Faculty of Sciences and Bioengineering Sciences
Vrije Universiteit Brussel (VUB), Belgium

Faculty of Sciences
Department of Plant Biotechnology and Bioinformatics
Ghent University (UGent), Belgium

How *Arabidopsis thaliana* dehydroascorbate reductase 2 and mitogen activated kinase 4 cope with cysteine sulfur oxidation

Nandita Bodra

Thesis submitted in partial fulfillment of the requirements
for the degree of

Doctor (PhD) in Bioengineering Sciences

Doctor (PhD) in Sciences, Biochemistry and Biotechnology

Academic year: 2017-2018

Promotor VUB:
Prof. Dr. Joris Messens
Faculty of Sciences and Bioengineering Sciences
Vrije Universiteit Brussel (VUB), Belgium

VIB Center for Structural Biology
Redox Signaling Lab
Pleinlaan 2, 1050 Brussel, Belgium

Promotor UGent:
Prof. Dr. Frank Van Breusegem
Faculty of Sciences, Department of Plant Biotechnology and Bioinformatics
Ghent University (UGent), Belgium

VIB Center for Plant Systems Biology
Oxidative Stress Signalling Lab
Technologiepark 927, 9052 Ghent, Belgium

This work was conducted at the Center for Structural Biology and the Center for Plant Systems Biology of the Flanders Institute for Biotechnology (VIB).

Nandita Bodra is indebted to Indian Council of Agricultural Research International fellowship.

EXAMINATION COMMISSION

Prof. Dr. Geert Angenon (Chair)
Faculty of Sciences and Bioengineering Sciences, Department of Bioengineering Sciences, Vrije Universiteit Brussel, Belgium

Prof. Dr. Jean-Pierre Hernalsteens (Secretary)
Faculty of Sciences and Bioengineering Sciences, Department of Biology, Vrije Universiteit Brussel, Belgium

Prof. Dr. Joris Messens (Promotor-VUB)
Faculty of Sciences and Bioengineering Sciences, Department of Bioengineering Sciences Vrije Universiteit Brussel, Belgium

Prof. Dr. Frank Van Breusegem (Promotor-UGent)
Faculty of Sciences, Department of Plant Biotechnology and Bioinformatics, Ghent University, Belgium

Prof. Dr. Ann Depicker
Faculty of Sciences, Department of Plant Biotechnology and Bioinformatics, Ghent University, Belgium

Prof. Dr. Jean-Philippe Reichheld
Genome and Plant Development Laboratory, National Center for Scientific Research, University of Perpignan, France

Prof. Dr. Natalie Verbruggen
Faculty of Sciences, Laboratory of Physiology and Molecular Genetics of Plants, Free University of Brussels (Universite libre de Bruxelles), Belgium

Prof. Dr. Godelieve Gheysen
Department Molecular Biotechnology, Applied Molecular Genetics, Ghent University, Belgium

Table of contents

Summary

How *Arabidopsis thaliana* dehydroascorbate reductase 2 and mitogen activated kinase 4 cope with cysteine sulfur oxidation

Reactive oxygen species (ROS) are unavoidable by-products of aerobic life. To prevent oxidative damage, cells maintain a dynamic balance between ROS production and removal by antioxidants. ROS can also function as signalling molecules, and today, thiol oxidation of cysteines is a well-recognized posttranslational protein modification. However, the signal transduction processes steered by such oxidations remain poorly understood. To gain insight into the cysteine thiol-dependent ROS signalling in plants, we first mapped out the hydrogen peroxide-dependent sulfenome of *Arabidopsis thaliana*: that is, proteins with at least one cysteine thiol (Cys-SH) oxidized to a sulfenic acid (Cys-SOH). In my PhD research project, I studied in detail dehydroascorbate reductase 2 (DHAR2) and mitogen activated kinase 4 (MPK4) which we identified as sulfenylated proteins.

DHAR2 regenerates the pool of ascorbate in a glutathione-dependent manner for the reduction of ROS. DHAR2 catalysis was shown to be driven by structural conformational flexibility with sulfenic acid formation and S-glutathionylation on its active site cysteine as part of its catalytic cycle. For MPK4, an enzyme located in the cytoplasm and induced by oxidative stress, the situation is different. Here, sulfenylation of one of its conserved cysteines significantly slows down its substrate phosphorylation activity.

From these studies, it becomes clear that understanding the role of sulfur oxidation of proteins from the sulfenome requires a detailed case-by-case biochemical approach. Ultimately, the molecular understanding of these oxidative stress induced protein modifications in plants might help to conceive new biotechnological approaches to improve performance of crops under stressful growth conditions.

Samenvatting

Het effect van cysteïne-zwaveloxidatie op dehydroascorbinezuurreductase 2 en mitogeen geactiveerd kinase 4 van *Arabidopsis thaliana*

Reactieve zuurstofmoleculen (ROS) zijn de onvermijdelijke nevenproducten van een aëroob leven. De cel wordt gespaard van door ROS geïnduceerde oxidatieve schade omdat er een dynamisch evenwicht is tussen ROS-productie en -verwijdering door antioxidantia. ROS hebben ook een functie als signaalmoleculen. Zo is de oxidatie van cysteïne-zwavels in eiwitten een bekende posttranslatiemodificatie, maar de onderliggende signaaltransductieprocessen worden nog steeds niet goed begrepen. Om een betere kijk te krijgen op de cysteïne-thiol-afhankelijke ROS-geïnduceerde signaalprocessen in planten, hebben we we allereerst het waterstofperoxide-afhankelijke sulfenoom van *Arabidopsis thaliana* kaart gebracht. Dit is de verzameling eiwitten met minstens een cysteïnethiolgroep (Cys-SH) geoxideerd tot sulfeenzuurcysteïne (Cys-SOH). In mijn doctoraatsonderzoeksproject heb ik de details bestudeerd van twee eiwitten van dit sulfenoom, dehydroascorbinezuur-reductase 2 (DHAR2) en mitogeen geactiveerd kinase 4 (MPK4).

DHAR2 regenereert op een glutathion-afhankelijke manier het ascorbaat dat nodig is om ROS te reduceren. Tijdens dit katalytisch proces wijzigt dit enzym zijn structurele conformatie door zowel de vorming van sulfeenzuur als een glutathionedisulfide op het cysteïne in zijn actieve centrum. Voor MPK4, een cytoplasmatisch enzym dat wordt aangemaakt onder oxidatieve stress, is de situatie anders. Sulfeenvorming op een van de geconserveerde cysteïnes heeft hier een significante verlaging van de autofosforylatie en substraatfosforylatie tot gevolg.

Deze studies tonen aan dat om de rol van zwaveloxidatie in eiwitten van het sulfenoom beter te begrijpen er voor ieder eiwit een afzonderlijke gedetailleerde biochemische studie nodig zal zijn. Uiteindelijk zullen inzichten in de moleculaire details van door oxidatieve stress geïnduceerde eiwitoxidaties in planten ons helpen bij het ontwerp van nieuwe biotechnologische technieken om gewassen onder stressvolle condities te doen groeien.

Abbreviations

ABA	abscisic acid
ATP	adenine triphosphate
BIAM	biotinylated iodoacetamide
CaMV	cauliflower mosaic virus
CaM	calmodulin
cCRD	c-terminal cysteine-rich domain c-terminal cysteine
CDS	coding sequence
Cys Ox-PTMs	cysteine oxidative posttranslational modifications
DHA	dehydroascorbate
DNaseI	deoxyribonuclease I
DTT	dithiothreitol
DYn-2	alkyne-functionalized dimedone analogous
EDTA	ethylenediaminetetraacetic acid
EGF	epidermal growth factor
GAPDH	glyceraldehyde 3-phosphate dehydrogenase
GEE	glutathione ethyl ester
Grx	glutaredoxin
GSH	glutathione
GSSG	oxidized form of glutathione
GST	glutathione s-transferase
IAA	indoleacetic acid
IAM	iodoacetamide
ICAT	isotope-coded affinity tag
LC-MS/MS	liquid chromatography tandem mass spectrometry
LDH	lactate dehydrogenase
JA	jasmonic acid
mBBr	monobromobimane
MBP	myelin basic protein
MEKK	mitogen activated protein kinase kinase kinase
MEK	mitogen activated protein kinase kinase
MPK	mitogen activated protein kinase
MV	methyl viologen
NADPH	nicotinamide adenine dinucleotide phosphate
NADH	nicotinamide adenine dinucleotide
NEM	N-ethylmaleimide
PA	poly arginine
PCR	polymerase chain reaction
PEP	phospho(enol)pyruvate
Pfu	proofreading polymerase
PK	pyruvate kinase
PTMs	posttranslational protein modifications
PTPs	protein tyrosine phosphatase
PTP-ABI2	protein tyrosine phosphatase abscisic acid insensitive 2
PVDF	polyvinylidene difluoride
ROS	reactive oxygen species

SA	salicylic acid
SDS	sodium dodecyl sulfate
SDS-PAGE	sodium dodecyl sulfate polyacrylamide gel electrophoresis
SOD	superoxide dismutase
SO_2H	sulfinic acid
SO_3H	sulfonic acid
SOH	sulfenic acid
TAIR	the Arabidopsis information resource
TCEP	tris 2-carboxyethyl phosphine
TCA	tricarboxylic acid
Trx	thioredoxin
YAP1	Yeast *Saccharomyces cerevisiae* activator protein1

Objective of the thesis

Plants encounter a variety of environmental stresses which diminish the productivity of various economically important crops. Each year, the world loses a huge amount of crop production through scarcity of water, extreme temperatures, high soil salinity and pathogen attack. The sessile nature of plants has resulted in the evolution of complicated protection mechanisms to survive different environmental challenges. One of the stress tolerance mechanisms is the ability to sense complex stress factors and respond appropriately. Activation of complex signaling pathways helps plants to achieve this. To better understand plant signaling pathways would enable us to modify plants to improve their adaptability.

As a response to stress plant produce reactive oxygen species (ROS) such as hydrogen peroxide (H_2O_2), singlet oxygen ($^1O_2$), superoxide radical ($O_2^{\bullet-}$), and hydroxyl radical ($HO^{\bullet-}$). The adverse growth conditions disturb the equilibrium between production and scavenging of ROS. Accumulation of ROS serves as an early hallmark for stress conditions and is rapidly perceived and transduced at the cellular and whole organism level. Based on this information, plants are able to tune the gene expression pattern that ultimately leads to a finely tailored response. The main target of ROS in the cell is cysteine residue and the foremost oxidation product of cysteine residue is sulfenic acid which can act as the decisive point for the plant to either proceed to survival or damage pathway.

Hydrogen peroxide acts a major redox metabolite involved in redox sensing, signaling and redox regulation. The role of the hydrogen peroxide as a signaling molecule in plants and its effects on cysteine residues have been reviewed in the chapter 1. In the beginning of this research we identified the hydrogen peroxide (H_2O_2)-dependent sulfenome of *Arabidopsis thaliana* with genetic and chemical probes. By using a genetic construct consisting of the fusion between the C-terminal domain of the yeast AP-1-like (YAP1) transcription factor and a tandem affinity purification tag, we identified ~100 sulfenic acid forming proteins. Next to the YAP1 probe, we used a dimedone based alkyne functionalized DYn-2 probe to trap the sulfenylated protein *in vivo*. With the DYn-2 approach, we identified 226 sulfenylated proteins.

Based on the biological relevance and protein biochemistry feasibility studies, we selected dehydroascorbate reductase 2, a cytosolic protein involved in regeneration of ascorbate which

is a major antioxidant in the cell and mitogen activated kinase 4, a nuclear and cytosol localized protein operating in intracellular signal perception and transduction via the mitogen activated kinase cascade signaling pathways from the list of protein which we have discussed in detail in chapter 2 and chapter 3. The major goal of this research was to identify and characterize the proteins that form sulfenic acid in stress condition and to understand the role of cysteine residue in the protein function and its physiological relevance under the oxidative stress to improve stress tolerance through *in vitro* validation and genetic approaches. Ultimately, we aim to translate our knowledge back to the crop, so that we can design crops with higher resilience against environmental stress conditions.

Introduction

Chapter 1

Abstract

Plants produce reactive oxygen species (ROS) in response to adverse environmental conditions, such as extreme temperature, drought, salinity, UV-irradiation, and pathogen attacks. Reactive oxygen species (ROS) have been considered highly reactive, comprising of toxic molecules that can cause oxidative damage to the cell. The most attractive targets of ROS are proteins, lipids, and nucleic acids. Under normal cellular conditions, ROS can also be produced through plant metabolic activities, such as respiration and photosynthesis. ROS, especially H_2O_2, play an important role as signalling molecules. The presence of mild concentrations of H_2O_2 plays a key role in cellular sensing and signalling involved in the regulation of plant growth, development, resistance responses, and signal transduction.

Over the last few years, the role of H_2O_2 as a signalling molecule has been extensively studied. However, it remains rather enigmatic how plant perceives the message of H_2O_2 that allow signalling, regulation and protection. The signalling function relies on the oxidation of proteins by H_2O_2 which results in changes in confirmation and activity of the proteins. One possible way to sense H_2O_2-driven oxidation by a protein is through cysteine sulfur oxidation. The initial oxidation product of cysteine is sulfenic acid (-SOH) which act as H_2O_2 sensor. Recently, with the YAP1C and DYn-2 probe, a list of sulfenic acid-forming proteins have been identified in *Arabidopsis thaliana* under H_2O_2 stress. This Ph.D. thesis focusses on in-depth study of two sulfenic acid forming proteins by exploring their biochemical, functional, and structural aspects to understand their role in signal perception and transduction under oxidative stress conditions.

This introductory chapter describes the hydrogen peroxide as a major redox metabolite and discusses the major H_2O_2 generation sites inside the plant cell. Next, it will cover the possible H_2O_2 scavenging strategies of plants including enzymatic and non-enzymatic scavengers. Furthermore, the reader will be introduced to various approaches to identify cysteine oxidative post-translational modifications and crosstalk between H_2O_2 and mitogen activated protein kinase signalling.

1.1 Hydrogen peroxide as a major redox metabolite

Plants live in an aerobic environment where oxygen is an integral part of their lifespans. During respiration and photosynthesis, plants utilize oxygen as a terminal oxidant. Though atmospheric oxygen itself is non-reactive, it has the capability to get partially reduced, which makes it very reactive and it transforms to become toxic intermediates, such as singlet oxygen ($^1O_2$), superoxide radical ($O_2^{\bullet-}$), hydrogen peroxide (H_2O_2), and hydroxyl radical ($HO^{\bullet-}$). These reactive oxygen species (ROS) have strong likenesses towards macromolecules such as proteins, DNA, carbohydrates, and lipids in plant cells (Anjum, Sofo et al. 2015). At the normal physiological level, H_2O_2 acts as a signalling molecule, whereas under biotic and abiotic stress conditions, it induces oxidative stress. Among ROS, H_2O_2 has a relatively long life span and small size, which permit it to traverse through cellular membranes to different cellular compartments, thus making it a suitable signaling molecule (Saxena, Srikanth et al. 2016) (Table 1).

Table. 1: Redox metabolites: H_2O_2 and other ROS derivatives and their properties (Nandini et al. 2016)

ROS	Half-life and mobility	Mode of Action	Main scavenging system
Superoxide radical ($O_2^{\bullet-}$)	1 µs, 30 nm	Reacts with double-bond compounds [such as iron-sulfur (Fe-S) clusters of proteins] and nitric oxide (NO) to form peroxynitrite ($ONOO^-$)	Superoxide dismutase (SODs)
Hydroxyl radical ($HO^{\bullet-}$)	1 ns,1 nm	Extremely reactive to proteins, lipids, DNA, and other macromolecules	Flavonoids
Hydrogen peroxide (H_2O_2)	1 ms, 1µm	Oxidizes proteins, reacts with $O_2^{\bullet-}$ in Fe-catalysed reaction to form $HO^{\bullet-}$	Catalase, various peroxidase, peroxiredoxin and flavonoids
Singlet oxygen ($^1O_2$)	1 µs, 30 nm	Directly oxidizes protein, polysaturated fatty acids, and DNA	Carotenoids and α-tocopherols

Hydrogen peroxide is a versatile molecule and ubiquitous to cell, and since its initial identification in living cell, it was considered as a toxic by-product of cellular metabolism. In the beginning of the 90s, H_2O_2 was predicted as a signalling molecule. H_2O_2 showed involvement in programmed cell death at high concentrations and its dual nature has been reported, where 600 µM H_2O_2 treatment causes an increase in the vase life of hybrid lily 'Manissa', and further increase in concentrations results in negative consequences (Liao et al. 2012). Nowadays, H_2O_2 is a very well-known signalling molecule. In plants, H_2O_2 functions as a messenger involved in intracellular signalling to regulate numerous biological functions

(Reczek and Chandel 2015). It also acts as a key regulator in a wide range of physiological processes, such as stomatal movement, senescence, photosynthesis and photorespiration, growth and development, and cell cycle. It has been proven to be involved under strict environmental conditions, which consist of various abiotic and biotic stresses in plants. Moreover, it has been identified as a transcription independent signalling molecule similar to Ca^{2+} and adenosine triphosphate. It facilitates a string of responses and activates several other signalling pathways, for instance, salicylic acid, abscisic acid, jasmonic acid, ethylene, and nitric oxide signalling in plants. A recent study has focused on ROS production and its integration with various hormonal signalling pathway in the regulation of plant growth and stress tolerance (Xia, Zhou et al. 2015). Exogenous application of H_2O_2 and its provocation in high light have shown different effects on gene expression (Golemiec, Tokarz et al. 2014).

As a messenger molecule, H_2O_2 can diffuse through the cells and initiates the cellular responses, such as the initiation of cell proliferation and recruitment of immune cells, change in cell shape, growth and developmental processes, and enabling of resistance responses. It has been described that through aquaporin channels, H_2O_2 crosses the cell membrane. Till date, it has become clear that H_2O_2 also assists in regulating metabolic functions.

As stated above, H_2O_2 cooperates with other signalling molecules, such as abscisic acid (ABA) and ethylene, which are important for plant development and senescence (Chen, Wu et al. 2012). ABA is a phytohormone and is an endogenous anti-transpirant responsible for lowering the water loss through stomatal pores on the leaf surface. Exogenous treatment of maize leaves with H_2O_2 significantly enhance the ABA content and involve in ABA-induced stomatal closure. Plants produce ABA under drought stress which stimulates stomatal guard cells to close. In this process, H_2O_2 is generated, and it acts as an essential signal and activates calcium-permeable channels in the plasma membrane and thus, in turn, mediates stomatal closure induced by ABA. The open stomatal 1(OST1) protein kinase mutant which lacks ABA-induced ROS production mediates stomatal closure upon H_2O_2 treatment.

Different H_2O_2 concentrations play diverse functions such as in intact cells, concentrations ranging between 0.1-0.5 mM H_2O_2 activate plant guard cell plasma membrane calcium channels (Kohler, Hills et al. 2003). Additionally, the exogenous treatment of 30-300 μM H_2O_2 inhibits the function of protein tyrosine phosphatase abscisic acid insensitive 2 (PTP-ABI2), which is a negative modulator of ABA signalling pathway, while 3–10 μM H_2O_2 does not

inhibit ABI2 action which is ten-fold higher than the physiologic intracellular level of H_2O_2 (Meinhard, Rodriguez et al. 2002). In Arabidopsis guard cells, 5 mM H_2O_2 enhances cytoplasmic calcium levels by the activation of plasma membrane cation channels (Pei, Murata et al. 2000).

Salicylic acid (SA) is a key signal in the establishment of systemic acquired resistance (SAR) in plants and the activation of localized resistance associated with hypersensitive reaction (HR) displays systemic acquired resistance (SAR). Benzoic acid is a precursor of SA and H_2O_2 further associates with SA synthesis as the conversion of benzoic acid into SA is catalysed by the H_2O_2 mediated activation of benzoic-acid-2 hydroxylase. The H_2O_2-SA interaction pattern have been suggested where H_2O_2 and SA constitute a self-amplifying system; H_2O_2 prompts SA accumulation and SA boosts H_2O_2 level (Van camp et al. 1998). The transgenic tobacco, Samsun NN, expressing salicylate hydroxylase (35S-SH-L) challenged with avirulent strains of *Pseudomonas syringae* delays H_2O_2 accumulation by 2 to 3 h, which implies the rise in SA potentate, the oxidative burst on accumulation of H_2O_2. In mung bean seedlings, salicylic acid is responsible for the formation of adventitious root and during this process H_2O_2 accumulation occurs which is further engaged in the downstream regulation process involved in salicylic acid-induced adventitious root formation (Yang, Zhu et al. 2013).

The plant hormone ethylene regulates various physiological processes, such as seed germination, pathogen and stress responses, fruit ripening, senescence. The catalase mutant pine needle induces ethylene production upon the exogenous treatment of H_2O_2 and Ozone-challenged tobacco produces H_2O_2 in apoplast and leads to ethylene accumulation (Shraudner, Moeder et al. 1998). It has been reported that during programmed cell death, ethylene is involved in H_2O_2 accumulation (de, Yakimova et al. 2002).

Calcium (Ca^{2+}) is a second messenger and can regulate various cellular processes in plant. It has been suggested that plasma membrane permeability enhances upon stress and thus, a calcium and proton influx emerges, which is adequate for the induction of H_2O_2 (Pei, Murata et al. 2000). Also, the study on H_2O_2 homeostasis in *Arabidopsis* reveals the link between H_2O_2 and Ca^{2+} signals (Yang and Poovaiah 2002). Continuous Ca^{2+} influx activates the plasma membrane-localized NADPH oxidase and subsequently calcium-dependent cellular responses are referred to anion and K^+ efflux. It has been shown that H_2O_2-challenged *Arabidopsis* triggers a biphasic Ca^{2+} elevation (Rentel and Knight 2004). Also, aequorin-expressing *Tobacco* cell cultures display a biphasic Ca^{2+} signature in response to the H_2O_2 challenge

(Lecourieux, Mazars et al. 2002). The Ca^{2+} inhibitors that decrease the Ca^{2+} concentration in cytosol delays the accumulation of endogenous H_2O_2. Both H_2O_2 and Ca^{2+} are involved in signalling cascades, resulting in stomata closure in *Arabidopsis* (Pei, Murata et al. 2000). Pie et al. reported that H_2O_2-activates Ca^{2+}channels and mediates influx of Ca^{2+} in protoplasts and increases Ca^{2+} in the cytosol in intact guard cells. The ubiquitous calcium-binding protein, calmodulin (CaM), has been assumed to increase H_2O_2 generation through Ca^{2+}/CaM-dependent NAD kinase that affects the concentration of available NADPH during the activation of NADPH oxidase. The exogenous Ca^{2+} signalling induces higher antioxidant enzymes activity and the expression level of antioxidant gene and H_2O_2 application decreases Ca^{2+} signalling but increases the transcript abundance of catalase and ascorbate peroxidase in Perennial ryegrass (*Lolium perenne*) (Hu, Chen et al. 2016).

Calcium-dependent protein kinases (CDPKs) are implicated as major primary Ca^{2+} sensors in plants. CDPK activation is triggered by biotic and abiotic stresses. N-terminal CDPK2 signalling has been reported to increase the levels of the phytohormones such as jasmonic acid, and ethylene, but not salicylic acid. Elevated CDPK signalling compromises stress-induced mitogen-activated protein kinases (MPKs) activation and this inhibition requires ethylene synthesis and perception (Ludwig, Saitoh et al. 2005). Ca^{2+}/CaM can down-regulate H_2O_2 levels in plants by stimulating the catalytic activity of plant catalase thus involved in controlling H_2O_2 homeostasis in plants (Yang and Poovaiah 2002). It has been observed that plants lacking K^+ ion can increase H_2O_2. The accumulation of H_2O_2 in roots has shown to be involved in K^+ uptake and translocation (Shin and Schachtman 2004) . Zhang et al. have been reported that H_2O_2 restricts calcium channels regulation as well as K^+ channel activity during stomatal closure (Zhang, Dong et al. 2001).

It is very interesting that the role of H_2O_2 as a signalling molecule in plants is quite similar in animals. In comparison to animals, plants have an extra potential source of H_2O_2, the chloroplasts. The steady state concentration of H_2O_2 in chloroplast is 0.37 μM, which is similar to physiologic levels of H_2O_2 in microbes and animals (Polle 2001). Plants also contain a cell wall and here, H_2O_2 serves in oxidative biosynthesis and remodelling of the cell wall (Apel and Hirt 2004). The evidences support that H_2O_2 participates in nitrosative stress-triggered cell death in kimchi cabbage (*Brassica rapa*) seedlings as well as involved in nitric oxide and hydrogen sulfide signalling to activate thermo-tolerance in maize seedlings. Furthermore,

H_2O_2, nitric oxide, and Ca^{2+} could mitigate copper stress in *Ulva compressa* (Gonzalez, Cabrera Mde et al. 2012).

1.2. Source of H_2O_2 in plants

It has been estimated that about 1% of O_2 consumed by plants is averted to produce reactive oxygen species (ROS) in various sub-cellular loci (Figure 1.) Plant chloroplasts capture light energy from the sun and produce the free energy stored in ATP and NADPH through photosynthesis. Chloroplasts are a major source of H_2O_2. It contains photo reaction system, photosystem I (PSI), photosystem II (PSII), as well as pigment protein. In PSI, the photoreduction of oxygen generates H_2O_2 (Mehler 1951)and the disproportionation of superoxide anion produces H_2O_2 and O_2 (Asada, Kiso et al. 1974). Additionally, in PSII, ground state oxygen ($^3O_2$) reacts to triplet excited state of chlorophyll and produces singlet oxygen ($^1O_2$). Generally, the electron flow from the excited PS centres is directed to $NADP^+$, which is then reduced to NADPH. Further NADPH enters the Calvin cycle and reduces CO_2 which is the final electron acceptor. When the electron flow exceeds from the electron transport chain (ETC), a part of the electron flow is diverted from ferredoxin to O_2. Then, O_2 reduces to superoxide anion ($O_2^{\bullet-}$) via a Mehler reaction. Studies have demonstrated that the acceptor side of ETC in the PS II -provided sides, such as Q_A and Q_B, with electron leakage to O_2 produces $O_2^{\bullet-}$. This $O_2^{\bullet-}$ either enzymatically by copper/zinc superoxide or spontaneously, dismutates to H_2O_2 on the stromal membrane surface (Pilon, Ravet et al. 2011). The ascorbate peroxidase in thylakoid and stroma catalyses the conversion of H_2O_2 into H_2O (Caverzan, Passaia et al. 2012). Also, peroxiredoxin and monodehydroascorbate reductase participate in regeneration of antioxidants. Tocopherols and ß-carotene function as quenchers of $^1O_2$.

Plant mitochondria are other common sites of production of H_2O_2 under aerobic condition. About 1–5% of the mitochondrial O_2 consumption leads to H_2O_2 generation (Moller 2001). It consists of four complex namely NADH dehydrogenase (C I), succinate dehydrogenase (C II), ubiquinol-cytochrome bc1(C III), and cytochrome c oxidase (C IV). There are five enzymes that are only present in plants; one alternative oxidase (AOX) and four NAD(P)H dehydrogenase assembled to flavoproteins and these are potential sources of ROS production. In mitochondria, H_2O_2 oxidizes alternative oxidase and enzymes involved in the tricarboxylic acid cycle and these are described to be the targets of the thioredoxin system. The ubiquinone site in complex III emerges as the main site of mitochondrial H_2O_2 production. The intra-

mitochondrial redox regulation has been studied in mammals, where they propose that reversible oxidation of Cys 39 of mitochondrial subunit ND3 can deactivate complex I, which results into avoiding an excessive $O_2^{\bullet-}$ release from reverse electron flow at reoxygenation after anoxia (Braun, Binder et al. 2014). Recently, Patterson et al. have proposed that mitochondrial superoxide dismutase produces H_2O_2 that can be perceived by the intermembrane space which lead to a phosphorylation cascade in animals (Patterson, Gerbeth et al. 2015). The mitochondrial matrix can sense the H_2O_2 -which is produced in the endoplasmic reticulum – and this H_2O_2 is responsible for glutathionylation of glycine decarboxylase subunit (Hoffmann, Plocharski et al. 2013). Although, it is not clear if the H_2O_2 produced in mitochondria is perceived by the endoplasmic reticulum or not. These experimental evidences provide clue that H_2O_2 sensing and signalling can be co-localized.

Peroxisomes are subcellular organelles and are also known as glyoxysomes. They have two sites that produce superoxide radicals ($O_2^{\bullet-}$) because of their normal metabolism (del Rio, Corpas et al. 2002). One is in the organelle matrix where xanthine oxidase (XOD) produces $O_2^{\bullet-}$ by catalysing the oxidation of xanthine and hypoxanthine into uric acid (Corpas, Barroso et al. 2001). Another site is in the peroxisome membranes, which are dependent on NADPH. Peroxisome membranes constitute flavoprotein NADH and cytochrome b, which produce $O_2^{\bullet-}$. Monodehydroascorbate reductase (MDHAR) participates in $O_2^{\bullet-}$ production by peroxisome membranes and CuZn-superoxide dismutase converts $O_2^{\bullet-}$ radicals into H_2O_2 and O_2.

The cell membrane NADPH-dependent oxidase (NADPH oxidase) acts as a source of H_2O_2 for the oxidative burst. It has been recognized that respiratory burst oxidase homologues (rboh), plant homologues of the catalytic subunit of the phagocyte NADPH oxidase as a source of ROS during the apoplastic oxidative burst (Agrawal, Iwahashi et al. 2003). Plant Rho-related GTPases (ROPs) are closely related to the mammalian Rac family proteins and initiate H_2O_2 production, thereby causing oxidative burst (Agrawal, Iwahashi et al. 2003). The pH-dependent cell wall peroxidase oxidizes NADH and catalyses the formation of the $O_2^{\bullet-}$. The cell wall oxidase catalyses the oxidation of NADH to NAD^+, reduces O_2 to $O_2^{\bullet-}$, and subsequently, $O_2^{\bullet-}$ disproportionates to H_2O_2. In apoplasts, germin-like oxalate oxidases and amine oxidases generates H_2O_2 (Hu, Bidney et al. 2003, Walters 2003).

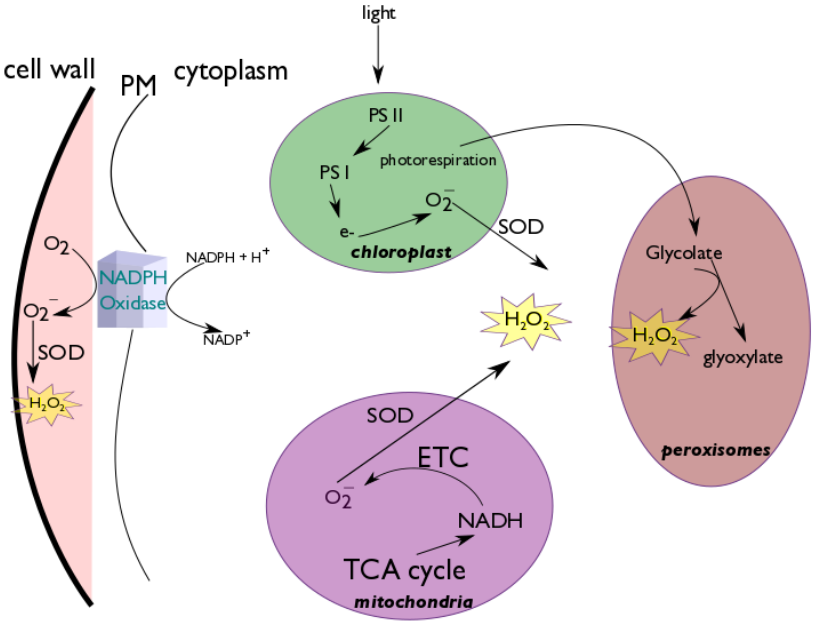

Figure 1: Major intracellular sources of H_2O_2 in a plant cell. The initiation of superoxide radical ($O_2^{\bullet-}$) production by NADPH oxidase in the plasma membrane and conversion of $O_2^{\bullet-}$ to H_2O_2 mediated by superoxide dismutase (SOD) in cell wall. The generation of $O_2^{\bullet-}$ by one-electron reduction of molecular oxygen by photosystem I (PSI) and its conversion to H_2O_2 by SOD and the generation of H_2O_2 by the peroxisomal glycolate oxidase reaction linked to photorespiration. The involvement of tricarboxylic acid cycle (TCA) and electron transport chain (ETC) in the production of H_2O_2.

1.3. H_2O_2 and cellular redox homeostasis

An intracellular balance between H_2O_2 production and its scavenging system exists in plant cells (Rogers and Munne-Bosch 2016). The redox homeostasis involves a complex network of non-enzymatic and enzymatic antioxidant systems located in different cellular compartments (Figure 2). Non-enzymatic processes involve ascorbate, carotenoids, tocopherol, and phenolic compounds and low molecular weight thiols like glutathione. On the other hand, enzymatic mechanisms include several enzymes, such as superoxide dismutase (SOD), ascorbate peroxidase (APX), glutathione peroxidase (GPX), peroxiredoxin (Prx), dehydroascorbate reductase (DHAR), and catalase (CAT).

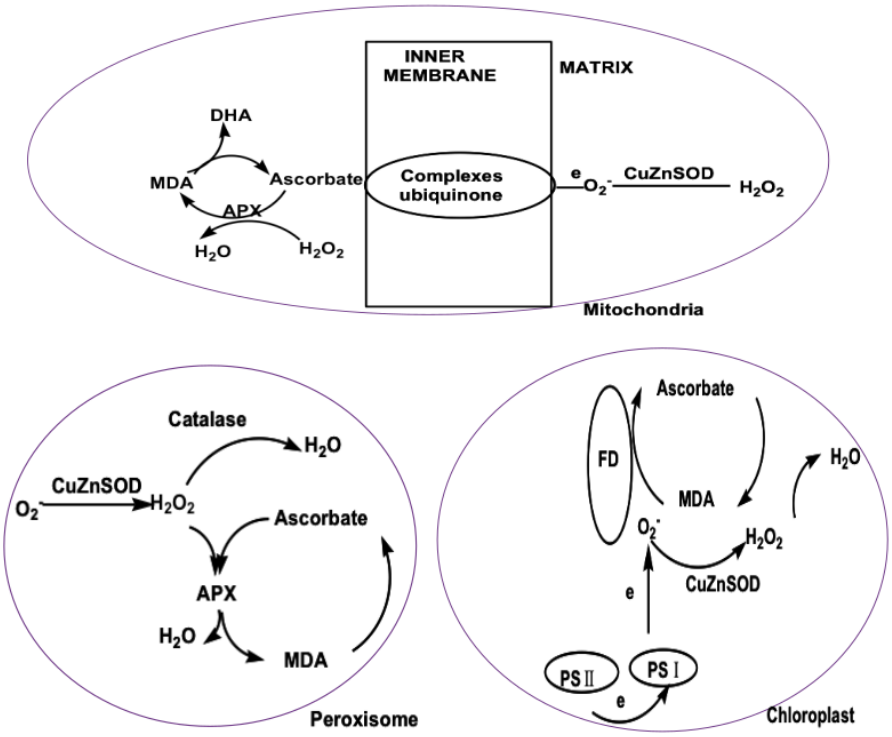

Figure 2: Hydrogen peroxide (H_2O_2) scavenging pathways in mitochondria, peroxisome and chloroplast. Catalase, ascorbate peroxidase (APX), superoxide dismutase (SOD) maintain the ascorbate pool inside the cell (Quan et al 2008).

1.3.1 Non-enzymatic scavengers

Ascorbate (AsA) is present in chloroplasts, cytosol, and vacuole and apoplastic spaces of leaf cells in high concentration and is an essential antioxidant in plants with a fundamental role in the removal of H_2O_2 (Polle, Chakrabarti et al. 1990). Ascorbate mostly occurs in the reduced form and it has been reported that 90% of the ascorbic acid pool and its intracellular concentration ranges from 20 mM in the cytosol to 20–300 mM in the chloroplast stroma (Noctor and Foyer 1998).

The biosynthesis of ascorbate occurs in the mitochondria and it is further transported to other cell components by a proton-electrochemical gradient or through facilitated diffusion (Horemans, Foyer et al. 2000), as it performs several functions in physiological processes including the regulation of growth and differentiation, as well as in plant metabolism. It reacts non-enzymatically with superoxide, hydrogen peroxide, and singlet oxygen. It scavenges free radicals and is involved in the ascorbate/glutathione cycle which is the most critical H_2O_2 detoxifying system in the chloroplasts, cytosol, peroxisomes, and mitochondria (Jimenez,

Hernandez et al. 1997). Ascorbate peroxidase utilizes two molecules of ascorbate to reduce H_2O_2 to water, with the concomitant production of monodehydroascorbate, which is a radical with a short lifetime and can disparate into dehydroascorbate (DHA) and ascorbate. Monodehydroascorbate directly reduces to ascorbate by using electrons derived from the photosynthetic electrons transport chain. Two enzymes are involved in the regeneration of reduced ascorbate, namely, monodehydroascorbate reductase (MDHAR) and dehydroascorbate reductase (DHAR). MDHAR utilizes NADPH directly to recycle ascorbate. MDHAR isozymes are present in mitochondria, chloroplasts, cytosol, and microbodies.

The enzyme catalysis mechanism of cytosolic DHAR2 of *Arabidopsis thaliana* in regeneration of ascorbate pool will be discussed in more detail in chapter 2. AsA and its synergetic action with other antioxidants minimize damages caused by the oxidative process (Pourcel, Routaboul et al. 2007). *Arabidopsis thaliana* MDAR 1 gene (*At MDAR1*) overexpression in tobacco plants has shown enhanced tolerance to ozone, salt, and PEG stress (Eltayeb, Kawano et al. 2007). The enhanced activity of MDAR results into the elevated levels of AsA. In *Picea aspertata*, high light conditions and drought significantly increased the AsA content. Also, UV radiation has been shown to increase the AsA content in *Cassia auriculata* seedlings. It is indirectly involved in the regeneration of tocopherol or in the synthesis of zeaxanthin in the xanthophylls cycle (Shao, Chu et al. 2007).

Tocopherol is another non-enzymatic antioxidant present in all parts of plants and algae. There are four tocopherol isomers, namely, α, β, γ, and δ, among which α-tocopherols are the most biologically active and prime antioxidants present in the chloroplast membranes. α-tocopherols are mainly responsible for protecting the chloroplast membrane against photo-oxidative damage. α-tocopherol is a lipid-soluble antioxidant linked with the biological membrane of cells, specifically the membrane of the photosynthetic apparatus (Halliwell 2006, Mullineaux, Karpinski et al. 2006) They quench singlet oxygen through a charge transfer mechanism. A single α-tocopherols molecule neutralizes 120 singlet oxygen molecules. It acts as polyunsaturated fatty acid (PUFA) radical terminator generated by lipid oxidation (Ledford, Chin et al. 2007). It scavenges lipid peroxy radicals and produces a tocopheroxyl radical that can be recycled back to the α-tocopherol by reacting with ascorbate or other antioxidants (Igamberdiev and Hill 2004). Lipid peroxidation is oxidative damage initiated by ROS mainly generated by plant photosynthesis and metabolism. During photosynthesis, α-tocopherol synthesis increases in the plant tissues upon abiotic stress. It has been reported that α-

tocopherol is involved in removing various ROS and lipid oxidation products (Kruk, Hollander-Czytko et al. 2005, Noctor 2006). It also modulates signal transduction and stabilizes membranes. Moreover, it inhibits chain propagation step of lipid auto-oxidation, which is an effective way of trapping free radicals. In higher plants, oxidative stress induces the expression of genes involved in the synthesis of tocopherol. Triazole which is a fungicide, treated plants have efficient free radical scavenging system. Triazole treatment in tomato increases α-tocopherol and ascorbic acid content, which further protects cellular membrane from oxidative damage. It has also been shown that triazole increases antioxidants and antioxidant enzymes levels in wheat. Also, an increase in the tocopherol level during water stress in plants have been reported. In grass species, it has been shown that drought stress lead to an increase in tocopherol content (Pourcel, Routaboul et al. 2007). The α-tocopherol content increases tremendously under high stress in *Arabidopsis*. It provides protection to the plant during oxidative stress, photo-inhibition, and photo-oxidative stress (Havaux, Eymery et al. 2005, Abbasi, Hajirezaei et al. 2007).

Glutathione (GSH) is another important antioxidant. It is a tripeptide called γ-glutamylcysteinylglycine, and exists in all cellular compartments like cytosol, chloroplasts, endoplasmic reticulum, vacuoles, and mitochondria (Millar, Mittova et al. 2003). It is a major cradle of non-protein thiols in the plant cells. The thiol group in glutathione is particularly reactive, which co-ordinates the biochemical functions in all organisms. The thiol group has a nucleophilic nature, which is crucial in forming mercaptide bonds with metals and for reacting with electrophiles. Chloroplasts contain the highest concentrations of reduced GSH, which is 1–4 mM. Glutathione and ascorbate biosynthesis is similar in plants, animals, and microorganisms. The GSH biosynthesis involves two adenosine triphosphate dependent steps, where γ-glutamylcysteine synthetase (γ-ECS) and glutathione synthetase (GSHS) link to form a tripeptide (Figure 3). These reactions take place in the chloroplastic and non-chloroplastic compartments, and the concentrations of GSH and redox state of the cell are critical in signalling (Noctor, Gomez et al. 2002).

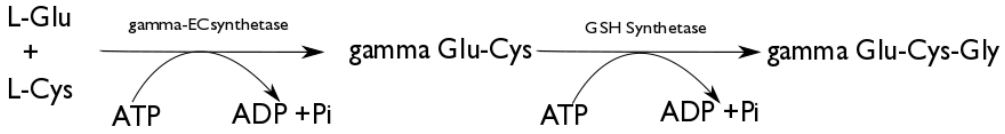

Figure 3: Pathway for glutathione biosynthesis in chloroplast and cytosol in plant leaves: The two ATP-dependent reactions lead to GSH synthesis.

GSH has been shown as a key player to maintain redox homeostasis (Noctor and Foyer 1998). GSH reduces DHA (dehydroascorbate), both enzymatically and non-enzymatically, in the ascorbate-glutathione cycle (Figure 4), and it itself gets oxidized to GSSG (oxidized glutathione). The regeneration from GSSG to GSH is catalysed by glutathione reductase, where NADPH behaves as a reducing agent. A nucleophilic cysteine residue of GSH is responsible for high redox potential of GSH. It detoxifies cytotoxic H_2O_2, and reacts non-enzymatically with other ROS, such as singlet oxygen, superoxide radicals, and hydroxyl radicals. GSH regenerates another powerful antioxidant, ascorbic acid, through the ascorbate–glutathione cycle (Millar, Mittova et al. 2003).

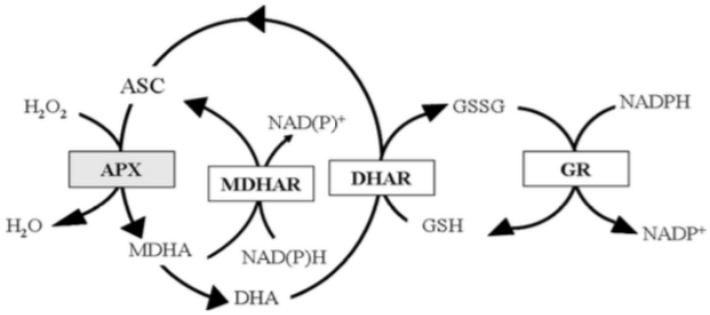

Figure 4: Foyer-Halliwell-Asada cycle. Ascorbate-glutathione cycle of H_2O_2 scavenging. Abbreviations – APX: ascorbate peroxidase; MDHAR: monodehydroascorbate reductase; DHAR: dehydroascorbate reductase; and GR: glutathione reductase. (Locato et al 2013).

It has been reported that glutathione assisted the endurance of oxidative stress in transgenic lines of tobacco (del Rio, Sandalio et al. 2006). It is an essential co-substrate, and reductant in defence against ROS, as well as is involved in maintenance of the redox imbalance. The glutathione also assists in the redox modification of metabolic enzymes and redox dependent changes of transcription factors and consequently, there is a change in the gene expression.

Likewise, the ROS-triggered post-translational modification of transcription factor activity has been suggested to be involved in developmental processes and stress-induced morphogenic responses (Potters, Pasternak et al. 2007).

Carotenoids are pigments that are found in plants and micro-organisms. The antioxidant activity of carotenoids is because of the conjugated double-bonded structure that delocalizes unpaired electrons (Mortensen, Skibsted et al. 2001). The β-carotene quenches singlet oxygen without degradation, and reacts with free radicals such as the peroxyl ($ROO^{\bullet-}$), hydroxyl ($HO^{\bullet}$), and superoxide radicals ($O_2^{\bullet-}$). At higher concentrations, carotenoids protect lipids from peroxidative damage. It has been suggested that carotenoids and tocopherols play an active role in photo protection (Penuelas and Munne-Bosch 2005).

Phenolic compounds such as flavonoids, tannins, hydroxycinnamate esters, and lignin are diverse secondary metabolites found in plant tissues. They have an ideal structural chemistry for free radical scavenging, and they are effective antioxidants compared to tocopherols and ascorbate. Polyphenols have high reactivity as hydrogen or electron donor, as well as polyphenol-derived radical to stabilize and delocalize the unpaired electron (chain-breaking function), and its ability to chelate transition metal ions. Flavonoids have been reported to mediate ROS homeostasis (Fini, Brunetti et al. 2011). They alter peroxidation kinetics by modifying the lipid packing order, thus decreasing the fluidity of the membranes. These changes result in sterically hindered diffusion of free radicals and inhibit per oxidative reactions. They also act as terminators of free radical chains, as well as chelators of redox-active metal ions, capable of lipid peroxidation catalysis (Schroeter, Boyd et al. 2002). Phenolic antioxidants interfere with lipids oxidation and other molecules by the rapid donation of hydrogen atom to radical. The phenoxy radical intermediates are relatively stable, so they do not allow further radical reactions to happen.

1.3.2 Enzymatic scavengers

Superoxide dismutase (SOD): Superoxide dismutase disproportionates $O_2^{\bullet-}$ to H_2O_2. It contains six isozymes and is classified based on the metal ion on its active site, namely, copper and zinc (Cu/Zn SOD), manganese (MnSOD), or iron (FeSOD) containing SODs. Kim et al have reported nickel superoxide dismutase in *Streptomyces* (Kim, Kim et al. 1996). SODs are located in different cellular compartments such as Cu/ZnSOD in the cytosol, MnSOD in matrix of the mitochondria and peroxisomes. Studies have shown that SOD activity increases under

stresses, such as salt stress, in pea, maize, and tea (Ahmad et al. 2008b; Tuna et al. 2008; Upadhyaya, Panda, and Dutta, 2008). It has been shown that in a salt-insensitive cultivar of tomato, SOD activity decreases, whereas the tolerant cultivars show an increase in activity in *Oryza sativa*, *Brassica napus*, and *Morus alba* (Shalata, Mittova et al. 2001, Sekmen, Turkan et al. 2007).

In *Picea asperata* (dragon spruce) seedlings, SOD activity has enhanced markedly under drought and high light condition (Yang et al. 2008). It has been noted that under high salt concentration, chloroplast SOD, thylakoid bound SOD, and stroma SOD has enhanced. The overexpression of 9-*cis*-epoxycarotenoid dioxygenase (NCED) gene *SgNCED1* in transgenic tobacco plants results in an induced activity of SOD, and the transgenic plants show an improved growth under 0.1 M mannitol-induced drought stress and 0.1 M NaCl-induced salinity stress (Qui-Fang et al. 2005). Transgenic plants show high levels of Cu/ZnSOD and ascorbate peroxidase gene transcripts under methyl viologen treatment. Camejo et al. showed that Fe-SODs may play a role in the development of heat-shock tolerance through heat acclimation in the seedlings of *Solanum esculentum* (Camejo, Marti Mdel et al. 2007). In ozone-sensitive varieties of tobacco plants, overexpression of Cu/Zn-SOD in the cytosol reduces ozone-induced necrosis (Pitcher and Zilinskas 1996). In *Ulva fasciata*, upregulation of gene expression of Mn-SOD/Fe-SOD has been reported under oxidative stress (Sung, Hsu et al. 2009).

Catalases: Catalases are tetrameric heme-containing enzymes that convert H_2O_2 into O_2 and H_2O. Plant catalases can be classified into three classes: Class 1, 2 and 3. The class 1 catalases are most prominent in photosynthetic tissues, and are involved in the removal of H_2O_2 produced during photorespiration; class 2 catalases are highly produced in vascular tissues and may play a role in lignification, though their exact biological role is unknown; class 3 catalases are highly abundant in seeds and young plants and their activity is linked with the removal of excessive H_2O_2 produced during fatty acid degradation in the glyoxylate cycle in glyoxisomes (Willekens, Villarroel et al. 1994).

Catalases do not require cellular reductants and capable to catalyse dismutase reaction (Mhamdi, Queval et al. 2010). It has been reported that the catalase activity is reduced under 200 mM H_2O_2 concentration (Ben Amor et al. 2005). The upregulation of catalase genes has been reported under abiotic stress in alfalfa nodule, tea, cotton, and tobacco (Sekmen, Türkan, and Takio 2007; Upadhyaya, Panda, and Dutta 2008; Vital et al. 2008; Zhang et al. 2008).

The class 2 catalases have been studied mostly under disease resistance. It has been shown that the expression of the tobacco *Cat*2Nt gene in transgenic potato plants leads to constitutive expression of the endogenous potato *Cat*2St gene and enhanced resistance to *Phytophthora infestans* in sensitive potato plants. The *E. coli* catalase gene with tomato *rbcS3C* promoter improves plant resistance to photooxidation caused by drought stress in tobacco (Shikanai, Takeda et al. 1998). The tobacco plants expressing catalase from *E. coli* fails to show destruction of chlorophyll (Miyagawa, Tamoi et al. 2000). The overexpression of the catalase gene under CaMV35S promoter in Japonica rice confers salt tolerance. The catalase activity has been shown to increase in *Citrumelo CPB 4475* and *Carrizo citrange* under continuous waterlogging (Arbona et al. 2008). In addition to that, draught and high light stress markedly increases the catalase activity in Dragon spruce (*Picea asperata* Mast.). In *Bassica napus*, an increase in the catalase activity has been shown under high salt concentration. Nevertheless, increase in the salt concentration in salt-tolerant mulberry cultivar does not show any response to catalase activity. Parida et al. have observed that under salt stress, catalase activity is decreased in the leaves of *Bruguiera parvi ora* (Parida, Das et al. 2004). It has been suggested that a decrease in the activity of catalase represents the importance of peroxidase and the SOD/ascorbate–glutathione cycle.

Glutathione peroxidases: Glutathione peroxidases (GPX) are the family of multiple isozymes that catalyse the reduction of H_2O_2. GPxs detoxify the products of lipid peroxidation formed due to an activity of ROS. There are three types, selenium-dependent GPxs, nonselenium-dependent phospholipids hydroperoxide GPxs (PHGPX), and glutathione transferases. GPx and glutathione transferases have differences in their subunits, the bonding nature of selenium at the active centre, and their catalytic mechanisms. It has been shown that constitutive overexpression of glutathione peroxidase gene or glutathione *S*-transferase gene enhances singlet oxygen resistance in *E. coli* (Ledford, Chin et al. 2007). The increase in the activity of Gpx has been observed in salt stress (Gueta-Dahan, Yaniv et al. 1997).

Ascorbate peroxidase (APX): APX scavenges H_2O_2 and is involved in water–water and ascorbate–glutathione cycles, besides engaging AsA as the electron donor. The reduction of H_2O_2 to water by ascorbate peroxidases (APXs) play an important role in the antioxidant system of plants (Kangasjarvi, Lepisto et al. 2008). APX family has five different isoforms, including thylakoid and microsomal membrane-bound forms, as well as soluble stromal, cytosolic, and apoplastic enzymes (Noctor and Foyer 1998). It has been purified from spinach,

pea, tea, and soybean plants. APX has high affinity for H_2O_2, compared to catalase. Wang et al has overexpressed *Arabidopsis* peroxisomal ascorbate peroxidase gene in tobacco and has conferred protection against aminotriazole, thereby causing oxidative stress in glyoxysomes and peroxisomes (Wang, Zhang et al. 1999), though the same transgenic tobacco plants do not show a decrease in the damage instigated by paraquat, which forms ROS in the chloroplast. These results suggest that the resistance provided by the expression of peroxisomal APX may be specific to the oxidative stress caused in peroxisomes rather than in the chloroplasts. In the leaves of sweet potato, the expression of APX gene has enhanced upon methyl viologen treatment. The level of cytosolic ascorbate peroxidase is upregulated during drought stress in the alfalfa nodule (Naya, Ladrera et al. 2007). Arbona et al demonstrates that during waterlogging, APX activity increases by 2.4-fold in *Citrumelo CPB 4475* and 1.9-fold *in Carrizo citrange*, higher than in the control plants (Arbona, Hossain et al. 2008). It has been explained that the activities of APX enhance significantly within 2 h under salt and paraquat-stressed cotton calli (Vital et al. 2008). The enhanced tolerance has been observed against salt stress in transgenic *Arabidopsis* plants, overexpressing cytosolic ascorbate peroxidases (Lu, Liu et al. 2007). Giacomelli et al. have shown that *Arabidopsis thaliana* deficient in two chloroplast ascorbate peroxidases, stromal APX, and thylakoid APX accelerates light-induced necrosis when levels of cellular AsA is low (Giacomelli et al. 2007). Simultaneous overexpressing of Cu/ZnSOD and APX genes in chloroplasts of transgenic tall fescue plants show tolerance to abiotic stresses (Lee, Ahsan et al. 2007).

Glutathione reductase (GR): GR is a highly-conserved enzyme and it catalyses the NADPH-dependent reaction of disulfide bond of GSSG and in this way, it maintains the reduced pool of glutathione. GR is localized in the chloroplast stroma, but is also found in mitochondria, cytosol, and peroxisomes. Plants contain multiple forms of this enzyme, such as eight in pea (Edwards, Rawsthorne et al. 1990) and two in wheat (Dalal and Khanna-Chopra 2001). The role of glutathione and GR in H_2O_2 scavenging is very well-demonstrated in the Halliwell–Asada enzyme pathway (Bray, Bailey-Serres, and Weretilnyk, 2000). It catalyses the rate-limiting last step of the ascorbate–glutathione pathway. Lee et al have demonstrated that chilling stress causes a significant increase in foliar levels of the GR activity in cucumber (*Cucumis sativas* L.) (Lee and Lee 2000). Similarly, the GR activity increases significantly in *Triticum aestivum* during high temperature stress (Keles and Öncel 2002), in alfalfa nodule during water stress (Naya, Ladrera et al. 2007), and in cotton calli during salt and paraquat stress (Vital et al. 2008). Cadmium encourages an increase in the messenger RNA level of

genes involved in GSH synthesis (*gsh1* and *gsh2*) (Semane et al. 2007). The constitutive expression of the bacterial *gor* gene coding for enzyme glutathione reductase under the CAMV35S promoter increases GR activity (Foyer, Lelandais et al. 1991). The overexpression of *E. coli* chimeric GR in chloroplasts increases GR activity, but fails to provide chilling stress. Also, an increase in salt concentration shows a decrease in GR activity in roots of salt sensitive genotypes of wheat (BR5001) (Azevedo Neto et al. 2006). Reduction in the GR activity has been observed in salt-sensitive *Plantago media* compared to salt tolerant *Plantago maritime* (Sekmen, Turkan et al. 2007). The exogenous application of oxalic acid or salicylic acid in mango increases the GR activity under chilling temperature stress. Ding et al. investigated the role of GR in protecting photosynthesis against chilling stress and under high light condition (Ding, Lei et al. 2012, Ding, Jiang et al. 2016).

Dehydroascorbate reductase (DHAR): Dehydroascorbate reductase enzymes are involved in the enzymatic ROS defence system. The oxidation of AsA by APX forms the short-lived MDHA radical, that converts to AsA by MDHAR or disproportionates non-enzymatically to AsA and dehydroascorbate (DHA). DHA is recycled to AsA by DHAR, which requires GSH as the reductant (Chen, Young et al. 2003). Salt stress significantly induces DHAR activity (Mittova, Tal et al. 2003) and a higher AsA and AsA/DHA ratio in salt-tolerant cultivar, whereas the activity remains unchanged in a salt-sensitive tomato cultivar. DHAR activity decreases upon salt and heavy metal stress in mung bean (Hossain, Hasanuzzaman et al. 2010, Hasanuzzaman, Hossain et al. 2011). Nevertheless, an increase in DHAR activity has been observed in rice shoot tissues under mild drought stress, but the activity decreases under severe drought stress. Heat treatment alters DHAR activity in tobacco BY-2 cells. Furthermore, Locato et al. suggest that an increase in DHAR activity may be a feedback regulation mechanism that occurs to improve AsA regeneration from DHA when AsA depletion occurs at its production sites due to enhanced ROS (Locato, de Pinto et al. 2009). Wang et al. have shown that DHAR overexpression in *Arabidopsis thaliana* increased AsA and GSH levels, and thus, the redox state relative to wild type shows oxidative stress tolerance, induced by high light and high temperature (Wang, Xiao et al. 2010). Therefore, it is evident that AsA content via enhanced ascorbate recycling limits the deleterious effects of environmental oxidative stress.

1.4. Hydrogen peroxide sensing/signalling and cysteine oxidation

H_2O_2 reacts with low molecular weight thiol like reduced glutathione (GSH) and cysteine at the rate of 2.9 $M^{-1}s^{-1}$ and 0.87 $M^{-1}s^{-1}$, respectively, at pH 7.4. The reaction of thiols with H_2O_2 engages a nucleophilic attack of the thiolate on H_2O_2. The pK_a of thiol governs the formation of thiolate anion (S^-). If the pK_a of cysteine is higher than the pH of the solution, it is more likely to exist in its protonated form. On the contrary, if pK_a is lower than the pH, thiols attain a thiolate form (Roos and Messens 2011). The pK_a is defined as the negative logarithm of acid dissociation constant (K_a) of an acid conjugate base equilibrium, and it represents the balance between thiol and thiolate. At neutral pH, cysteines have pK_a of ~8.3, which means they are protonated and not reactive (Winterbourn and Hampton 2008). The sulfur atom in cysteine is large, polarizable, and electron-rich with empty 3D orbital, which makes it susceptible to adopt a multiple range of oxidation states (Lindahl, Mata-Cabana et al. 2011). The protein thiols, particularly with low pK_a, ionizes at physiological pH and are often referred to as reactive cysteines. H_2O_2 reacts with cysteine thiol and thiolate to form sulfenic (-SOH) acid which can be reduced to thiol (-SH) by enzymatic and non-enzymatic antioxidant pathways in the cell. Furthermore, high concentrations of oxidants lead to the formation of sulfinic (SO_2H) and sulfonic (SO_3H) acid derivatives (Figure 5).

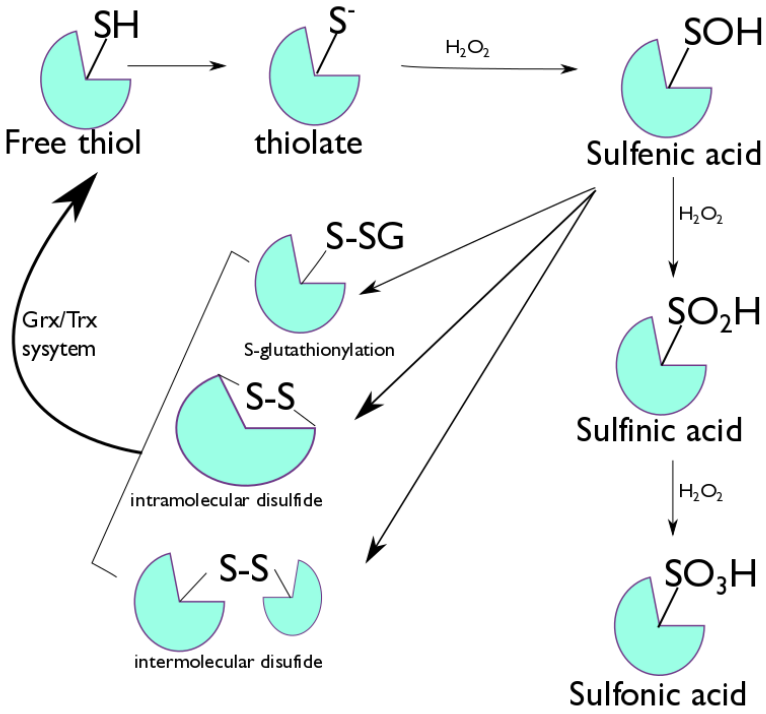

Figure 5: Cysteine oxidation by H_2O_2. In the presence of H_2O_2, cysteine thiolate form leads to reversible oxidation of cysteine residue, which is sulfenic acid. This transient oxo-form of cysteine can either form S-

glutathionylated and intramolecular or intermolecular disulfide which can further be reduced to free thiols by glutaredoxin and thioredoxin (Grx/Trx) systems. In excess of H_2O_2, sulfenic acid can oxidize to form sulfinic and sulfonic acid.

Various factors such as an alkaline environment, adjacent positively charged amino acids can decrease the pK_a of the cysteine, thus making it more reactive (Smith and MacQuarrie 1979, Kortemme and Creighton 1995). The solvent-exposed thiol (SH) group is more sensitive to oxidation and can ionize to form a nucleophilic thiolate anion (Lo Conte and Carroll 2013). Additionally, the presence of a cysteine at the N-terminal end of an α-helix (N_{cap}) effects cysteine reactivity. For instance, N_{cap} effects on cysteine reactivity have been reported for peroxiredoxin 1 (Prx1), which is a thiol peroxidase, and for the epidermal growth factor receptor (EGFR) kinase. The two active-site cysteines in DsbA, which is a bacterial disulfide oxidoreductase, have pKa values of 3.5 and 10. The reactivity of the thiol determines whether cysteine thiol can adopt different oxidation states and its ability to react with hydrogen peroxide to mediate redox regulation. A cysteine sulfur in its thiolate form is less stable and behaves as a nucleophile and is more reactive towards H_2O_2 (Winterbourn and Metodiewa 1999).

The notion of redox signalling by H_2O_2 has become more popular because of the proteins involved in signalling, such as phosphatases, kinases, and transcription factors. These signalling proteins contain cysteine residues, whose thiol groups can oxidize and change the biological activity of these proteins. According to this archetype, upon an increase in the concentration of H_2O_2, proteins oxidize which follows a cascade of molecular events. The reactivity of H_2O_2 with signalling proteins, like phosphatases Cdc25B and protein tyrosine phosphatase 1B (PTB1B), is much lower than the reactivity with peroxiredoxins (Prxs), glutathione peroxidases (GPx), and catalase. Although it is noteworthy that the cellular abundance of antioxidant enzymes like GPx, Prxs, and catalase is much larger than that of signalling proteins like phosphatases or transcription factors. Also, reaction of H_2O_2 with thiols deals with second-order rate constants, *i.e.,* the rate of the reaction is proportional to the concentrations of H_2O_2 and the thiol. Therefore, the consequent signalling molecules cannot compete with known protein antioxidant systems that remove H_2O_2. It has been concluded that the signalling protein, PTP1B, has a lower reactivity towards H_2O_2 (Denu and Tanner 1998). Also, PTP1B has been reported to be redox regulated by H_2O_2 (Mahadev, Zilbering et al. 2001, Meng, Fukada et al. 2002, Salmeen, Andersen et al. 2003).

1.5. Approaches to identify low-pK_a cysteine residues

Cysteine reactivity relies on protein microenvironment. Several approaches have been developed to identify low pK_a cysteine residues in proteins. One of them is the computational method which identifies reactive cysteines in the proteome based on the conservation of cysteine residues involved catalysis (Fomenko, Xing et al. 2007). Another is the chemical approach that employs chemical reagents such as N- ethylmaleimide (NEM) or iodoacetamide (IAM), which form covalent adducts with sulfhydryl groups by Michael addition or nucleophilic substitution respectively. Thiols predominantly reacts with IAM as the unprotonated thiolate anion and this reagent is most often used to detect low pK_a cysteines which form reactive thiol proteome (Shaked, Szajewski et al. 1980, Ying, Clavreul et al. 2007). NEM reacts with thiols faster than IAM and is less dependent on pH (Shaked, Szajewski et al. 1980). Nevertheless, IAM is more specific for thiols than NEM, which can modify the side chain amines like histidine and lysine if used in excess or at basic pH. NEM and IAM can be conjugated to biotin or fluorophores to enable enrichment of labeled proteins and are followed by one or two-dimensional gel electrophoresis with consequent identification by liquid chromatography tandem mass spectrometry (LC-MS/MS). N-(biotinoyl)-N′-(iodoacetyl) ethylenediamine, commonly indicated as biotinylated iodoacetamide (BIAM), identifies surface-exposed reactive cysteine residues in *Saccharomyces cerevisiae* (Marino, Li et al. 2010). Also, BIAM and 5-iodoacetamido fluorescein at low micromolar concentrations and at mildly acidic pH identifies reactive thiols (Kim, Yoon et al. 2000). Recently Chen et al have reported a heteroaromatic alkylsulfone, 4-(5- Methanesulfonyl-[1,2,3,4]tetrazol-1-yl)-phenol (MSTP), as a selective and highly reactive thiol blocking reagent compatible with biological applications (Chen, Wu et al. 2017).

The cysteine oxidation products, such as sulfenic acid, disulfide, and S- glutathionylation are reversible and therefore, they can rheostat protein function during cell signaling. Moreover, cysteine sulfinic acids have emerged to be involved in potential regulatory mechanism, because of the identification of sulfiredoxin (Srx) proteins (Lei, Townsend et al. 2008), which can revert the sulfinic acid to its sulfenic form. Several methods have been developed to study changes in protein cysteine oxidative post translational modification (oxPTM). Most methods detect cysteine oxidation, which rely upon the loss of reactivity with thiol-modifying reagents or restoration of labeling by reducing agents such as dithiothreitol (DTT).

Chemical biology approaches have facilitated the development of small molecule and protein-

based methods for direct detection of distinct oxidative cysteine modifications. It is notable to consider the rate at which these chemical probes react with the modified cysteine residue. If the reaction rate is low, it is more likely that transient cysteine oxidation events will be missed. On the contrary, if the reaction is too fast, it could fade the chemical selectivity of the probe or interrupt the biological process. Thus, reactive probes should have a minimal biological impact. Increasing the concentration of probe can counterbalance for modest rates of reaction and along with that, proper controls must be performed to ensure that the underlying biology is not disturbed.

The common chemical used to detect ROS sensitive cysteines is BIAM alkylating reagent attached with acid cleavable isotope-coded affinity tag (ICAT) which allows both identification and quantification of oxidant-sensitive cysteine thiols by analyzing the ratio of light (^{12}C) and heavy (^{13}C) ICAT label by LC-MS/MS (Sethuraman, McComb et al. 2004). Apart from BIAM, alternative biotinylated or fluorophore-modified alkylating reagents can be used to alkylate thiols and are used to monitor protein oxidation in response to exogenous oxidants such as H_2O_2 or diamide or to ROS- promoting stimuli such as peptide growth factors (Le Moan, Clement et al. 2006, Marino, Li et al. 2010).

1.6 Cysteine oxidative post translational modifications and detection

Cysteine is one of the most functionally diverse amino acids among twenty amino acids. The sulfhydryl (-SH) group of a cysteine has a negatively charged thiolate group, which is ionised and formed after deprotonation that enhances its reactivity (Figure 6). Furthermore, the thiolate group of a cysteine is prone to oxidation by reactive oxygen species and alkylation by electrophiles that lead to posttranslational modifications (PTMs), an important biological event related to the protein's function. One of the reversible redox-based PTMs is the oxidation of a cysteine thiol group to a sulfenic acid (Cys-SOH) that acts as regulatory switch in oxidative stress signal transduction pathways (Ma, Takanishi et al. 2007, Roos and Messens 2011).

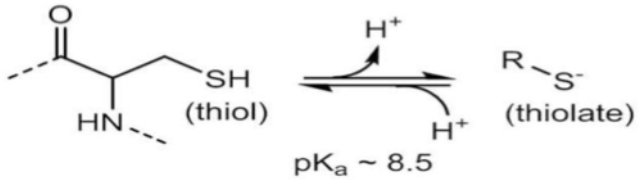

Figure 6: Structures of cysteinyl residues within proteins. The dotted line represents peptide bonds to the next residue on either side of the aminoacyl groups. Both protonated (left) and deprotonated (right) forms of the amino acid are depicted with average pK_a value (that can vary depending on protein microenvironments).

Thiol peroxidases exhibit an H_2O_2-dependent signalling function and can function as receptor and transducer (Fomenko, Koc et al. 2011). In *Saccharomyces cerevisiae*, the H_2O_2 sensor oxidant receptor peroxidase1 (ORP1/glutathione peroxidase 3) together with the transcription factor YAP1 (yeast AP-1–like) mediates a redox regulation through a sulfenic acid thiol-disulfide relay mechanism (Delaunay, Pflieger et al. 2002). In this process, the peroxidatic cysteine of ORP1 oxidizes upon reaction with H_2O_2 and forms sulfenic acid that reacts with the YAP1 C-terminal cysteine-rich domain (cCRD) and forms a disulfide. Takanishi et.al adapted a redox-regulated domain from the YAP1 transcription factor to trap proteins that form cysteine sulfenic acid (Cys-SOH) *in vivo*. They showed that the formation of these protein complexes is time-dependent and peroxide concentration-dependent. They identified six proteins in *Escherichia coli* that contain redox-active cysteine residues known to form Cys-SOH as part of their catalytic cycle (Takanishi, Ma et al. 2007). Waszczak et al also exploited mixed disulfide formation and designed YAP1-based probe for trapping plant sulfenylated proteins *in vivo* (Waszczak, Akter et al. 2014). With this, they identified and functionally characterized 97 sulfenylated proteins during the early and late oxidative stress responses. These proteins involved in signal perception and transduction, protein degradation, primary metabolism, redox-related proteins, and protein transport.

Four redox-related proteins, Monothiol Glutaredoxin17 (GRXS17), Thioredoxin-dependent peroxidase1 (TPX1), Glutaredoxin c2 (GRXC2), and dehydroascorbate reductase (DHAR2) have been detected with YAP 1 based probe. TPX1 functions as a target of *Arabidopsis* cytosolic thioredoxin h3 (Trxh3) (Marchand, Le Marechal et al. 2006). GRXC2 and GRXS17 function in early plant development during embryonic and temperature-dependent postembryonic growth (Cheng, Liu et al. 2011, Roos and Messens 2011, Riondet, Desouris et al. 2012). DHAR2 has found to be sulfenylated in both the early and late oxidative stress responses. DHAR functions in counterbalancing oxidative stress by catalysing the regeneration of ascorbate, a major antioxidant in plants. The perturbation of DHAR has been shown to limit ascorbate recycling and influence the rate of plant growth and leaf aging due to ROS-mediated damage (Chen and Gallie 2006). Waszczak et al. validated sulfenylation on DHAR2 and demonstrated glutathione (GSH)-dependent redox switch on its sulfenylated nucleophilic cysteine that reversibly regulates the DHAR activity. We have further investigated the enzyme catalysis mechanism of DHAR2 and more detailed study on DHAR2 are presented in chapter 2 of this thesis.

In the signal perception and transduction category, three mitogen activated protein kinases (MAPKs) have been found to be sulfenylated namely MPK2, MPK4, and MPK7. MAP kinases are redox regulated through upstream regulators and direct cysteine oxidation events in yeast and humans (Truong and Carroll 2013). In human, p38 MPK acts as a functional regulatory switch via cysteine oxidation (Templeton, Aye et al. 2010), whereas in plant MAP kinase modules, no such thiol modification has been reported yet. This result has prompted us to investigate the function of MPK4 as a redox sensor. The more detailed study on MPK4 will be discussed in chapter 3.

To identify the cysteine oxidative modification, chemical probes have been developed. A condensation reaction between the electrophilic sulfenic acid and the nucleophile dimedone (5,5-dimethyl-1,3-cyclohexanedione) that produces thioether derivative has been reported, and this chemistry has been exploited to detect dimedone-modified sulfenic acids using mass spectrometry (Benitez and Allison 1974, Carballal, Radi et al. 2003). DYn-2 is a sulfenic acid specific chemical probe that constitutes two functional units, a dimedone scaffold for sulfenic acid recognition and an alkyne chemical handle for enrichment of labelled proteins (Leonard and Carroll 2011). With click reaction that involves copper (I)-catalysed azide-alkyne cycloaddition reaction forms alkyne functionalized DYn-2 and the azide functionalized biotin complex (Wang, Hong et al. 2011). The DYn-2 chemical probe has been introduced in a human epidermoid carcinoma A431 cell line to investigate the epidermal growth factor (EGF) mediated protein sulfenylation and identification of intracellular protein targets of H_2O_2 during cell signalling. Further, DYn-2 probe has also been applied to plant cells to identify the sulfenome under oxidative stress. Akter et al. identified 226 sulfenylated proteins in response to an H_2O_2 treatment of *Arabidopsis* cell suspensions, of which 123 proteins are new candidates for cysteine oxidative post-translational modification events (Akter, Huang et al. 2015).

Apart from YAP1 based probe and DYn-2 probes which are utilised for sulfenic acid detection, several other cysteine post-translational modifications (PTMs) have been reported such a disulfide bond formation, glutathionylation, sulfinic, and sulfonic acid modifications. The identification and detection of these PTMs are discussed in more detail in the following section.

1.6.1 Disulfides: Disulfide bond formation plays an important role in protein folding and stability. This post translational modification occurs largely in the extracellular space or the endoplasmic reticulum (ER). Here, protein disulfide isomerases (PDI) create disulfide bonds

in nascent proteins that are destined for export to the extracellular environment (Nakamura, Yamamoto et al. 2008). Although disulfide bonds can be formed in the cytoplasm, mitochondria, or nucleus, where thiol-dependent reductases maintain a reducing environment, it is rare. Under oxidative stress conditions, the intracellular redox balance can shift to encourage disulfide bond formation in reducing compartments till redox homeostasis is being re-established.

Thiol condensation with a sulfenic acid drives the formation of a disulfide bond. This reaction can either be intramolecular or intermolecular, and the rate of disulfide bond formation depends on the distance between the two cysteine residues. The rate constants for intra- and inter-molecular disulfide bond formation have been estimated to be 10 s^{-1} and 10^5 $M^{-1}s^{-1}$, respectively (Nagy and Ashby 2007). Disulfides can be cleaved by other thiols via a thiol-disulfide exchange reaction. The thiol in a disulfide with a lower pK_a is a better leaving group and determines which cysteine will be released in a thiol-disulfide exchange reaction. This has been shown in the case of PDI (Gahl and Scheraga 2009). Disulfides can also be oxidized to generate a thiosulfinate, which can subsequently react with a thiol to give disulfide and sulfenic acid products. Further disulfide oxidation produces thiosulfonate, which releases a disulfide and sulfinic acid after reaction with a thiol.

To detect protein disulfide formation, mostly reducing and non-reducing SDS-PAGE gel electrophoresis are employed. Intermolecular disulfides are detected as reducing agent-sensitive protein complexes that migrate at a molecular mass equal to the that of the two oxidized proteins, which have been shown for PKG1α (Burgoyne, Madhani et al. 2007), Src (Kemble and Sun 2009) and ATM (Guo, Deshpande et al. 2010) dimers. Intramolecular disulfide bond formation can also lead to altered migration on gels, which has been observed for *S. cerevisiae* thiol peroxidase Gpx3 (Delaunay, Pflieger et al. 2002, Paulsen and Carroll 2009). Differential alkylation approaches can also be used to identify disulfide bond formation where thiols are alkylated prior to sample separation on a non-reducing SDS-PAGE gel, and the protein band corresponding to the oxidized proteins of interest can then be reduced in-gel with DTT or TCEP. Further, proteins can be digested in-gel, and the differentially alkylated cysteine residues are identified by LC-MS/MS analysis (Klamt, Zdanov et al. 2009, Guo, Deshpande et al. 2010).

The differential migration of disulfide containing proteins by non-reducing and reducing gel electrophoresis have been directed to acquire a high-throughput method to identify oxidant

induced disulfide-bonded protein complexes. The diagonal SDS-PAGE (Sommer and Traut 1974) or redox 2D-PAGE (Cumming 2008) uses sequential non-reducing/reducing two-dimensional SDS-PAGE. Further, LC-MS/MS analysis can identify and determine proteins. The limitation of this method is that it cannot reliably visualize or generate analytical quantities of low abundant proteins that are present in <1000 copies per cell (Leonard and Carroll 2011). Nevertheless, this method has been used to detect disulfide-linked proteins in cell lysates derived from oxidant-treated rodent nerve cell cultures (Cumming, Andon et al. 2004) and cardiac myocytes (Brennan, Wait et al. 2004). This method has also been applied in plants (Winger, Taylor et al. 2007).

With a redox SDS-PAGE approach, it is not possible to attain quantitative information of the fraction of cysteine oxidized under a given condition. To allow identification and quantification of reversibly oxidized protein cysteine residues involving disulfides bonds, an extension of the ICAT technology, known as OxICAT has been reported (Leichert, Gehrke et al. 2008). In this approach, lysates are first generated in the presence of TCA to precipitate proteins and inhibit thiol/disulfide exchange. Thereafter, free thiols are alkylated with a light (^{12}C) ICAT reagent and then followed by reduction of with TCEP, which serves to reduce reversible modifications. Subsequently, nascent thiols are labelled with a heavy (^{13}C) ICAT reagent and protein samples are digested and ICAT- modified peptides are isolated by avidin affinity chromatography. Then the eluted peptides are analysed by LC-MS/MS, and the fraction of oxidation for a particular cysteine is determined by the ratio of the heavy to light MS signals. The OxICAT method appears to be the best suited method for disulfide detection for both protein and low molecular weight thiols, for instance mixed-disulfides formed by S-glutathionylation.

Proteins, which undergo disulfide bond formation, involve in the regulation of redox homeostasis, chaperone activity, metabolism, transcriptional regulation, and protein translation (Le Moan, Clement et al. 2006, Leichert, Gehrke et al. 2008). Disulfide bonds alter enzyme activity, subcellular localization, and protein-protein interactions (Paulsen and Carroll 2010). For instance, the activity of certain protein tyrosine phosphatases were inhibited by disulfide bond formation (Sohn and Rudolph 2003, Michalek, Nelson et al. 2007). The involvement of disulfide bond in regulatory mechanism has been observed in certain members of the caspase family of cysteine proteases (Choi, Ryu et al. 2010). Also, various studies have demonstrated an increase in protein phosphorylation in response to receptor activation that depends upon endogenous H_2O_2 production (Dickinson, Peltier et al. 2011, Paulsen, Truong et al. 2011,

Prosser, Ward et al. 2011). Protein tyrosine phosphatases have been anticipated as the major cellular targets of H_2O_2-derived signalling (Ostman, Hellberg et al. 2006).

Kinases are now also supposed to be redox-regulated, but in most of the cases, exact molecular details are not well characterized. Nevertheless, it has been demonstrated that serine/threonine kinases (Kemble and Sun 2009) and ATM kinase (Guo, Deshpande et al. 2010) are activated by intermolecular disulfide formation between homodimers. On the contrary, intermolecular disulfide formation between Src tyrosine kinase monomer inhibits kinase activity (Kemble and Sun 2009). Although Src has been revealed to be activated by H_2O_2 (Giannoni, Buricchi et al. 2005), the oxidative inhibition of Src involves Cys277, which is not conserved in all Src family kinases (Kemble and Sun 2009). The Src-family kinase Lyn, which has glutamine at the site corresponding to Cys277, activates ROS in neutrophils suggesting that oxidative activation of Src-family kinase involves a different cysteine residue (Yoo, Starnes et al. 2011). Other proteins whose activity has been exposed to be regulated by disulfide bond formation comprise the bacterial chaperone Hsp33 (Winter, Ilbert et al. 2008), the nonspecific cation channel TRPA1 (Takahashi, Kuwaki et al. 2011), and the glycolytic enzyme pyruvate kinase M2 (PKM2) (Anastasiou, Poulogiannis et al. 2011).

Disulfide bond formation can affect the subcellular localization of a protein. For instance, intramolecular disulfide formation in the *Saccharomyces cerevisiae* transcription factor YAP1 induces a conformational change that masks the nuclear export signal (NES) and prohibits interaction with the nuclear export receptor, Crm1. This further results in nuclear accumulation of YAP1, which activates transcription of genes involved in the oxidative stress response (Wood, Storz et al. 2004). The intramolecular disulfide between DnaJb5, which is chaperone, and HDAC4, a class II histone deacetylase, results in the dissociation of the DnaJb5-HDAC4 complex that removes the mask of the HDCA4 NES and mediates its cytoplasmic localization and derepression of target genes involved in hypertrophy (Ago, Liu et al. 2008, Paulsen and Carroll 2010). The oxidative stress induced formation of two intramolecular disulfides in cofilin, an actin regulatory protein, leads to the dissociation of the actin cofilin complex. Additionally, cofilin oxidation assists in its mitochondrial accumulation where it interacts with the mPTP to foster mitochondrial swelling, cytochrome c release, and eventually induction of apoptosis (Klamt, Zdanov et al. 2009).

1.6.2 S-Glutathionylation: Glutathione (GSH), which is a thiol-containing tripeptide, present in millimolar concentrations in cells. Approximately, 98% of GSH exists in its reduced state under normal conditions but under oxidative stress, an pliable amount of the GSH pool exists in its oxidized state GSSG (Townsend, Tew et al. 2003). Protein S-glutathionylation occurs during disulfide reduction by the glutathione/glutaredoxin/glutathione reductase (GSH/Grx/GR) system, which is reversible. Protein S-glutathionylation acts as a regulatory mechanism where, in oxidizing state, the GSH/GSSG redox balance shifts to a more oxidizing state and thus it protects against irreversible oxidation. The GSH/Grx/GR system maintains protein thiols in their reduced state via redox reactions and thiol-disulfide exchange reactions. Also, GSH undergoes nucleophilic addition and displacement reactions to purge the cell of toxic electrophilic and oxidizing reagents as catalysed by glutathione-S-transferase, glyoxalase, glutaredoxin, and Glutathione reductase (Rudolph and Freeman 2009).

Protein S-glutathionylation occurs via two possible mechanisms which involves (a) thiol-disulfide exchange of GSSG with a thiolate or (b) condensation of GSH with a sulfenic acid. S-glutathionylation has been estimated to occur with a rate constant of 2-100 $M^{-1}s^{-1}$. The thiol-disulfide exchange between GSSG and a protein thiolate is very slow and Grx catalyses this reaction that promotes S-glutathionylation of the electron transport chain (ETC) complex I (Starke, Chock et al. 2003, Beer, Taylor et al. 2004). Beer et al. reported Grx-mediated S-glutathionylation (Beer, Taylor et al. 2004). The specificity of S-glutathionylation depends on the steric properties, oxidation sensitivity of the cysteine, and surrounding environment. The members of the Grx family, Srx, Trx, and PDI perform deglutathionylation albeit with decreased efficiency (Park, Mieyal et al. 2009).

The protein S-glutathionylation activates enzymes such as collagenase (Macartney and Tschesche 1983), trypsin (Steven, Griffin et al. 1981), and fructose-1, 6- bisphosphatase whereas glyceraldehyde 3-phosphate dehydrogenase (GAPDH) (Eaton, Wright et al. 2002), 26S proteasome (Hurd, Requejo et al. 2008), cysteine protease caspase-1, and ETC complex I (Meissner, Molawi et al. 2008) are inactivated by this post translational modification. In case of PTP1B, the phosphatase undergoes S-glutathionylation to protect against hyperoxidation (Barrett, DeGnore et al. 1999). Apart from the regulation of enzyme activity, S-glutathionylation also influences protein-DNA and protein-protein interactions. For instance, S-glutathionylation of cysteines in the DNA binding domain of transcriptional regulator, p53

lessens its association with DNA (Velu, Niture et al. 2007). Similarly, S-glutathionylation of the transcriptional regulator, interferon regulatory factor 3 (IRF3) hinders its interaction with CBP/p300 coactivators and inhibits activation of target genes involved in the induction of an antiviral response (Prinarakis, Chantzoura et al. 2008).

To detect protein S-glutathionylation, several immunological, metabolic labelling and differential alkylation approaches have been developed. A usual method to detect S-glutathionylation in proteins employs an antibody specific for the protein-S-GSH adduct. This antibody is pliable to immunoprecipitation, Western blot on non-reducing gels, and immunofluorescence analysis. The anti-GSH antibody has also been used in combination with 2D SDS- PAGE. In HeLa cells, samples separated by isoelectric focusing in the first dimension and by molecular weight in the second dimension and with MALDI-TOF MS identifies S-glutathionylated proteins. Also, antibodies specific for protein-S-GSH adducts have been used to identify S-glutathionylation. The differences in the surrounding environment of the modified cysteine is a limitation of the antibody because not all protein-S-GSH adducts are detected with the same affinity. Another immunological approach employs the specificity and affinity of GST for GSH. In this method, Western blots from non-reducing SDS-PAGE gels are exposed to biotinylated-GST, which recognizes and binds selectively to protein-S-GSH disulfides and subsequently avidin blot detects biotin-GST. Protein S-glutathionylation can also be monitored by differential alkylation where free thiols are alkylated and protein-S-GSH adducts are selectively reduced by Grx, and nascent thiols are tagged by a biotinylated or fluorescent alkylating reagent. In principle, this approach could also be coupled to the OxICAT method to measure the extent of protein-S-GSH disulfides.

Approaches have been developed to enable the detection of S-glutathionylated proteins in cells. One such method includes inhibiting protein synthesis with cycloheximide, which does not affect GSH synthesis and subsequent metabolic labelling of the GSH pool with ^{35}S-cysteine incorporation. Cells are subsequently lysed in the presence of a thiol alkylating agent to minimize thiol-disulfide exchange, and samples are separated under non-reducing conditions and analysed by radiography. This technique identifies proteins, such as enolase and 6-phosphogluconolactonase, that endure S-glutathionylation in human T lymphocytes exposed to exogenous oxidants such as H_2O_2 and diamide. Alternatively, biotinylated-GSH ethyl ester (BioGEE) and N, N-biotinyl glutathione disulfide have been used to monitor protein S-

glutathionylation in lysates, isolated cells, and tissues (Brennan, Miller et al. 2006). Although biotin tag assists enrichment and identification of proteins that undergo S-glutathionylation, the limitations of these methods include steric occlusion of biotinylated GSH analogues and poor cellular trafficking of biotinylated probes.

1.6.3 Sulfenic Acids: Sulfenic acids are unstable intermediates of sulfur oxidation. The foremost oxidation state of the sulfur atom in a sulfenic acid is 0 that makes it a weak nucleophile and a soft electrophile. By condensation reaction, two sulfenic acids generate thiosulfinate. The occurrence of thiosulfinates in cells has yet to be reported. However, given the abundance of cellular thiols, interfacing of two sulfenic acids is a rare phenomenon. This thesis focusses on the study of sulfenic acid forming proteins of *Arabidopsis thaliana*. Sulfenic acid modification represents the initial product of two-electron oxidants with the thiolate anion and therefore serve as a marker for oxidant-sensitive cysteine residues.

The first pK_a measurement for the sulfenyl group of a protein sulfenic acid reported in a mutant form of 2-Cys Prx from *Salmonella typhimurium*, AhpC where the resolving cysteine mutated to serine. In this study, the sulfenic acid and sulfenate forms display discrete spectral shifts in AhpC that allowed a pK_a determination of 6.1. There are three classes of Prxs namely typical 2-Cys, atypical 2-Cys, and 1-Cys Prxs. Typical and atypical 2-Cys Prxs form sulfenic acid at their active site cysteine after reaction with H_2O_2 which condenses with a second cysteine in the same (atypical) or neighbouring (typical) Prx to generate a disulfide followed by thioredoxin/thioredoxin reductase (Trx/TrxR) reduction system. 1-Cys Prxs do not have a resolving cysteine and thus the sulfenic acid intermediate gets reduced by GSH or ascorbate. The pK_a for the sulfenic acid in a 1-Cys Prx from *Mycobacterium tuberculosis* has been reported to be 6.6 by a tryptophan fluorescence study. The susceptibility for sulfenic acid to undergo further oxidation to sulfinic acid is influenced by the local protein environment, just like cysteine thiolate reactivity with H_2O_2. The 2-Cys Prxs from eukaryotes incline to be sensitive to hyperoxidation. For instance, oxidation of bacterial peroxiredoxin AhpE sulfenic acid by H_2O_2 occurs at 40 $M^{-1}s^{-1}$.

Sulfenic acids have been involved in the catalytic cycle of multiple enzymes such as Prx, NADH peroxidase, and methionine sulfoxide and formylglycine-generating enzymes. Also, it has been related to oxidative stress-induced transcriptional changes in bacteria due to altered

DNA binding of OxyR and OhrR and changes in the activity of the yeast Prx and YAP1 protein. The sulfenic acid-mediated regulation has been reported in mammalian protein function and signalling pathways where cysteines from several transcription factors (i.e., NF-κB, Fos, and Jun) or proteins involved in cell signalling or metabolism (e.g., GAPDH, GR, PTPs, kinases, and proteases) can be converted to sulfenic acid *in vitro*. Sulfenic acid formation has been studied in the regulation of apoptosis, immune cell activation and proliferation, and growth factor (GF) signalling pathways.

The cysteine sulfenic acid formation has not only been observed in oxidoreductases, but also significantly in transferases and hydrolases and to a lesser extent in other functional classes. Waszczak et al. and Akter et al. have identified cysteine sulfenic acid proteins involved in redox regulation, signal perception and transduction, primary metabolism, protein transport, protein degradation, and several unknown proteins (Waszczak, Akter et al. 2014, Akter, Huang et al. 2015).

Various chemical methods have been established to detect protein sulfenic acid modifications (also termed sulfenylation). An indirect approach involves thiol alkylation, reduction of sulfenic acids by arsenite and labelling of nascent thiols with biotinylated NEM. In rat kidney cell extracts, formation of sulfenic acid has been profiled. The method of sulfenic acid detection involves nucleophilic substitution of halonitroarenes, such as 4-chloro-7-nitrobenzo-2-oxa-1,3-diazole (NBD-Cl), and nucleophilic addition to electron-deficient alkynes, alkenes, and triphenyl phosphines. Among these, the common method for sulfenic acid detection is NBD-Cl. This chemical reagent reacts with thiols, sulfenic acids, and at higher pHs, with amine-containing residues; therefore, a variety of protein functional groups seems best suited for use with recombinant proteins more precisely with a single cysteine residue.

Benitez and Allison et al reported that protein sulfenic acids react with cyclic 1,3-diketone carbon nucleophiles, like 5,5-dimethyl-1,3-cyclohexadione (dimedone) and with hydrazines or amines (Benitez and Allison 1974). Dimedone has been used to detect protein sulfenic acid modifications in the *Saccharomyces cerevisiae* YAP1-Gpx3 H_2O_2 sensing pathway (Paulsen and Carroll 2009), T cell activation, and EGFR signalling (Paulsen, Truong et al. 2011).The chemo-selective method for detecting protein sulfenic acids reported till date depend upon this chemistry. The lack of an enrichment or visualisation for protein-S-dimedone adducts further motivated the development of biotinylated (Poole, Klomsiri et al. 2007) and fluorophore-

conjugated analogues. These probes have been used in isolated rat hearts and AKT2 has been identified as a target of PDGF-induced H_2O_2 (Wani, Qian et al. 2011) in a proteomic study. The demerit of direct conjugation of any probe to biotin or a fluorophore is its bulky chemical tags that reduce cell permeability (Prinarakis, Chantzoura et al. 2008). Although DCP-Biol is not entirely impermeant, however, comparative studies suggest time and again that tagged derivatives suffer from diminished cell uptake and trafficking properties. Alternative mechanisms of uptake are possible, such as active transport of BioGEE, but may limit probe distribution to specific cellular compartments.

An alternative approach that has emerged is the development of azido-and alkyne-functionalized dimedone analogue such as DAz-1, DAz-2, DYn-1, and DYn-2, which allow trapping and tagging of protein sulfenic acid modifications directly in living cells. Proteins are covalently modified by DAz or DYn probes coupled to biotin or fluorophores by Staudinger ligation or Huisgen cycloaddition reactions (Gupta and Carroll 2014). DAz-2 identified proteins that undergo sulfenic acid modifications in HeLa cells, which include a majority of known sulfenic acid modified proteins. Azido dimedone analogues trapped sulfenic acid modification of the thiol peroxidase Gpx3, which is essential for yeast to sense oxidative stress, and identified a unique reducing system in the bacterial periplasm that protects single cysteine residues from oxidation (Paulsen and Carroll 2009).

DYn-2 has been reported to be involved in trapping dynamic protein sulfenylation during EGF signalling in human epidermoid A431 cells and identified the EGFR kinase as a prominent target of sulfenic acid forming protein under endogenous H_2O_2. Also, three PTPs involved in the regulation of EGFR signalling PTP1B, PTEN, and SHP2 have shown to undergo sulfenic acid modification in response to EGF stimulation of cells. It is notable that PTPs and EGFR displayed differential sensitivity to oxidation by EGF-induced endogenous H_2O_2. In 2015, our lab had identified sulfenic acid forming proteins in *Arabidopsis thaliana* cell suspension cultures with DYn-2 approach (Akter, Huang et al. 2015). Kate et al reported the method to detect protein sulfenic acid modifications where antibodies elicited by a synthetic hapten mimicking dimedone modified cysteine conjugated to KLH are highly specific and sensitive for detecting protein-S-dimedone adducts by Western blot and immunofluorescence. This method demonstrated the cysteine sulfenylation and co-localization of oxidized proteins with NOX2 during EGF signalling.

To capture sulfenic acid form in a protein for X-ray analysis was difficult until cryo conditions were used (PDB ID 1JOA) (Yeh, Claiborne et al. 1996). The crystallographic proof for a sulfenic acid in the oxidized form of enterococcal NADH peroxidase, a cysteine-based peroxidase with a highly stabilized sulfenic acid formed at the active site proximal to the flavin (Poole and Claiborne 1989) produced high quality crystallographic information regarding the hyperoxidized, sulfonic acid form (Stehle, Claiborne et al. 1993). The crystallized proteins are highly resistant to air oxidation and synchrotron radiation, which generates highly reactive hydroxyl radicals that promote non-physiological cysteine oxidation (Xu and Chance 2005). A human PrxVI, a cysteine-based peroxidase belonging to the peroxiredoxin family, has been deposited to protein data bank (PDB) in its sulfenic acid form (PDB ID 1PRX) (Choi, Kang et al. 1998). There are about 400 protein structures in the PDB, which includes an annotated S-hydroxy or S-oxycysteine proteins.

NMR using proteins labelled with ^{13}C cysteine has been used to monitor changes in cysteine protonation state, which enables NMR-based pK_a analyses or redox state in proteins exhibiting high quality NMR spectra (Jeng, Holmgren et al. 1995, Wilson, Barbar et al. 1995). The studies with the sulfenic acid form of the NADH peroxidase provided the first NMR-based analysis of this redox form of a protein (Crane, Vervoort et al. 1997). With the chemical shift, predictions built by the C-13 NMR Module of ChemIntosh (SoftShell International), the Cys42 sulfenic acid was found to correspond to a chemical shift of 41.3 ppm; the predicted value is 39.6 ppm, which is higher than the 30.8 ppm observed for the reduced thiolate form of the enzyme, which is predicted to be 28.5 ppm. Furthermore, oxidatively-inactivated NADH peroxidase, reflecting sulfinic and/or sulfonic acid formation at Cys42 (Poole and Claiborne 1989) provided a ^{13}C chemical shift of 57.0 ppm because the expected chemical shifts of Cys sulfinic and sulfonic acids are very similar (predicted values of 58.8 and 56.0 ppm, respectively). This 57 ppm species could not be assigned to either oxidation state. It is considerable that the secondary structure and overall protein microenvironment exerts additional influence on the actual chemical shifts observed in a given protein (Wishart and Sykes 1994). NMR and crystallographic evidence have indicated the bond lengths between the O and S of stabilized sulfenic acids and supported the predominance of the sulfenic acid form (Crane, Vervoort et al. 1997).

1.6.4 Sulfinic Acids: Sulfenic acid can be oxidized to sulfinic acid in the presence of excess oxidant. The oxidation number of the sulfur atom in sulfinic acid is +2, which enhances

electrophilicity of sulfinic acid as compared to sulfenic acid. The sulfinic acid does not undergo self-condensation or nucleophilic attack by thiols because of the increase in partial positive charge on the sulfur in sulfinic acid, which converts the sulfur atom into a harder electrophile and makes it less prone to reaction with soft nucleophiles. At physiological pH, sulfinic acid has *pKa* of 2. Cysteine sulfinylation modifies protein and its metal binding properties. In matrix metalloproteases (MMPs), sulfinic acid oxidation of a zinc-coordinated active site cysteine thiolate activates protease function by reducing the ability to coordinate with the zinc cation. Cysteine oxidation is essential for hydratase activity.

Till date, the cysteine sulfinic acid modification has been mostly studied in Prxs and the Parkinson's disease protein, DJ-1. Eukaryotic Prxs seems to be most liable to sulfinic acid modification, a feature that evolutionarily coincides with sulfiredoxin expression, which is the single known sulfinic acid reductase. Sulfiredoxin has been identified in cyanobacteria, which appears to have 2-Cys peroxiredoxins that are prone to hyperoxidation.

The identification of protein sulfinic acids modifications involves the increase of 32 Da molecular mass in acidic electrophoretic gel shifts and antibodies that recognize a sulfinic acid peptide from a specific protein. Kate et al. investigated the reaction of sulfinic acids with aryl-nitroso compounds. The initial sulfinic acid-derived N-sulfonyl hydroxylamine product is reversible and can be trapped by ester-functionalized aryl-nitroso 34 to give an irreversible N-sulfonylbenzisoxazolone adduct. The reaction of ester-functionalized aryl-nitroso 34 with a thiol gives a sulfenamide species, which can be cleaved with nucleophiles. It is notable that ester-functionalized aryl-nitroso 34 does not cross react with other sulfur and non-sulfur containing biological functional groups.

1.6.5 Sulfonic Acids: The sulfinic acid modification is quite stable but still it can undergo further oxidization to form sulfonic acid. The sulfur atom in sulfonic acid has a formal oxidation number of +4, thus sulfonic acid functions as a hard electrophile. It does not undergo self-condensation or nucleophilic attack by thiols. The sulfonic acid modification has been characterized in a small group of proteins such as in mammalian Cu, Zn-SOD. Chang et al developed a probe that permits selective enrichment of sulfonic acid-modified peptides using poly arginine (PA)-coated nano-diamonds as high affinity probes (Chang, Huang et al. 2010). In this study, BSA has been used as a model system. Here, they oxidized BSA with performic acid and digested, further sulfonic acid-containing peptides were enriched and eluted from PA-

coated nano-diamonds with phosphoric acid and peptides were identified by MALDI-MS analysis.

1.7 Crosstalk between ROS and MAP kinase module during stress signalling

The crosstalk between redox metabolites and MAP kinases in plant signalling systems enables the adaptation and survival of plants under diverse environmental stresses. MAP kinases were reported to regulate gene expression by controlling transcription factor activity and other cellular and physiological responses to facilitate resistance to stresses (Figure. 7).

Reactive oxygen species (ROS) act as redox metabolites and are common by-products of aerobic metabolisms and are induced by various abiotic stresses such as extreme temperatures, genotoxic irradiation, draught and under pathogen attacks (O'Brien, Daudi et al. 2012, Suzuki, Koussevitzky et al. 2012). ROS produced by oxygen metabolism are rapidly quenched by antioxidant enzymes like superoxide dismutase and catalase, which prevents the accumulation of toxic levels H_2O_2 (Gill and Tuteja 2010). The detoxification of H_2O_2 by several non-enzymatic and enzymatic systems have been extensively discussed in the preceded section. However, prior to the removal of ROS, these involve in cell signalling and homeostasis, which are linked with MAP kinase signalling. Mostly high levels of ROS cause the activation of MAP kinase 3 (MPK3), MAP kinase 6 (MPK6) (Lumbreras, Vilela et al. 2010) and MAP kinase 4 (MPK4). The activation of MPK4 is well-established in the MEKK1-MKK1/2 pathway (Pitzschke, Djamei et al. 2009). H_2O_2 induces MPK3/MPK6 activation and it has been demonstrated that the OXIDATIVE SIGNAL-INDUCIBLE1(OXI 1) gene also gets activated by H_2O_2 in *Arabidopsis thaliana*. The OXI 1 gene encodes serine threonine kinase and is involved in normal root hair growth under stress conditions. It has been shown that the OXI1 mutant failed to activate MPK3 and MPK6 activation upon H_2O_2 treatment which implies that OXI1 is required for full activation of MPK3 and MPK6. In Arabidopsis, MKK5 mediates transcriptional upregulation of superoxide dismutase upon mutagenic irradiation that causes formation of ROS. It has been shown that MKK5 phosphorylates MPK3 and MPK6 in response to ozone stress (Xing, Cao et al. 2013). MPK phosphatase 2 (MKP2) activation is triggered by oxidative stress. MKP2 dephosphorylates MPK3 and MPK6 thus stimulating oxidative stress tolerance (Lee and Ellis 2007) in Arabidopsis.

The remodelling of gene expression takes place under drought stress in plants. These processes

are known to be mediated by transcription factors, which include WRKYs and basic leucine zipper factors (Shen, Liu et al. 2012, Tang, Zhang et al. 2012). MAP kinases have been found to be involved in the regulation of drought-induced transcription factors such as nuclear factor-Y (NF-YA5) (Sinha, Jaggi et al. 2011). It has been reported that MPK9 and MPK12 regulates stomatal movements under drought stress. Yu et al. reported that MPK6 is activated due to ROS accumulation under drought stress (Yu, Nie et al. 2010). In agriculturally important plants such as maize, rice and cotton, drought induces activation of MAP kinases, for instance OsMPK3, 4, 7, 14 in rice (Shen, Liu et al. 2012), ZmMPK3 in maize (Wang, Ding et al. 2010), and GhMPK2 and GhMPK16 in cotton (Shi, Zhang et al. 2011, Zhang, Xi et al. 2011). These results exemplify the cross talk and inherent redundancy of MPK signalling.

Cold stress has been reported to elicit gene expression and induce MAP kinase activation (Mishra, Tuteja et al. 2006, Huang, Ma et al. 2012). Under cold stress, MPK4 and MPK6 have been shown to be activated in Arabidopsis plants within two minutes, where MPK4 has shown its peak activity after 60 minutes while MPK6 activity increased rapidly and peaked within 10 minutes (Ichimura, Mizoguchi et al. 2000, Teige, Scheikl et al. 2004). Further studies have shown that MPK4 interacts with MEKK1 and MKK2 by yeast two hybrid experiment (Ichimura, Mizoguchi et al. 2000). It has been also demonstrated that MPK4 interacts with the N-terminal regulatory domain of MEKK1 (Ichimura, Mizoguchi et al. 1998). MKK2 functions as a signalling enzyme involved in cold stress responses of Arabidopsis (Teige, Scheikl et al. 2004). MEKK1 activates MKK2 and its phosphorylation prompts the activation of both MPK4 and MPK6 (Teige, Scheikl et al. 2004, Pitzschke, Djamei et al. 2009).

Secondary messengers produced by salt and hyper-osmosis activate MAP kinase cascade. High salt concentration activates drought hypersensitive mutant 1 (DSM1), which is a MAP kinase kinase kinase (MEKK) gene in rice (Ning, Li et al. 2010). It has been reported that high salt concentrations activate MEKK20, which is upstream of MPK6 (Kim, Woo et al. 2012) in Arabidopsis plant. Arabidopsis MEKK1 mutants show improved growth under high salinity environments. Furthermore, it has been reported that MPK4 and MPK6 are activated upon salt stress and MAP kinase kinase 2 (MKK2) lies upstream to these MAP kinases. In addition, null mkk2 mutants have shown to be hypersensitive to salinity (Teige, Scheikl et al. 2004). It has been shown that MPK6 regulates salt-induced transcriptional transactivation of responsive genes by phosphorylating the ZAT6 zinc finger transcription factor (Liu, Nguyen et al. 2013).

Zhou et al. have reported that MKK9 expression increases in response to mechanical wounding (Zhou, Cai et al. 2009).

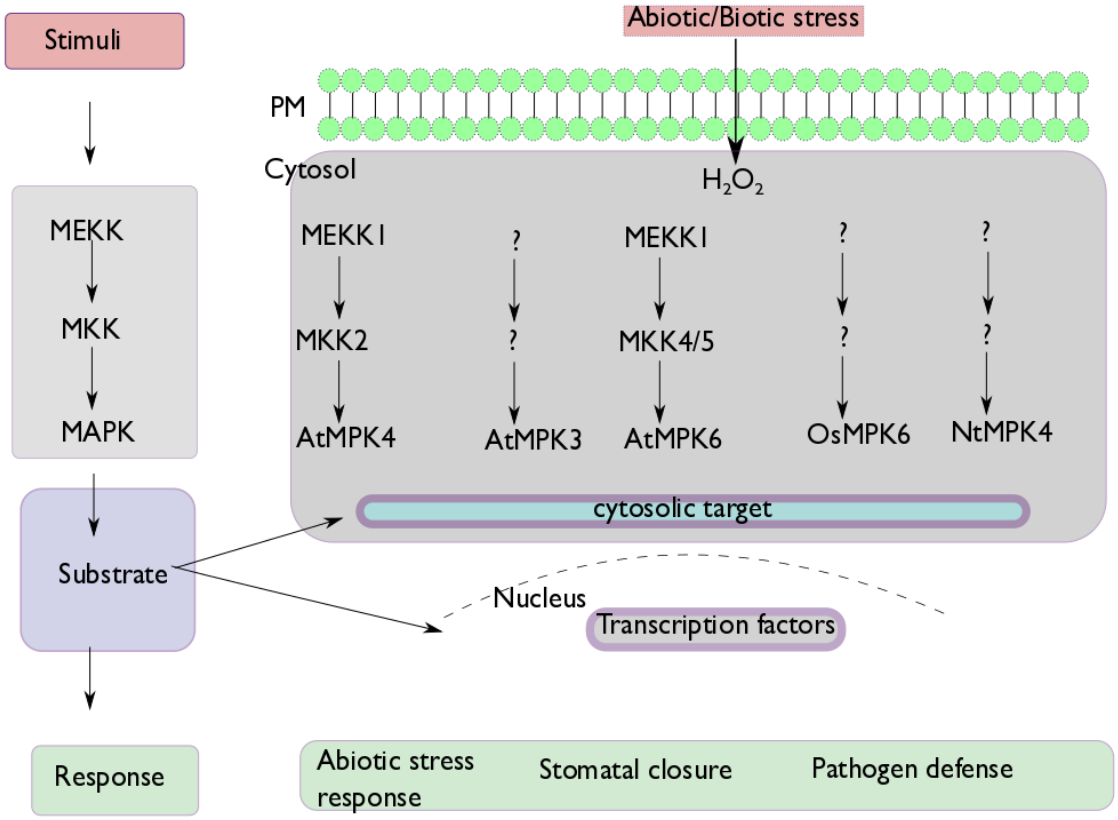

Figure 7: Diagram depicting the activation of mitogen activated kinases (MAPK) cascade by abiotic and biotic stress induced hydrogen peroxide. The area on the left highlights a typical MAPK signalling pathway. MAP kinase activates cytosolic or nuclear targets to facilitate the cellular function.
MEKK- mitogen activated kinase, kinase; kinase MEK-mitogen activated kinase kinase; MAPK/MPK-mitogen activated kinase

1.8 Research gap

Abiotic and biotic factors such as drought, temperature, high light, herbicides, and pathogen attacks influence the growth and development of plants. These stress factors cause oxidative stress in plants by producing H_2O_2, which acts as a potential signalling molecule. Also, under normal cellular metabolism plant produces H_2O_2 in large amounts in mitochondria, chloroplasts, peroxisomes/glyoxysomes, and at the plasma membrane and cell wall. It has been suggested that H_2O_2 plays a versatile role in plant defence and in physiological aspects. H_2O_2 accumulation is maintained at low levels inside cells because of the existence of enzymatic and non-enzymatic antioxidant systems in plant, which eliminate excess H_2O_2 production and maintains the level of H_2O_2 at a normal dynamic balance. With the help of genetic and chemical

probes, and proteomic studies, several proteins have been identified, which undergo post-translational modification and form cysteine sulfenic acid (-SOH) upon H_2O_2 treatment.

The function and physiological relevance of sulfenylation of protein in oxidative stress response is one of the important research question to understand the role of ROS induced signal perception and transduction in plant protection. The main objective of my PhD thesis was to investigate and characterize sulfenylated proteins of *Arabidopsis thaliana* dehydroascorbate reductase (DHAR2), and mitogen activated kinase 4 (MPK4) to understand the mechanism of sulfenylation and their behaviour under H_2O_2 stress. More precisely, we have revealed that cysteine residue of DHAR2 is crucial for enzyme catalysis and showed localized conformational differences around the active site of DHAR2 with its crystal structure. Further we unravelled an enzymatic step where DHAR2 releases oxidized glutathione (GSSG). With *Arabidopsis thaliana* MPK4 (AtMPK4), we have confirmed that it is sulfenylated on cysteine 181. Furthermore, we have shown that wild type AtMPK4 has higher phosphorylation activity than MPK4 C181S mutant in which Cys181 is mutated to Ser.

In the coming years, we expect to explore more sulfenylated proteins, both by *in vitro* and *in vivo* studies, to get a better understanding of the role of H_2O_2 signalling in plants. Difficulty to produce recombinant plant proteins using *Escherichia coli,* dearth of suitable activity assays, absence of mutant phenotype, and lack of information about the role and function of the identified proteins are still a few bottlenecks at this stage.

Eventually, these findings might help the future plant biologists to manipulate stress tolerant genes, and this knowledge will be translated to the design of stress resistant crop species.

References

Abbasi, A. R., M. Hajirezaei, D. Hofius, U. Sonnewald and L. M. Voll (2007). "Specific roles of alpha- and gamma-tocopherol in abiotic stress responses of transgenic tobacco." Plant Physiol **143**(4): 1720-1738.

Ago, T., T. Liu, P. Zhai, W. Chen, H. Li, J. D. Molkentin, S. F. Vatner and J. Sadoshima (2008). "A redox-dependent pathway for regulating class II HDACs and cardiac hypertrophy." Cell **133**(6): 978-993.

Agrawal, G. K., H. Iwahashi and R. Rakwal (2003). "Small GTPase 'Rop': molecular switch for plant defense responses." FEBS Lett **546**(2-3): 173-180.

Ahmad P, Jhon R, Sarwat M, Umar S. 2008b. Responses of proline, lipid per- oxidation and antioxidative enzymes in two varieties of *Pisum sativum* L. under salt stress. Int J Plant Prod **2**: 353–366.

Akter, S., J. Huang, N. Bodra, B. De Smet, K. Wahni, D. Rombaut, J. Pauwels, K. Gevaert, K. Carroll, F. Van Breusegem and J. Messens (2015). "DYn-2 Based Identification of *Arabidopsis Sulfenomes*." Mol Cell Proteomics **14**(5): 1183-1200.

Anastasiou, D., G. Poulogiannis, J. M. Asara, M. B. Boxer, J. K. Jiang, M. Shen, G. Bellinger, A. T. Sasaki, J. W. Locasale, D. S. Auld, C. J. Thomas, M. G. Vander Heiden and L. C. Cantley (2011). "Inhibition of pyruvate kinase M2 by reactive oxygen species contributes to cellular antioxidant responses." Science **334**(6060): 1278-1283.

Anjum, N. A., A. Sofo, A. Scopa, A. Roychoudhury, S. S. Gill, M. Iqbal, A. S. Lukatkin, E. Pereira, A. C. Duarte and I. Ahmad (2015). "Lipids and proteins--major targets of oxidative modifications in abiotic stressed plants." Environ Sci Pollut Res Int **22**(6): 4099-4121.

Apel, K. and H. Hirt (2004). "Reactive oxygen species: metabolism, oxidative stress, and signal transduction." Annu Rev Plant Biol **55**: 373-399.

Arbona, V., Z. Hossain, M. F. Lopez-Climent, R. M. Perez-Clemente and A. Gomez-Cadenas (2008). "Antioxidant enzymatic activity is linked to waterlogging stress tolerance in citrus." Physiol Plant **132**(4): 452-466.

Asada, K., K. Kiso and K. Yoshikawa (1974). "Univalent reduction of molecular oxygen by spinach chloroplasts on illumination." J Biol Chem **249**(7): 2175-2181.

Azevedo-Neto AD, Prisco JT, Enéas-Filho J, Braga-de-Abreu CE, Gomes-Filho E. 2006. E ect of salt stress on antioxidative enzymes and lipid peroxidation in leaves and roots of salt tolerant and salt sensitive maize genotypes. Env Exp Bot **56**: 87–94.

Barrett, W. C., J. P. DeGnore, S. Konig, H. M. Fales, Y. F. Keng, Z. Y. Zhang, M. B. Yim and P. B. Chock (1999). "Regulation of PTP1B via glutathionylation of the active site cysteine 215." Biochemistry **38**(20): 6699-6705.

Beer, S. M., E. R. Taylor, S. E. Brown, C. C. Dahm, N. J. Costa, M. J. Runswick and M. P. Murphy (2004). "Glutaredoxin 2 catalyzes the reversible oxidation and glutathionylation of mitochondrial membrane thiol proteins: implications for mitochondrial redox regulation and antioxidant DEFENSE." J Biol Chem **279**(46): 47939-47951.

Ben-Amor N, Hamed KB, Debez A, Grignon C, Abdelly C. 2005. Physiological and antioxidant

response of the perennial halophytes *Crithmum mariti- mum* to salinity. Plant Sci **168**: 889–899.

Benitez, L. V. and W. S. Allison (1974). "The inactivation of the acyl phosphatase activity catalyzed by the sulfenic acid form of glyceraldehyde 3-phosphate dehydrogenase by dimedone and olefins." J Biol Chem **249**(19): 6234-6243.

Braun, H. P., S. Binder, A. Brennicke, H. Eubel, A. R. Fernie, I. Finkemeier, J. Klodmann, A. C. Konig, K. Kuhn, E. Meyer, T. Obata, M. Schwarzlander, M. Takenaka and A. Zehrmann (2014). "The life of plant mitochondrial complex I." Mitochondrion **19 Pt B**: 295-313.

Bray EA, Bailey-Serres J, Weretilnyk E. 2000. Responses to abiotic stresses. In Buchanan BB, W Gruissem W, Jones RL, eds. Biochemistry and Molecular Biology of Plants (pp. 1158). ASPP: Rockville

Brennan, J. P., J. I. Miller, W. Fuller, R. Wait, S. Begum, M. J. Dunn and P. Eaton (2006). "The utility of N,N-biotinyl glutathione disulfide in the study of protein S-glutathiolation." Mol Cell Proteomics **5**(2): 215-225.

Brennan, J. P., R. Wait, S. Begum, J. R. Bell, M. J. Dunn and P. Eaton (2004). "Detection and mapping of widespread intermolecular protein disulfide formation during cardiac oxidative stress using proteomics with diagonal electrophoresis." J Biol Chem **279**(40): 41352-41360.

Burgoyne, J. R., M. Madhani, F. Cuello, R. L. Charles, J. P. Brennan, E. Schroder, D. D. Browning and P. Eaton (2007). "Cysteine redox sensor in PKGIa enables oxidant-induced activation." Science **317**(5843): 1393-1397.

Camejo, D., C. Marti Mdel, E. Nicolas, J. J. Alarcon, A. Jimenez and F. Sevilla (2007). "Response of superoxide dismutase isoenzymes in tomato plants (*Lycopersicon esculentum*) during thermo-acclimation of the photosynthetic apparatus." Physiol Plant **131**(3): 367-377.

Carballal, S., R. Radi, M. C. Kirk, S. Barnes, B. A. Freeman and B. Alvarez (2003). "Sulfenic acid formation in human serum albumin by hydrogen peroxide and peroxynitrite." Biochemistry **42**(33): 9906-9914.

Caverzan, A., G. Passaia, S. B. Rosa, C. W. Ribeiro, F. Lazzarotto and M. Margis-Pinheiro (2012). "Plant responses to stresses: Role of ascorbate peroxidase in the antioxidant protection." Genet Mol Biol **35**(4 (suppl)): 1011-1019.

Chang, Y. C., C. N. Huang, C. H. Lin, H. C. Chang and C. C. Wu (2010). "Mapping protein cysteine sulfonic acid modifications with specific enrichment and mass spectrometry: an integrated approach to explore the cysteine oxidation." Proteomics **10**(16): 2961-2971.

Chen, H. J., S. D. Wu, G. J. Huang, C. Y. Shen, M. Afiyanti, W. J. Li and Y. H. Lin (2012). "Expression of a cloned sweet potato catalase SPCAT1 alleviates ethephon-mediated leaf senescence and H(2)O(2) elevation." J Plant Physiol **169**(1): 86-97.

Chen, X., H. Wu, C. M. Park, T. H. Poole, G. Keceli, N. O. Devarie-Baez, A. W. Tsang, W. T. Lowther, L. B. Poole, S. B. King, M. Xian and C. M. Furdui (2017). "Discovery of heteroaromatic sulfones as a new class of biologically compatible thiol-selective reagents." ACS Chem Biol **12**(8): 2201-2208.

Chen, Z. and D. R. Gallie (2006). "Dehydroascorbate reductase affects leaf growth, development, and function." Plant Physiol **142**(2): 775-787.

Chen, Z., T. E. Young, J. Ling, S. C. Chang and D. R. Gallie (2003). "Increasing vitamin C content of plants through enhanced ascorbate recycling." Proc Natl Acad Sci U S A **100**(6): 3525-3530.

Cheng, N. H., J. Z. Liu, X. Liu, Q. Wu, S. M. Thompson, J. Lin, J. Chang, S. A. Whitham, S. Park, J. D. Cohen and K. D. Hirschi (2011). "Arabidopsis monothiol glutaredoxin, AtGRXS17, is critical for temperature-dependent postembryonic growth and development via modulating auxin response." J Biol Chem **286**(23): 20398-20406.

Choi, H. J., S. W. Kang, C. H. Yang, S. G. Rhee and S. E. Ryu (1998). "Crystal structure of a novel human peroxidase enzyme at 2.0 A resolution." Nat Struct Biol **5**(5): 400-406.

Choi, K., S. W. Ryu, S. Song, H. Choi, S. W. Kang and C. Choi (2010). "Caspase-dependent generation of reactive oxygen species in human astrocytoma cells contributes to resistance to TRAIL-mediated apoptosis." Cell Death Differ **17**(5): 833-845.

Corpas, F. J., J. B. Barroso and L. A. del Rio (2001). "Peroxisomes as a source of reactive oxygen species and nitric oxide signal molecules in plant cells." Trends Plant Sci **6**(4): 145-150.

Crane, E. J., 3rd, J. Vervoort and A. Claiborne (1997). "13C NMR analysis of the cysteine-sulfenic acid redox center of enterococcal NADH peroxidase." Biochemistry **36**(28): 8611-8618.

Cumming, R. C. (2008). "Analysis of global and specific changes in the disulfide proteome using redox two-dimensional polyacrylamide gel electrophoresis." Methods Mol Biol **476**: 165-179.

Cumming, R. C., N. L. Andon, P. A. Haynes, M. Park, W. H. Fischer and D. Schubert (2004). "Protein disulfide bond formation in the cytoplasm during oxidative stress." J Biol Chem **279**(21): 21749-21758.

Dalal, M. and R. Khanna-Chopra (2001). "Differential response of antioxidant enzymes in leaves of necrotic wheat hybrids and their parents." Physiol Plant **111**(3): 297-304.

de, J., E. T. Yakimova, V. M. Kapchina and E. J. Woltering (2002). "A critical role for ethylene in hydrogen peroxide release during programmed cell death in tomato suspension cells." Planta **214**(4): 537-545.

del Rio, L. A., F. J. Corpas, L. M. Sandalio, J. M. Palma, M. Gomez and J. B. Barroso (2002). "Reactive oxygen species, antioxidant systems and nitric oxide in peroxisomes." J Exp Bot **53**(372): 1255-1272.

del Rio, L. A., L. M. Sandalio, F. J. Corpas, J. M. Palma and J. B. Barroso (2006). "Reactive oxygen species and reactive nitrogen species in peroxisomes. Production, scavenging, and role in cell signaling." Plant Physiol **141**(2): 330-335.

Delaunay, A., D. Pflieger, M. B. Barrault, J. Vinh and M. B. Toledano (2002). "A thiol peroxidase is an H_2O_2 receptor and redox-transducer in gene activation." Cell **111**(4): 471-481.

Denu, J. M. and K. G. Tanner (1998). "Specific and reversible inactivation of protein tyrosine phosphatases by hydrogen peroxide: evidence for a sulfenic acid intermediate and implications for redox regulation." Biochemistry **37**(16): 5633-5642.

Dickinson, B. C., J. Peltier, D. Stone, D. V. Schaffer and C. J. Chang (2011). "Nox2 redox signaling maintains essential cell populations in the brain." Nat Chem Biol **7**(2): 106-112.

Ding, S., R. Jiang, Q. Lu, X. Wen and C. Lu (2016). "Glutathione reductase 2 maintains the function of photosystem II in *Arabidopsis* under excess light." Biochim Biophys Acta **1857**(6): 665-677.

Ding, S., M. Lei, Q. Lu, A. Zhang, Y. Yin, X. Wen, L. Zhang and C. Lu (2012). "Enhanced sensitivity and characterization of photosystem II in transgenic tobacco plants with decreased chloroplast glutathione reductase under chilling stress." Biochim Biophys Acta **1817**(11): 1979-1991.

Eaton, P., N. Wright, D. J. Hearse and M. J. Shattock (2002). "Glyceraldehyde phosphate dehydrogenase oxidation during cardiac ischemia and reperfusion." J Mol Cell Cardiol **34**(11): 1549-1560.

Edwards, E. A., S. Rawsthorne and P. M. Mullineaux (1990). "Subcellular distribution of multiple forms of glutathione reductase in leaves of pea (*Pisum sativum L.*)." Planta **180**(2): 278-284.

Eltayeb, A. E., N. Kawano, G. H. Badawi, H. Kaminaka, T. Sanekata, T. Shibahara, S. Inanaga and K. Tanaka (2007). "Overexpression of monodehydroascorbate reductase in transgenic tobacco confers enhanced tolerance to ozone, salt and polyethylene glycol stresses." Planta **225**(5): 1255-1264.

Fini, A., C. Brunetti, M. Di Ferdinando, F. Ferrini and M. Tattini (2011). "Stress-induced flavonoid biosynthesis and the antioxidant machinery of plants." Plant Signal Behav **6**(5): 709-711.

Fomenko, D. E., A. Koc, N. Agisheva, M. Jacobsen, A. Kaya, M. Malinouski, J. C. Rutherford, K. L. Siu, D. Y. Jin, D. R. Winge and V. N. Gladyshev (2011). "Thiol peroxidases mediate specific genome-wide regulation of gene expression in response to hydrogen peroxide." Proc Natl Acad Sci U S A **108**(7): 2729-2734.

Fomenko, D. E., W. Xing, B. M. Adair, D. J. Thomas and V. N. Gladyshev (2007). "High-throughput identification of catalytic redox-active cysteine residues." Science **315**(5810): 387-389.

Foyer, C., M. Lelandais, C. Galap and K. J. Kunert (1991). "Effects of elevated cytosolic glutathione reductase activity on the cellular glutathione pool and photosynthesis in leaves under normal and stress conditions." Plant Physiol **97**(3): 863-872.

Gahl, R. F. and H. A. Scheraga (2009). "Oxidative folding pathway of onconase, a ribonuclease homologue: insight into oxidative folding mechanisms from a study of two homologues." Biochemistry **48**(12): 2740-2751.

Giannoni, E., F. Buricchi, G. Raugei, G. Ramponi and P. Chiarugi (2005). "Intracellular reactive oxygen species activate Src tyrosine kinase during cell adhesion and anchorage-dependent cell growth." Mol Cell Biol **25**(15): 6391-6403.

Giacomelli L, Masi A, Ripoll DR, Lee MJ, van Wijk KJ. 2007. *Arabidopsis thaliana* deficient in two chloroplast ascorbate peroxidases shows accelerated light-induced necrosis when levels of cellular ascorbate are low. Plant Mol Biol **65**: 627–644.

Gill, S. S. and N. Tuteja (2010). "Reactive oxygen species and antioxidant machinery in abiotic stress tolerance in crop plants." Plant Physiol Biochem **48**(12): 909-930.

Golemiec, E., K. Tokarz, M. Wielanek and E. Niewiadomska (2014). "A dissection of the effects of ethylene, H_2O_2 and high irradiance on antioxidants and several genes associated with stress and senescence in tobacco leaves." J Plant Physiol **171**(3-4): 269-275.

Gonzalez, A., L. Cabrera Mde, M. J. Henriquez, R. A. Contreras, B. Morales and A. Moenne (2012). "Cross talk among calcium, hydrogen peroxide, and nitric oxide and activation of gene expression involving calmodulins and calcium-dependent protein kinases in *Ulva compressa* exposed to copper excess." Plant Physiol **158**(3): 1451-1462.

Gueta-Dahan, Y., Z. Yaniv, B. A. Zilinskas and G. Ben-Hayyim (1997). "Salt and oxidative stress: similar and specific responses and their relation to salt tolerance in citrus." Planta **203**(4): 460-469.

Guo, Z., R. Deshpande and T. T. Paull (2010). "ATM activation in the presence of oxidative stress." Cell Cycle **9**(24): 4805-4811.

Gupta, V. and K. S. Carroll (2014). "Sulfenic acid chemistry, detection and cellular lifetime." Biochim Biophys Acta **1840**(2): 847-875.

Halliwell, B. (2006). "Reactive species and antioxidants. Redox biology is a fundamental theme of aerobic life." Plant Physiol **141**(2): 312-322.

Hasanuzzaman, M., M. A. Hossain and M. Fujita (2011). "Selenium-induced up-regulation of the antioxidant defense and methylglyoxal detoxification system reduces salinity-induced damage in rapeseed seedlings." Biol Trace Elem Res **143**(3): 1704-1721.

Havaux, M., F. Eymery, S. Porfirova, P. Rey and P. Dormann (2005). "Vitamin E protects against photoinhibition and photooxidative stress in *Arabidopsis thaliana*." Plant Cell **17**(12): 3451-3469.

Hoffmann, C., B. Plocharski, I. Haferkamp, M. Leroch, R. Ewald, H. Bauwe, J. Riemer, J. M. Herrmann and H. E. Neuhaus (2013). "From endoplasmic reticulum to mitochondria: absence of the *Arabidopsis* ATP antiporter endoplasmic reticulum adenylate transporter1 perturbs photorespiration." Plant Cell **25**(7): 2647-2660.

Horemans, N., C. H. Foyer and H. Asard (2000). "Transport and action of ascorbate at the plant plasma membrane." Trends Plant Sci **5**(6): 263-267.

Hossain, M. A., M. Hasanuzzaman and M. Fujita (2010). "Up-regulation of antioxidant and glyoxalase systems by exogenous glycinebetaine and proline in mung bean confer tolerance to cadmium stress." Physiol Mol Biol Plants **16**(3): 259-272.

Hu, T., K. Chen, L. Hu, E. Amombo and J. Fu (2016). "H2O2 and Ca(2+)-based signaling and associated ion accumulation, antioxidant systems and secondary metabolism orchestrate the response to NaCl stress in perennial ryegrass." Sci Rep **6**: 36396.

Hu, X., D. L. Bidney, N. Yalpani, J. P. Duvick, O. Crasta, O. Folkerts and G. Lu (2003). "Overexpression of a gene encoding hydrogen peroxide-generating oxalate oxidase evokes defense responses in sunflower." Plant Physiol **133**(1): 170-181.

Huang, G. T., S. L. Ma, L. P. Bai, L. Zhang, H. Ma, P. Jia, J. Liu, M. Zhong and Z. F. Guo (2012). "Signal transduction during cold, salt, and drought stresses in plants." Mol Biol Rep **39**(2): 969-987.

Hurd, T. R., R. Requejo, A. Filipovska, S. Brown, T. A. Prime, A. J. Robinson, I. M. Fearnley and M. P. Murphy (2008). "Complex I within oxidatively stressed bovine heart mitochondria is glutathionylated on Cys-531 and Cys-704 of the 75-kDa subunit: potential role of CYS residues in decreasing oxidative damage." J Biol Chem **283**(36): 24801-24815.

Ichimura, K., T. Mizoguchi, K. Irie, P. Morris, J. Giraudat, K. Matsumoto and K. Shinozaki (1998). "Isolation of ATMEKK1 (a MAP kinase kinase kinase)-interacting proteins and analysis of a MAP kinase cascade in Arabidopsis." Biochem Biophys Res Commun **253**(2): 532-543.

Ichimura, K., T. Mizoguchi, R. Yoshida, T. Yuasa and K. Shinozaki (2000). "Various abiotic stresses rapidly activate Arabidopsis MAP kinases ATMPK4 and ATMPK6." Plant J **24**(5): 655-665.

Igamberdiev, A. U. and R. D. Hill (2004). "Nitrate, NO and haemoglobin in plant adaptation to hypoxia: an alternative to classic fermentation pathways." J Exp Bot **55**(408): 2473-2482.

Jeng, M. F., A. Holmgren and H. J. Dyson (1995). "Proton sharing between cysteine thiols in Escherichia coli thioredoxin: implications for the mechanism of protein disulfide reduction." Biochemistry **34**(32): 10101-10105.

Jimenez, A., J. A. Hernandez, L. A. Del Rio and F. Sevilla (1997). "Evidence for the presence of the ascorbate-glutathione cycle in mitochondria and peroxisomes of Pea leaves." Plant Physiol **114**(1): 275-284.

Kangasjarvi, S., A. Lepisto, K. Hannikainen, M. Piippo, E. M. Luomala, E. M. Aro and E. Rintamaki (2008). "Diverse roles for chloroplast stromal and thylakoid-bound ascorbate peroxidases in plant stress responses." Biochem J **412**(2): 275-285.

Keles Y, Oncel I. 2002. Response of antioxidative defence system to temper- ature and water stress combinations in wheat seedlings. Plant Sci **163**: 783–790.

Kemble, D. J. and G. Sun (2009). "Direct and specific inactivation of protein tyrosine kinases in the Src and FGFR families by reversible cysteine oxidation." Proc Natl Acad Sci U S A **106**(13): 5070-5075.

Kim, F. J., H. P. Kim, Y. C. Hah and J. H. Roe (1996). "Differential expression of superoxide dismutases containing Ni and Fe/Zn in Streptomyces coelicolor." Eur J Biochem **241**(1): 178-185.

Kim, J. M., D. H. Woo, S. H. Kim, S. Y. Lee, H. Y. Park, H. Y. Seok, W. S. Chung and Y. H. Moon (2012). "Arabidopsis MKKK20 is involved in osmotic stress response via regulation of MPK6 activity." Plant Cell Rep **31**(1): 217-224.

Kim, J. R., H. W. Yoon, K. S. Kwon, S. R. Lee and S. G. Rhee (2000). "Identification of proteins containing cysteine residues that are sensitive to oxidation by hydrogen peroxide at neutral pH." Anal Biochem **283**(2): 214-221.

Klamt, F., S. Zdanov, R. L. Levine, A. Pariser, Y. Zhang, B. Zhang, L. R. Yu, T. D. Veenstra and E. Shacter (2009). "Oxidant-induced apoptosis is mediated by oxidation of the actin-regulatory protein cofilin." Nat Cell Biol **11**(10): 1241-1246.

Kohler, B., A. Hills and M. R. Blatt (2003). "Control of guard cell ion channels by hydrogen peroxide and abscisic acid indicates their action through alternate signaling pathways." Plant Physiol **131**(2): 385-388.

Kortemme, T. and T. E. Creighton (1995). "Ionisation of cysteine residues at the termini of model alpha-helical peptides. Relevance to unusual thiol pKa values in proteins of the thioredoxin family." J Mol Biol **253**(5): 799-812.

Kruk, J., H. Hollander-Czytko, W. Oettmeier and A. Trebst (2005). "Tocopherol as singlet oxygen scavenger in photosystem II." J Plant Physiol **162**(7): 749-757.

Le Moan, N., G. Clement, S. Le Maout, F. Tacnet and M. B. Toledano (2006). "The Saccharomyces cerevisiae proteome of oxidized protein thiols: contrasted functions for the thioredoxin and glutathione pathways." J Biol Chem **281**(15): 10420-10430.

Lecourieux, D., C. Mazars, N. Pauly, R. Ranjeva and A. Pugin (2002). "Analysis and effects of cytosolic free calcium increases in response to elicitors in *Nicotiana plumbaginifolia* cells." Plant Cell **14**(10): 2627-2641.

Ledford, H. K., B. L. Chin and K. K. Niyogi (2007). "Acclimation to singlet oxygen stress in *Chlamydomonas reinhardtii*." Eukaryot Cell **6**(6): 919-930.

Lee, D. H. and C. B. Lee (2000). "Chilling stress-induced changes of antioxidant enzymes in the leaves of cucumber: in gel enzyme activity assays." Plant Sci **159**(1): 75-85.

Lee, J. S. and B. E. Ellis (2007). "Arabidopsis MAPK phosphatase 2 (MKP2) positively regulates oxidative stress tolerance and inactivates the MPK3 and MPK6 MAPKs." J Biol Chem **282**(34): 25020-25029.

Lee, S. H., N. Ahsan, K. W. Lee, D. H. Kim, D. G. Lee, S. S. Kwak, S. Y. Kwon, T. H. Kim and B. H. Lee (2007). "Simultaneous overexpression of both CuZn superoxide dismutase and ascorbate peroxidase in transgenic tall fescue plants confers increased tolerance to a wide range of abiotic stresses." J Plant Physiol **164**(12): 1626-1638.

Lei, K., D. M. Townsend and K. D. Tew (2008). "Protein cysteine sulfinic acid reductase (sulfiredoxin) as a regulator of cell proliferation and drug response." Oncogene **27**(36): 4877-4887.

Leichert, L. I., F. Gehrke, H. V. Gudiseva, T. Blackwell, M. Ilbert, A. K. Walker, J. R. Strahler, P. C. Andrews and U. Jakob (2008). "Quantifying changes in the thiol redox proteome upon oxidative stress in vivo." Proc Natl Acad Sci U S A **105**(24): 8197-8202.

Leonard, S. E. and K. S. Carroll (2011). "Chemical 'omics' approaches for understanding protein cysteine oxidation in biology." Curr Opin Chem Biol **15**(1): 88-102.

Liao W. B., Zhang M. L., Huang G. B., Yu J. H. (2012). Hydrogen peroxide in the vase solution increases vase life and keeping quality of cut Oriental × Trumpet hybrid lily "manissa." Sci. Hortic.**139** 32–38. 10.4161/psb.3.9.5757

Lindahl, M., A. Mata-Cabana and T. Kieselbach (2011). "The disulfide proteome and other reactive cysteine proteomes: analysis and functional significance." Antioxid Redox Signal **14**(12): 2581-2642.

Liu, X. M., X. C. Nguyen, K. E. Kim, H. J. Han, J. Yoo, K. Lee, M. C. Kim, D. J. Yun and W. S. Chung (2013). "Phosphorylation of the zinc finger transcriptional regulator ZAT6 by MPK6 regulates Arabidopsis seed germination under salt and osmotic stress." Biochem Biophys Res Commun **430**(3): 1054-1059.

Lo Conte, M. and K. S. Carroll (2013). "The redox biochemistry of protein sulfenylation and sulfinylation." J Biol Chem **288**(37): 26480-26488.

Locato V, Cimini S, Gara LD. 2013 Startegies to increase vitamin C in plants from plant defense perspective to food biofortification. Front Plant Sci.**4**:152

Locato, V., M. C. de Pinto and L. De Gara (2009). "Different involvement of the mitochondrial, plastidial and cytosolic ascorbate-glutathione redox enzymes in heat shock responses." Physiol Plant **135**(3): 296-306.

Lu, Z., D. Liu and S. Liu (2007). "Two rice cytosolic ascorbate peroxidases differentially improve salt tolerance in transgenic *Arabidopsis*." Plant Cell Rep **26**(10): 1909-1917.

Ludwig, A. A., H. Saitoh, G. Felix, G. Freymark, O. Miersch, C. Wasternack, T. Boller, J. D. Jones and T. Romeis (2005). "Ethylene-mediated cross-talk between calcium-dependent protein kinase and MAPK signaling controls stress responses in plants." Proc Natl Acad Sci U S A **102**(30): 10736-10741.

Lumbreras, V., B. Vilela, S. Irar, M. Sole, M. Capellades, M. Valls, M. Coca and M. Pages (2010). "MAPK phosphatase MKP2 mediates disease responses in *Arabidopsis* and functionally interacts with MPK3 and MPK6." Plant J **63**(6): 1017-1030.

Ma, L. H., C. L. Takanishi and M. J. Wood (2007). "Molecular mechanism of oxidative stress perception by the Orp1 protein." J Biol Chem **282**(43): 31429-31436.

Macartney, H. W. and H. Tschesche (1983). "Characterisation of beta 1-anticollagenase from human plasma and its reaction with polymorphonuclear leukocyte collagenase by disulfide/thiol interchange." Eur J Biochem **130**(1): 85-92.

Mahadev, K., A. Zilbering, L. Zhu and B. J. Goldstein (2001). "Insulin-stimulated hydrogen peroxide reversibly inhibits protein-tyrosine phosphatase 1b in vivo and enhances the early insulin action cascade." J Biol Chem **276**(24): 21938-21942.

Marchand, C., P. Le Marechal, Y. Meyer and P. Decottignies (2006). "Comparative proteomic approaches for the isolation of proteins interacting with thioredoxin." Proteomics **6**(24): 6528-6537.

Marino, S. M., Y. Li, D. E. Fomenko, N. Agisheva, R. L. Cerny and V. N. Gladyshev (2010). "Characterization of surface-exposed reactive cysteine residues in *Saccharomyces cerevisiae*." Biochemistry **49**(35): 7709-7721.

Mehler, A. H. (1951). "Studies on reactions of illuminated chloroplasts. I. Mechanism of the reduction of oxygen and other Hill reagents." Arch Biochem Biophys **33**(1): 65-77.

Meinhard, M., P. L. Rodriguez and E. Grill (2002). "The sensitivity of ABI2 to hydrogen peroxide links the abscisic acid-response regulator to redox signalling." Planta **214**(5): 775-782.

Meissner, F., K. Molawi and A. Zychlinsky (2008). "Superoxide dismutase 1 regulates caspase-1 and endotoxic shock." Nat Immunol **9**(8): 866-872.

Meng, T. C., T. Fukada and N. K. Tonks (2002). "Reversible oxidation and inactivation of protein tyrosine phosphatases in vivo." Mol Cell **9**(2): 387-399.

Mhamdi, A., G. Queval, S. Chaouch, S. Vanderauwera, F. Van Breusegem and G. Noctor (2010). "Catalase function in plants: a focus on Arabidopsis mutants as stress-mimic models." J Exp Bot **61**(15): 4197-4220.

Michalek, R. D., K. J. Nelson, B. C. Holbrook, J. S. Yi, D. Stridiron, L. W. Daniel, J. S. Fetrow, S. B. King, L. B. Poole and J. M. Grayson (2007). "The requirement of reversible cysteine sulfenic acid formation for T cell activation and function." J Immunol **179**(10): 6456-6467.

Millar, A. H., V. Mittova, G. Kiddle, J. L. Heazlewood, C. G. Bartoli, F. L. Theodoulou and C. H. Foyer (2003). "Control of ascorbate synthesis by respiration and its implications for stress responses." Plant Physiol **133**(2): 443-447.

Mishra, N. S., R. Tuteja and N. Tuteja (2006). "Signaling through MAP kinase networks in plants." Arch Biochem Biophys **452**(1): 55-68.

Mittova, V., M. Tal, M. Volokita and M. Guy (2003). "Up-regulation of the leaf mitochondrial and peroxisomal antioxidative systems in response to salt-induced oxidative stress in the wild salt-tolerant tomato species *Lycopersicon pennellii*." Plant Cell Environ **26**(6): 845-856.

Miyagawa, Y., M. Tamoi and S. Shigeoka (2000). "Evaluation of the defense system in chloroplasts to photooxidative stress caused by paraquat using transgenic tobacco plants expressing catalase from *Escherichia coli*." Plant Cell Physiol **41**(3): 311-320.

Moller, I. M. (2001). "PLANT MITOCHONDRIA AND OXIDATIVE STRESS: Electron Transport, NADPH turnover, and metabolism of reactive oxygen species." Annu Rev Plant Physiol Plant Mol Biol **52**: 561-591.

Mortensen, A., L. H. Skibsted and T. G. Truscott (2001). "The interaction of dietary carotenoids with radical species." Arch Biochem Biophys **385**(1): 13-19.

Mullineaux, P. M., S. Karpinski and N. R. Baker (2006). "Spatial dependence for hydrogen peroxide-directed signaling in light-stressed plants." Plant Physiol **141**(2): 346-350.

Nagy, P. and M. T. Ashby (2007). "Reactive sulfur species: kinetics and mechanisms of the oxidation of cysteine by hypohalous acid to give cysteine sulfenic acid." J Am Chem Soc **129**(45): 14082-14091.

Nakamura, T., T. Yamamoto, M. Abe, H. Matsumura, Y. Hagihara, T. Goto, T. Yamaguchi and T. Inoue (2008). "Oxidation of archaeal peroxiredoxin involves a hypervalent sulfur intermediate." Proc Natl Acad Sci U S A **105**(17): 6238-6242.

Nandini Y, Sharma S. 2016 Reactive oxygen species, oxidative stress and ROS scavenging system in plants. J Chem Pharm Res **8**(5):595-604

Naya, L., R. Ladrera, J. Ramos, E. M. Gonzalez, C. Arrese-Igor, F. R. Minchin and M. Becana (2007). "The response of carbon metabolism and antioxidant defenses of alfalfa nodules to drought stress and to the subsequent recovery of plants." Plant Physiol **144**(2): 1104-1114.

Ning, J., X. Li, L. M. Hicks and L. Xiong (2010). "A Raf-like MAPKKK gene DSM1 mediates drought resistance through reactive oxygen species scavenging in rice." Plant Physiol **152**(2): 876-890.

Noctor, G. (2006). "Metabolic signalling in defence and stress: the central roles of soluble redox couples." Plant Cell Environ **29**(3): 409-425.

Noctor, G. and C. H. Foyer (1998). "ASCORBATE AND GLUTATHIONE: Keeping active oxygen under control." Annu Rev Plant Physiol Plant Mol Biol **49**: 249-279.

Noctor, G., L. Gomez, H. Vanacker and C. H. Foyer (2002). "Interactions between biosynthesis, compartmentation and transport in the control of glutathione homeostasis and signalling." J Exp Bot **53**(372): 1283-1304.

O'Brien, J. A., A. Daudi, V. S. Butt and G. P. Bolwell (2012). "Reactive oxygen species and their role in plant defence and cell wall metabolism." Planta **236**(3): 765-779.

Ostman, A., C. Hellberg and F. D. Bohmer (2006). "Protein-tyrosine phosphatases and cancer." Nat Rev Cancer **6**(4): 307-320.

Parida, A. K., A. B. Das and P. Mohanty (2004). "Defense potentials to NaCl in a mangrove, Bruguiera parviflora: differential changes of isoforms of some antioxidative enzymes." J Plant Physiol **161**(5): 531-542.

Park, J. W., J. J. Mieyal, S. G. Rhee and P. B. Chock (2009). "Deglutathionylation of 2-Cys peroxiredoxin is specifically catalyzed by sulfiredoxin." J Biol Chem **284**(35): 23364-23374.

Patterson, H. C., C. Gerbeth, P. Thiru, N. F. Vogtle, M. Knoll, A. Shahsafaei, K. E. Samocha, C. X. Huang, M. M. Harden, R. Song, C. Chen, J. Kao, J. Shi, W. Salmon, Y. D. Shaul, M. P. Stokes, J. C. Silva, G. W. Bell, D. G. MacArthur, J. Ruland, C. Meisinger and H. F. Lodish (2015). "A respiratory chain controlled signal transduction cascade in the mitochondrial intermembrane space mediates hydrogen peroxide signaling." Proc Natl Acad Sci U S A **112**(42): E5679-5688.

Paulsen, C. E. and K. S. Carroll (2009). "Chemical dissection of an essential redox switch in yeast." Chem Biol **16**(2): 217-225.

Paulsen, C. E. and K. S. Carroll (2010). "Orchestrating redox signaling networks through regulatory cysteine switches." ACS Chem Biol **5**(1): 47-62.

Paulsen, C. E., T. H. Truong, F. J. Garcia, A. Homann, V. Gupta, S. E. Leonard and K. S. Carroll (2011). "Peroxide-dependent sulfenylation of the EGFR catalytic site enhances kinase activity." Nat Chem Biol **8**(1): 57-64.

Pei, Z. M., Y. Murata, G. Benning, S. Thomine, B. Klusener, G. J. Allen, E. Grill and J. I. Schroeder (2000). "Calcium channels activated by hydrogen peroxide mediate abscisic acid signalling in guard cells." Nature **406**(6797): 731-734.

Penuelas, J. and S. Munne-Bosch (2005). "Isoprenoids: an evolutionary pool for photoprotection." Trends Plant Sci **10**(4): 166-169.

Pilon, M., K. Ravet and W. Tapken (2011). "The biogenesis and physiological function of chloroplast superoxide dismutases." Biochim Biophys Acta **1807**(8): 989-998.

Pitcher, L. H. and B. A. Zilinskas (1996). "Overexpression of Copper/Zinc Superoxide Dismutase in the Cytosol of Transgenic Tobacco Confers Partial Resistance to Ozone-Induced Foliar Necrosis." Plant Physiol **110**(2): 583-588.

Pitzschke, A., A. Djamei, F. Bitton and H. Hirt (2009). "A major role of the MEKK1-MKK1/2-MPK4 pathway in ROS signalling." Mol Plant **2**(1): 120-137.

Polle, A. (2001). "Dissecting the superoxide dismutase-ascorbate-glutathione-pathway in chloroplasts by metabolic modeling. Computer simulations as a step towards flux analysis." Plant Physiol **126**(1): 445-462.

Polle, A., K. Chakrabarti, W. Schurmann and H. Renneberg (1990). "Composition and properties of hydrogen peroxide decomposing systems in extracellular and total extracts from needles of Norway Spruce (*Picea abies* L., Karst.)." Plant Physiol **94**(1): 312-319.

Poole, L. B. and A. Claiborne (1989). "The non-flavin redox center of the streptococcal NADH peroxidase. II. Evidence for a stabilized cysteine-sulfenic acid." J Biol Chem **264**(21): 12330-12338.

Poole, L. B., C. Klomsiri, S. A. Knaggs, C. M. Furdui, K. J. Nelson, M. J. Thomas, J. S. Fetrow, L. W. Daniel and S. B. King (2007). "Fluorescent and affinity-based tools to detect cysteine sulfenic acid formation in proteins." Bioconjug Chem **18**(6): 2004-2017.

Potters, G., T. P. Pasternak, Y. Guisez, K. J. Palme and M. A. Jansen (2007). "Stress-induced morphogenic responses: growing out of trouble?" Trends Plant Sci **12**(3): 98-105.

Pourcel, L., J. M. Routaboul, V. Cheynier, L. Lepiniec and I. Debeaujon (2007). "Flavonoid oxidation in plants: from biochemical properties to physiological functions." Trends Plant Sci **12**(1): 29-36.

Prinarakis, E., E. Chantzoura, D. Thanos and G. Spyrou (2008). "S-glutathionylation of IRF3 regulates IRF3-CBP interaction and activation of the IFN beta pathway." EMBO J **27**(6): 865-875.

Prosser, B. L., C. W. Ward and W. J. Lederer (2011). "X-ROS signaling: rapid mechano-chemo transduction in heart." Science **333**(6048): 1440-1445.

Qiu-Fang Z, Yuan-Yuan L, Cai-Hong P, Cong-Ming L, Bao-Shan W.. 2005. NaCl enhances thylakoid-bound SOD activity in the leaves of C_3 halophyte *Suaeda salsa* L. Plant Sci **168**: 423–430.

Quan LJ, Zhang B, Shi WW, Li HY.2008. Hydrogen peroxide in plants: a versatile molecule of the reactive oxygen species network. J Integr Plant Biol. **50**(1):2-18

Reczek, C. R. and N. S. Chandel (2015). "ROS-dependent signal transduction." Curr Opin Cell Biol **33**: 8-13.

Rentel, M. C. and M. R. Knight (2004). "Oxidative stress-induced calcium signaling in *Arabidopsis*." Plant Physiol **135**(3): 1471-1479.

Riondet, C., J. P. Desouris, J. G. Montoya, Y. Chartier, Y. Meyer and J. P. Reichheld (2012). "A dicotyledon-specific glutaredoxin GRXC1 family with dimer-dependent redox regulation is functionally redundant with GRXC2." Plant Cell Environ **35**(2): 360-373.

Rogers, H. and S. Munne-Bosch (2016). "Production and scavenging of reactive oxygen species and redox gignaling during leaf and flower senescence: similar but different." Plant Physiol **171**(3): 1560-1568.

Roos, G. and J. Messens (2011). "Protein sulfenic acid formation: from cellular damage to redox regulation." Free Radic Biol Med **51**(2): 314-326.

Rudolph, T. K. and B. A. Freeman (2009). "Transduction of redox signaling by electrophile-protein reactions." Sci Signal **2**(90): re7.

Salmeen, A., J. N. Andersen, M. P. Myers, T. C. Meng, J. A. Hinks, N. K. Tonks and D. Barford (2003). "Redox regulation of protein tyrosine phosphatase 1B involves a sulphenyl-amide intermediate." Nature **423**(6941): 769-773.

Saxena, I., S. Srikanth and Z. Chen (2016). "Cross Talk between H_2O_2 and interacting signal molecules under plant stress response." Front Plant Sci **7**: 570.

Schraudner, M., W. Moeder, C. Wiese, W. V. Camp, D. Inze, C. Langebartels and H. Sandermann, Jr. (1998). "Ozone-induced oxidative burst in the ozone biomonitor plant, tobacco Bel W3." Plant J **16**(2): 235-245.

Schroeter, H., C. Boyd, J. P. Spencer, R. J. Williams, E. Cadenas and C. Rice-Evans (2002). "MAPK signaling in neurodegeneration: influences of flavonoids and of nitric oxide." Neurobiol Aging **23**(5): 861-880.

Sekmen, A. H., I. Turkan and S. Takio (2007). "Differential responses of antioxidative enzymes and lipid peroxidation to salt stress in salt-tolerant *Plantago maritima* and salt-sensitive Plantago media." Physiol Plant **131**(3): 399-411.

Sethuraman, M., M. E. McComb, H. Huang, S. Huang, T. Heibeck, C. E. Costello and R. A. Cohen (2004). "Isotope-coded affinity tag (ICAT) approach to redox proteomics: identification and quantitation of oxidant-sensitive cysteine thiols in complex protein mixtures." J Proteome Res **3**(6): 1228-1233.

Shaked, Z., R. P. Szajewski and G. M. Whitesides (1980). "Rates of thiol-disulfide interchange reactions involving proteins and kinetic measurements of thiol pKa values." Biochemistry **19**(18): 4156-4166.

Shalata, A., V. Mittova, M. Volokita, M. Guy and M. Tal (2001). "Response of the cultivated tomato and its wild salt-tolerant relative *Lycopersicon pennellii* to salt-dependent oxidative stress: The root antioxidative system." Physiol Plant **112**(4): 487-494.

Shao, H. B., L. Y. Chu, Z. H. Lu and C. M. Kang (2007). "Primary antioxidant free radical scavenging and redox signaling pathways in higher plant cells." Int J Biol Sci **4**(1): 8-14.

Shen, H., C. Liu, Y. Zhang, X. Meng, X. Zhou, C. Chu and X. Wang (2012). "OsWRKY30 is activated by MAP kinases to confer drought tolerance in rice." Plant Mol Biol **80**(3): 241-253.

Shi, J., L. Zhang, H. An, C. Wu and X. Guo (2011). "GhMPK16, a novel stress-responsive group D MAPK gene from cotton, is involved in disease resistance and drought sensitivity." BMC Mol Biol **12**: 22.

Shikanai, T., T. Takeda, H. Yamauchi, S. Sano, K. I. Tomizawa, A. Yokota and S. Shigeoka (1998). "Inhibition of ascorbate peroxidase under oxidative stress in tobacco having bacterial catalase in chloroplasts." FEBS Lett **428**(1-2): 47-51.

Shin, R. and D. P. Schachtman (2004). "Hydrogen peroxide mediates plant root cell response to nutrient deprivation." Proc Natl Acad Sci U S A **101**(23): 8827-8832.

Sinha, A. K., M. Jaggi, B. Raghuram and N. Tuteja (2011). "Mitogen-activated protein kinase signaling in plants under abiotic stress." Plant Signal Behav **6**(2): 196-203.

Smith, R. E. and R. MacQuarrie (1979). "The role of cysteine residues in the catalytic activity of glycerol-3-phosphate dehydrogenase." Biochim Biophys Acta **567**(2): 269-277.

Sohn, J. and J. Rudolph (2003). "Catalytic and chemical competence of regulation of cdc25 phosphatase by oxidation/reduction." Biochemistry **42**(34): 10060-10070.

Sommer, A. and R. R. Traut (1974). "Diagonal polyacrylamide-dodecyl sulfate gel electrophoresis for the identification of ribosomal proteins crosslinked with methyl-4-mercaptobutyrimidate." Proc Natl Acad Sci U S A **71**(10): 3946-3950.

Starke, D. W., P. B. Chock and J. J. Mieyal (2003). "Glutathione-thiyl radical scavenging and transferase properties of human glutaredoxin (thioltransferase). Potential role in redox signal transduction." J Biol Chem **278**(17): 14607-14613.

Stehle, T., A. Claiborne and G. E. Schulz (1993). "NADH binding site and catalysis of NADH peroxidase." Eur J Biochem **211**(1-2): 221-226.

Steven, F. S., M. M. Griffin and R. H. Smith (1981). "Disulphide exchange reactions in the control of enzymic activity. Evidence for the participation of dimethyl disulphide in exchanges." Eur J Biochem **119**(1): 75-78.

Sung, M. S., Y. T. Hsu, Y. T. Hsu, T. M. Wu and T. M. Lee (2009). "Hypersalinity and hydrogen peroxide upregulation of gene expression of antioxidant enzymes in Ulva fasciata against oxidative stress." Mar Biotechnol (NY) **11**(2): 199-209.

Suzuki, N., S. Koussevitzky, R. Mittler and G. Miller (2012). "ROS and redox signalling in the response of plants to abiotic stress." Plant Cell Environ **35**(2): 259-270.

Takahashi, N., T. Kuwaki, S. Kiyonaka, T. Numata, D. Kozai, Y. Mizuno, S. Yamamoto, S. Naito, E. Knevels, P. Carmeliet, T. Oga, S. Kaneko, S. Suga, T. Nokami, J. Yoshida and Y. Mori (2011). "TRPA1 underlies a sensing mechanism for O2." Nat Chem Biol **7**(10): 701-711.

Takanishi, C. L., L. H. Ma and M. J. Wood (2007). "A genetically encoded probe for cysteine sulfenic acid protein modification in vivo." Biochemistry **46**(50): 14725-14732.

Tang, N., H. Zhang, X. Li, J. Xiao and L. Xiong (2012). "Constitutive activation of transcription factor OsbZIP46 improves drought tolerance in rice." Plant Physiol **158**(4): 1755-1768.

Teige, M., E. Scheikl, T. Eulgem, R. Doczi, K. Ichimura, K. Shinozaki, J. L. Dangl and H. Hirt (2004). "The MKK2 pathway mediates cold and salt stress signaling in *Arabidopsis*." Mol Cell **15**(1): 141-152.

Templeton, D. J., M. S. Aye, J. Rady, F. Xu and J. V. Cross (2010). "Purification of reversibly oxidized proteins (PROP) reveals a redox switch controlling p38 MAP kinase activity." PLoS One **5**(11): e15012.

Townsend, D. M., K. D. Tew and H. Tapiero (2003). "The importance of glutathione in human disease." Biomed Pharmacother **57**(3-4): 145-155.

Truong, T. H. and K. S. Carroll (2013). "Redox regulation of protein kinases." Crit Rev Biochem Mol Biol **48**(4): 332-356.

Tuna AL, Kaya C, Dikilitas M, Higgs D. 2008. e combined e ects of gib- berellic acid and salinity on some antioxidant enzyme activities, plant growth parameters and nutritional status in maize plants. Environ Exp Bot **62**: 1–9.

Upadhyaya H, Panda SK, Dutta BK. 2008. Variation of physiological and anti- oxidative responses in tea cultivars subjected to elevated water stress fol- lowed by rehydration recovery. Acta Physiol. Plant **30**: 457–468.

Vital SA, Fowler RW, Virgen A, Gossett DR, Banks SW, Rodriguez J. 2008. Opposing roles for superoxide and nitric oxide in the NaCl stress-in- duced upregulation of antioxidant enzyme activity in cotton callus tissue. Environ Exp Bot **62**: 60–68

Velu, C. S., S. K. Niture, C. E. Doneanu, N. Pattabiraman and K. S. Srivenugopal (2007). "Human p53 is inhibited by glutathionylation of cysteines present in the proximal DNA-binding domain during oxidative stress." Biochemistry **46**(26): 7765-7780.

Walters, D. R. (2003). "Polyamines and plant disease." Phytochemistry **64**(1): 97-107.

Wang, J., H. Ding, A. Zhang, F. Ma, J. Cao and M. Jiang (2010). "A novel mitogen-activated protein kinase gene in maize (Zea mays), ZmMPK3, is involved in response to diverse environmental cues." J Integr Plant Biol **52**(5): 442-452.

Wang, J., H. Zhang and R. D. Allen (1999). "Overexpression of an *Arabidopsis* peroxisomal ascorbate peroxidase gene in tobacco increases protection against oxidative stress." Plant Cell Physiol **40**(7): 725-732.

Wang, W., S. Hong, A. Tran, H. Jiang, R. Triano, Y. Liu, X. Chen and P. Wu (2011). "Sulfated ligands for the copper(I)-catalyzed azide-alkyne cycloaddition." Chem Asian J **6**(10): 2796-2802.

Wang, Z., Y. Xiao, W. Chen, K. Tang and L. Zhang (2010). "Increased vitamin C content accompanied by an enhanced recycling pathway confers oxidative stress tolerance in Arabidopsis." J Integr Plant Biol **52**(4): 400-409.

Wani, R., J. Qian, L. Yin, E. Bechtold, S. B. King, L. B. Poole, E. Paek, A. W. Tsang and C. M. Furdui (2011). "Isoform-specific regulation of Akt by PDGF-induced reactive oxygen species." Proc Natl Acad Sci U S A **108**(26): 10550-10555.

Waszczak, C., S. Akter, D. Eeckhout, G. Persiau, K. Wahni, N. Bodra, I. Van Molle, B. De Smet, D. Vertommen, K. Gevaert, G. De Jaeger, M. Van Montagu, J. Messens and F. Van Breusegem (2014). "Sulfenome mining in *Arabidopsis thaliana*." Proc Natl Acad Sci U S A **111**(31): 11545-11550.

Willekens, H., R. Villarroel, M. Van Montagu, D. Inze and W. Van Camp (1994). "Molecular identification of catalases from Nicotiana plumbaginifolia (L.)." FEBS Lett **352**(1): 79-83.

Wilson, N. A., E. Barbar, J. A. Fuchs and C. Woodward (1995). "Aspartic acid 26 in reduced Escherichia coli thioredoxin has a pKa > 9." Biochemistry **34**(28): 8931-8939.

Winger, A. M., N. L. Taylor, J. L. Heazlewood, D. A. Day and A. H. Millar (2007). "Identification of intra- and intermolecular disulphide bonding in the plant mitochondrial proteome by diagonal gel electrophoresis." Proteomics **7**(22): 4158-4170.

Winter, J., M. Ilbert, P. C. Graf, D. Ozcelik and U. Jakob (2008). "Bleach activates a redox-regulated chaperone by oxidative protein unfolding." Cell **135**(4): 691-701.

Winterbourn, C. C. and M. B. Hampton (2008). "Thiol chemistry and specificity in redox signaling." Free Radic Biol Med **45**(5): 549-561.

Winterbourn, C. C. and D. Metodiewa (1999). "Reactivity of biologically important thiol compounds with superoxide and hydrogen peroxide." Free Radic Biol Med **27**(3-4): 322-328.

Wishart, D. S. and B. D. Sykes (1994). "The 13C chemical-shift index: a simple method for the identification of protein secondary structure using 13C chemical-shift data." J Biomol NMR **4**(2): 171-180.

Wood, M. J., G. Storz and N. Tjandra (2004). "Structural basis for redox regulation of Yap1 transcription factor localization." Nature **430**(7002): 917-921.

Xia, X. J., Y. H. Zhou, K. Shi, J. Zhou, C. H. Foyer and J. Q. Yu (2015). "Interplay between reactive oxygen species and hormones in the control of plant development and stress tolerance." J Exp Bot **66**(10): 2839-2856.

Xing, Y., Q. Cao, Q. Zhang, L. Qin, W. Jia and J. Zhang (2013). "MKK5 regulates high light-induced gene expression of Cu/Zn superoxide dismutase 1 and 2 in Arabidopsis." Plant Cell Physiol **54**(7): 1217-1227.

Xu, G. and M. R. Chance (2005). "Radiolytic modification of sulfur-containing amino acid residues in model peptides: fundamental studies for protein footprinting." Anal Chem **77**(8): 2437-2449.

Yang, T. and B. W. Poovaiah (2002). "Hydrogen peroxide homeostasis: activation of plant catalase by calcium/calmodulin." Proc Natl Acad Sci U S A **99**(6): 4097-4102.

Yang Y, Han C, Liu Q, Lin B, Wang J. 2008. E ect of drought and low light on growth and enzymatic antioxidant system of *Picea asperata* seedlings. Acta Physiol Plant **30**: 433–440.

Yang, W., C. Zhu, X. Ma, G. Li, L. Gan, D. Ng and K. Xia (2013). "Hydrogen peroxide is a second messenger in the salicylic acid-triggered adventitious rooting process in mung bean seedlings." PLoS One **8**(12): e84580.

Yeh, J. I., A. Claiborne and W. G. Hol (1996). "Structure of the native cysteine-sulfenic acid redox center of enterococcal NADH peroxidase refined at 2.8 A resolution." Biochemistry **35**(31): 9951-9957.

Ying, J., N. Clavreul, M. Sethuraman, T. Adachi and R. A. Cohen (2007). "Thiol oxidation in signaling and response to stress: detection and quantification of physiological and pathophysiological thiol modifications." Free Radic Biol Med **43**(8): 1099-1108.

Yoo, S. K., T. W. Starnes, Q. Deng and A. Huttenlocher (2011). "Lyn is a redox sensor that mediates leukocyte wound attraction in vivo." Nature **480**(7375): 109-112.

Yu, L., J. Nie, C. Cao, Y. Jin, M. Yan, F. Wang, J. Liu, Y. Xiao, Y. Liang and W. Zhang (2010). "Phosphatidic acid mediates salt stress response by regulation of MPK6 in *Arabidopsis thaliana*." New Phytol **188**(3): 762-773.

Zhang, L., D. Xi, S. Li, Z. Gao, S. Zhao, J. Shi, C. Wu and X. Guo (2011). "A cotton group C MAP kinase gene, GhMPK2, positively regulates salt and drought tolerance in tobacco." Plant Mol Biol **77**(1-2): 17-31.

Zhang Y, Yang J, Lu S, Cai J, Guo Z. 2008. Overexpressing *SgNCED1* in tobacco increases aba level, antioxidant enzyme activities, and stress tolerance. J Plant Growth Regul **27**: 151–158

Zhang, X., F. C. Dong, J. F. Gao and C. P. Song (2001). "Hydrogen peroxide-induced changes in intracellular pH of guard cells precede stomatal closure." Cell Res **11**(1): 37-43.

Zhou, C., Z. Cai, Y. Guo and S. Gan (2009). "An arabidopsis mitogen-activated protein kinase cascade, MKK9-MPK6, plays a role in leaf senescence." Plant Physiol **150**(1): 167-177.

Chapter 2

Arabidopsis thaliana dehydroascorbate reductase 2: Conformational flexibility during catalysis

Nandita Bodra, David Young, Leonardo Astolfi Rosado, Anna Pallo, Khadija Wahni, Frank De Proft, Jingjing Huang, Frank Van Breusegem, Joris Messens

This work has been published in a modified version in Nature Scientific Reports.2017 Feb 14;7:42494. doi: 10.1038/srep42494.

Author Contributions

All authors contributed to the design of the experiments, which were performed by Nandita Bodra, David Young, Leonardo Astolfi Rosado, Anna Pallo, and Khadija Wahni. Nandita Bodra, David Young, Leonardo Astolfi Rosado, Frank Van Breusegem and Joris Messens wrote the manuscript. Joris Messens and Frank Van Breusegem supervised the project.

Chapter 2

Arabidopsis thaliana dehydroascorbate reductase 2: Conformational flexibility during catalysis

Abstract

Dehydroascorbate reductase (DHAR) catalyzes the glutathione (GSH) dependent reduction of dehydroascorbate and plays a direct role in regenerating ascorbic acid, an essential plant antioxidant vital for defense against oxidative stress. DHAR enzymes bear close structural homology to the glutathione transferase (GST) superfamily of enzymes and contain the same active site motif, but most GSTs do not exhibit DHAR activity. The presence of a cysteine at the active site is essential for the catalytic functioning of DHAR, as mutation of this cysteine abolishes the activity. Here we present the crystal structure of DHAR2 from *Arabidopsis thaliana* with GSH bound to the catalytic cysteine. This structure reveals localized conformational differences around the active site which distinguishes the GSH-bound DHAR2 structure from that of DHAR1. We also unraveled the enzymatic step in which DHAR releases oxidized glutathione (GSSG). To consolidate our structural and kinetic findings, we investigated potential conformational flexibility in DHAR2 by normal mode analysis and found that subdomain mobility could be linked to GSH binding or GSSG release.

2.1 Introduction

Oxidative stress has a significant impact on the cellular environment of organisms. Control of the reactive oxygen species (ROS) that cause such stress is essential for effective redox homeostasis. Generation of ROS can occur endogenously through leakage from respiratory complexes or photosystems, or can be induced by external stressors, such as UV radiation, drought, temperature extremes, or elevated salinity (Price, Atherton et al. 1989, Hernandez, Jimenez et al. 2000, Sharma and Dubey 2005, Krieger-Liszkay, Fufezan et al. 2008, Vass and Cser 2009). Once released, ROS inflict cellular damage through oxidative inactivation of enzymes, metal oxidation, and mutagenesis (Breen and Murphy 1995, Wu, O'Doherty et al. 2011). Soluble small-molecule antioxidants, such as ascorbate (AsA) or glutathione (GSH),

neutralize ROS either by direct reduction or by acting as cofactors for redox enzymes, such as peroxidases ((Koussevitzky, Suzuki et al. 2008, Gill and Tuteja 2010) Cellular compartments maintain a reducing environment by constant recycling of oxidized antioxidants back to their reduced forms, a reaction catalyzed by glutathione reductase (GR) in the case of oxidized glutathione (GSSG) and dehydroascorbate reductase (DHAR) for dehydroascorbate (DHA), the oxidized form of AsA (Foyer and Halliwell 1977). Intracellular concentration of GSH and AsA in plants are typically maintained within the range of 2–6 mM and 2–25 mM, respectively. GSH (5 mM) is able to directly reduce DHA through a non-enzymatic mechanism, albeit at a rate of 17 $nmol.min^{-1}$ (Winkler, Orselli et al. 1994, Meyer and Fricker 2000), which is significantly lower than the reduction catalyzed by DHAR (20–370 $\mu mol.min^{-1}.mg^{-1}$). AsA typically behaves as a single-electron donor and is converted to its semi-oxidized radical form, monodehydroascorbate (MDHA) upon ROS reduction. Two molecules of MDHA then disproportionate into AsA and DHA or, alternatively, MDHA can be enzymatically reduced to AsA by MDHA reductase (Shigeoka, Yasumoto et al. 1987). Whereas GSH is relatively stable in its oxidized form, DHA undergoes irreversible hydrolysis to diketogulonate (DKG) (Washko, Welch et al. 1992), and therefore, rapid reduction of DHA in cells is critical for effective AsA recycling. AsA is the major antioxidant of plants and, accordingly, the majority of the characterized DHAR enzymes are of plant origin. Plant DHAR enzymes contain a conserved catalytic motif CPFS/C and are largely categorized into four isoforms, DHAR1, DHAR2, DHAR3 and DHAR4 (Zhang, Wang et al. 2015) . To date, four independent structures of plant DHAR have been deposited in the Protein Data Bank: the crystallographic structures of *Oryza sativa* (rice) (OsDHAR1; PDB, 5D9T) (Do, Kim et al. 2016), *Pennisetum glaucum* (pearl millet) (PgDHAR1; PDB, 5EV0, 5IQY), the nuclear magnetic resonance solution structure of DHAR3A from *Populus trichocarpa* (black cottonwood) (PtDHAR3A; PDB, 2N5F) (Krishna Das, Kumar et al. 2016, Lallement, Roret et al. 2016), and the recently deposited crystal structure of *Arabidopsis thaliana* DHAR1 (AtDHAR1; PDB, 5EL8). In addition, crystal structures of *P. trichocarpa* GST Lambda (PtGSTL) (Lallement, Meux et al. 2014) and *Homo sapiens* GST Omega (HsGSTO) (Zhou, Brock et al. 2012) with DHAR activity have been determined with GSH bound at the catalytic cysteine. As the AtDHAR1 structure is yet to be published, we will not discuss it here.

DHAR is also structurally homologous to chloride intracellular channel (CLIC) proteins which, in their soluble globular state, have been shown to exhibit low levels of DHAR activity, although they primarily function as multimeric membrane-integrated ion channels (Littler,

Harrop et al. 2004, Bryan and Orban 2010, Al Khamici, Brown et al. 2015). Intriguingly, AtDHAR1 also appears to be capable of transmembrane ion conductance, but the relevance of such activity has still to be explored (Elter, Hartel et al. 2007). Recently, a mechanism for DHA reduction by DHAR has been proposed, based on the oxidized and AsA-bound structures of OsDHAR1 (Do, Kim et al. 2016). Here, from the structural and biochemical investigation of *Arabidopsis* DHAR2 (AtDHAR2), we provide further support for this mechanism and use elastic network modeling to explore the apparently allosteric behavior in the enzymatic DHAR2 mechanism.

2.2 Materials and methods

Cloning, purification, and glutathionylation of AtDHAR2

Recombinant AtDHAR2 was expressed in *Escherichia coli* C41 (DE3) and purified as described (Waszczak, Akter et al. 2014). Glutathionylated AtDHAR2 was prepared by a 5-min pre-equilibration of 20 μM DHAR2 with 1 mM GSH, followed by a 30-min incubation with 1 mM H_2O_2 at room temperature. Excess GSH was removed by gel filtration with a 16/60 Superdex75 column (GE Healthcare) equilibrated in 20 mM Hepes (pH 7.5), 150 mM NaCl, and 1 mM EDTA and eluted protein was concentrated by centrifugal filtration.

Derivatization of GSH with monobromobimane (mBBr)

For mBBr derivatization of GSSG-derived GSH, enzyme samples, known standards, and controls were prepared as described previously (Cotgreave and Moldeus 1986, Winters, Zukowski et al. 1995). Samples of 0.001–1 mM GSH, 1–100 μM GSSG, 100 μM of glutathionylated DHAR2, and 100 μM of glutathionylated DHAR2 with 1 mM GSH were prepared in 300 mM MOPS (pH 7), 150 mM NaCl, and 1 mM EDTA (freshly flushed with argon gas). Of each sample, 20 μL was mixed with 25 μL acetonitrile, 5 μL of 10 mM N-ethylmaleamide for alkylation of free thiols, and incubated at room temperature for 30 min. Sample pH was brought to pH 10.5 by 0.5 M NaOH and, after 5 min, the pH was readjusted to pH 7 with 1M HCl. After centrifugation for 5min at 20,000×g, tris(2-carboxyethyl) phosphine was added to a final concentration of 1 mM and samples were incubated for 20 min. Subsequently, mBBr (in acetonitrile) was added to a final concentration of 10 mM and samples were incubated in the dark at room temperature for 20 min. The mBBr derivatization was stopped by addition of 40 mM methane sulfonic acid at a 10:1 acid:sample ratio. Protein

aggregates were removed by centrifugation (5 min, 20,000×g) and syringe filtration (with a 0.2-µm filter).

HPLC reversed-phase analysis

Of each of the derivative samples described above, 100 µL was injected onto a C18 column (ACE 5 C18 AR 250 × 4.6 mm) on an Alliance HPLC system (Waters) operated at 25°C. Fluorescence was monitored with a detector at an excitation λ of 390 nm and emission λ filter of 478 nm. Mobile phases used were 10% (v/v) methanol, 0.25% (v/v) acetic acid (solvent A) to 90% (v/v) methanol, 0.25% (v/v) acetic acid (solvent B), at a flow rate of 0.7 $mL.min^{-1}$. Upon sample injection, the mobile phase was held at 100% (v/v) solvent A for 7.14 min, then a gradient was applied with sequential composition targets of 90% (v/v) solvent A and 10% (v/v) solvent B for 21.42 min, 80% (v/v) solvent A and 20% (v/v) solvent B for 42.85 min, 20% (v/v) solvent A and 80% (v/v) solvent B for 57.14 min, 100% (v/v) solvent B for 64.28, and 100% (v/v) solvent A for 78.57 min. Data were analyzed by means of the Empower®3 software.

Steady-state kinetics

The steady-state kinetics of AtDHAR2 were measured in a spectrophotometric assay in 0.5-cm and 1.0-cm path-length quartz cuvettes with 100 Bio UV-visible spectrophotometer (Cary) equipped with a temperature-controlled cuvette holder. The AtDHAR2 activity was determined by following the formation of AsA at 265 nm (with a molar extinction coefficient of 7000 $M^{-1}.cm^{-1}$) under saturated conditions of DHA (200 µM) with varying concentrations of GSH, ranging from 0.5 mM to 15 mM. Both enzymes and substrates were prepared in assay buffer (300 mM MOPS, pH 7.0, 150 mM NaCl, and 1 mM EDTA). The reaction began with the addition of AtDHAR2-SG at a final concentration of 100 nM to a starting sample mixture of GSH and DHA in a 0.5-mL final volume. All experiments were done in duplicate. One unit of enzyme activity (U) was defined as the amount of enzyme required for the conversion of 1 µmol of substrate into product per minute at 30°C. The experimental data were fitted to an allosteric sigmoidal equation (Eq. 1), where v is the steady state velocity, S is the substrate concentration, V_{max} is the maximum rate velocity, $K_{0.5}$ is the substrate concentration that gives

half the maximal velocity, and h is the Hill coefficient. All the data were analyzed with the GraphPad Prism 6.0 software.

$$v = V_{max}[S]^h/(K_{0.5}^h + [S]^h) \qquad \text{Eq. 1}$$

Fluorescence spectroscopy and stopped-flow analysis

AtDHAR2 contains four tryptophan residues (Trp50, Trp69, Trp171, and Trp207), of which one (Trp207) is located at the H-site and is expected to interact directly with GSH. The overall change in fluorescence of S-glutathionylated AtDHAR2 (prepared as described above) upon rapid mixing with GSH was determined with a SX-20 stopped-flow spectrometer equipped with a fluorescence detector. The final concentration of AtDHAR2-SG was 1 µM in the assay buffer with the GSH concentrations ranging from 0.5 to 17.5 mM. Samples were excited at 295 nm with an emission cut-off of 320 nm. All measurements were done at 30°C and in triplicate. A single exponential function was used to determine the observable rate constant (k_{obs}). The k_{obs} values were fitted as a function of varied substrate concentration (S) to an equation describing a linear relationship, where k_{+1} is the forward and k_{-1} the reverse rate constant (Figure 4A).

$$k_{obs} = k_{+1}S + k_{-1} \qquad \text{Eq. 2}$$

Crystallization and diffraction data collection

Glutathionylated AtDHAR2 (prepared as described above) at 20 mg. mL^{-1} was crystallized by vapor diffusion in a hanging droplet consisting of 1 µL protein, 1 µL precipitant solution (2 M ammonium sulfate, 0.1 M sodium acetate, pH 4.8) at 20°C. Crystals were cryoprotected by 20% (v/v) glycerol. X-ray diffraction data were collected on a PILATUS 6M detector (Dectris) at the Proxima1 beamline of the SOLEIL Synchrotron (Paris). Diffraction data were indexed and integrated in XDS (Kabsch 2010) and the space group of P21221 assigned in POINTLESS (Evans 2006) based on systematic absences on axial reflections. Scaling and merging of reflections was carried out in AIMLESS (Evans and Murshudov 2013) of the CCP4 program suite (Collaborative Computational Project 1994), with 5% of unique reflections set aside as R-free set.

Structure determination

Initial phases were determined in Phaser (McCoy, Grosse-Kunstleve et al. 2007) by molecular replacement with the structure of OsDHAR1 as search model. Initial model building and further iterative structural modifications were carried out in COOT (Emsley and Cowtan 2004), and maximum-likelihood refinement performed in REFMAC5 (Murshudov, Skubak et al. 2011) and Phenix.refine (Heinig and Frishman 2004). Stereochemistry of the model was checked with MolProbity (Chen, Arendall et al. 2010). The Ramachandran plot showed 94.4% of residues to be favored, 5% allowed, and 0.6% generously allowed. Diffraction data collection and refinement statistics are presented in Table 1. The atomic coordinates and structure factors of AtDHAR2 have been deposited in the PDB under the accession code 5LOL.

Table. 1

Data collection	
Wavelength (Å)	0.9786
Resolution range (Å)	38.73 - 2.3 (2.382 - 2.3)
Space group	$P2_122_1$
Unit cell dimensions (Å)	a = 47.107, b = 67.002, c = 68.026
Total reflections	59565 (2217)
Unique reflections	9622 (733)
Multiplicity	6.2 (3.0)
Completeness (%)	96 (75)
Mean I/σ(I)	15.01 (1.7)
Wilson B-factor (Å^2)	32.57
R_{merge} (%)	9.996 (67.64)
R_{meas} (%)	10.85 (70.28)
$CC_{1/2}$	0.997 (0.573)
CC*	0.999 (0.854)
Refinement	
Reflections used in refinement	9619 (733)
Reflections used for R_{free}	460 (29)
R_{work} (%)	21.18 (26.80)
R_{free} (%)	22.20 (28.57)
CC_{work}	0.938 (0.768)
CC_{free}	0.908 (0.762)
Number of non-hydrogen atoms	1739
Macromolecules	1658
Ligands	31
Protein residues	207
RMS bonds (Å)	0.011
RMS angles (°)	1.34
Ramachandran favored (%)	98
Ramachandran allowed (%)	1.9
Ramachandran outliers (%)	0
Rotamer outliers (%)	0.53
Clashscore	3.52
Molprobity score	1.14
Average B-factor (Å^2)	36.25
Macromolecules	36.2
Ligands	41.14
Solvent	34.92

It is pertinent to highlight the presence of unmodeled electron density at the H-site of AtDHAR2 (Figure. 1). After failed efforts to model components of the purification buffer, mother liquor, or cryoprotectant, an attempt was made to model GSH in this region. Two putative conformations of the H-site GSH were placed, one with the glycinyl terminus oriented inward toward Asp19 and the other in a reverse orientation with the γ-glutamyl directed inward. The modeled GSH gave an acceptable fit to the electron density (Real-space R= 23%) and an average B-factor of 50Å^2. However, placement of the H-site GSH was unjustified because of a significant lack of stabilizing protein interactions and relatively unfavorable stereochemistry (bond length/angle root-mean-square Z score of 2.2–4, depending on conformer orientation).

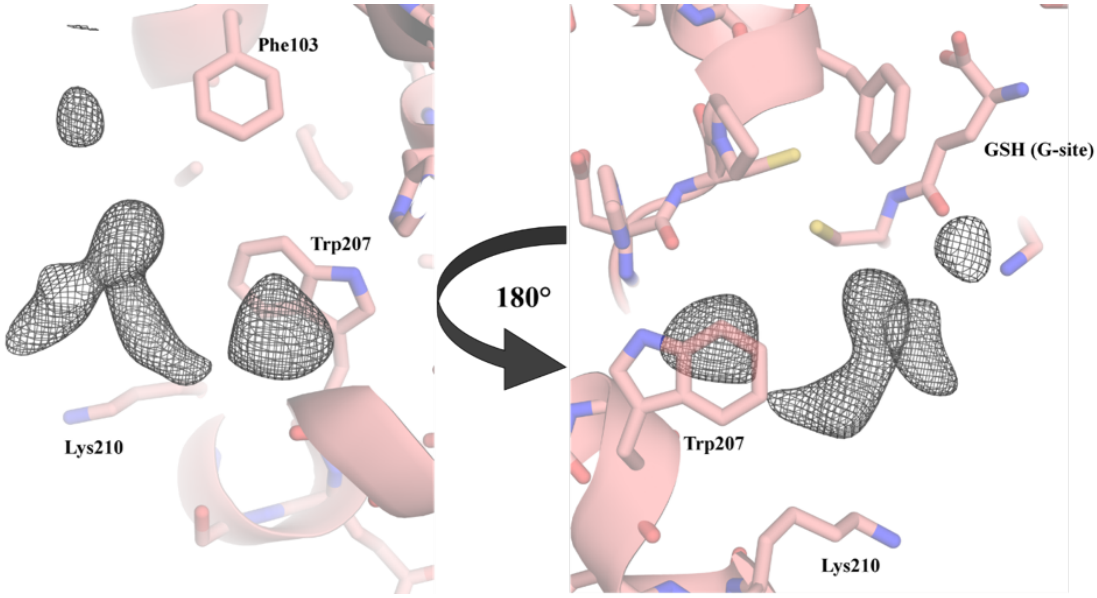

Figure 1. Unmodeled density at the H-site of AtDHAR2. The G-site GSH and the H-site residues, Phe103, Lys210, and Trp207 are indicated. Electron density from a mF_O-DF_C difference map contoured at 3 σ is presented as grey isomesh.

Structural analysis

Subdomains and hinge axes were identified with the DynDom web server (http://fizz. cmp.uea.ac.uk/dyndom/) (Hayward, Kitao et al. 1997). Secondary structure elements were assigned with Stride (http://webclu.bio.wzw.tum. de/stride/) (Chen, Arendall et al. 2010). Normal mode analysis was carried out in the elNémo (http://igs-server.cnrs-mrs.fr/elnemo/index. html) (Suhre and Sanejouand 2004) and ANM 2.0 (http://anm.csb.pitt.edu) (Eyal, Lum et al. 2015) web servers with default parameters.

Structural superposition was performed in the Superpose module of CCP4 by means of the Gesamt algorithm. All structural figures were prepared with PyMOL (Schrodinger 2015).

2.3 Result and discussions

The kinetic parameters and the release of GSSG as reaction product

Previously, DHAR has been reported to have a bi-uni-uni-uni ping-pong enzymatic mechanism, with GSH and DHA interacting with the catalytic cysteine (Cys20 in AtDHAR2) in separate, sequential binding events (Shimaoka, Miyake et al. 2003). This catalytic cysteine is essential for enzymatic activity, and mutation to a serine (to mimic the catalytic motif common to GSTs) has been shown to abolish the DHA reductase activity (Shimaoka, Miyake et al. 2003). The reduction of DHA by DHAR has been proposed to result in the formation of a sulfenic acid at the catalytic cysteine, based on the crystallographic identification of Cys20 over-oxidation in OsDHAR1 upon soaking crystals with DHA (Zhang, Wang et al. 2015). A sulfenic acid at Cys20 of AtDHAR2 has also been identified in Arabidopsis cell suspensions subjected to oxidative stress (Waszczak, Akter et al. 2014). Cysteinyl sulfenic acids readily form mixed disulfides with GSH under physiological conditions, thereby protecting against irreversible over-oxidation of the cysteine sulfur (Turell, Botti et al. 2008, Roos and Messens 2011, Gupta and Carroll 2014, Bak and Weerapana 2015). Such S-glutathionylation of a sulfenylated Cys20 comprises reaction step 1 of the mechanistic scheme (Figure. 2), of which the formation in AtDHAR2 had previously been confirmed by mass spectrometric analysis (Waszczak, Akter et al. 2014). Nucleophilic attack of a second molecule of GSH on the Cys20 mixed disulfide then generates the reduced enzyme form with a thiol at catalytic Cys20 (Figure. 2, step 2) and releases GSSG as by-product. However, as of yet, no direct biochemical evidence exists to support this mechanistic step.

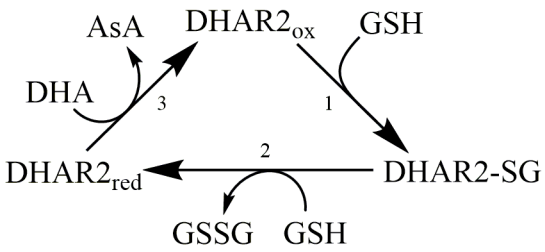

Figure 2. Reaction scheme for the catalytic cycle of DHA reduction by DHAR2. In a mechanistic scheme, the ping-pong mechanism for the enzymatic reduction of DHA is shown. DHAR2 is sulfenylated at the catalytic cysteine (Cys20) and GSH performs a nucleophilic attack on the sulfenylated Cys20 to form mixed

disulfide, DHAR2-S-SG (step 1). A second GSH molecule reacts with mixed disulfide, producing GSSG and the cysteine is released in its reduced thiolate form (step 2). DHA enters the active site of the reduced form of DHAR2 and is converted to AsA (step 3).

To experimentally validate reaction step 2, we detected the generation of GSSG from S-glutathionylated AtDHAR2 through thiol-labeling of the GSSG reduction product, GSH, by monobromobimane (mBBr). This mBBr is an essentially non-fluorescent compound that can form a conjugate with GSH via nucleophilic attack of the glutathione thiolate at the alkyl halide with formation of a thioether bond. The resulting conjugate is highly fluorescent and mBBr derivatization has been effectively applied in the quantification of free GSH in the pmol range (Fahey and Newton 1987). The reactivity of mBBr is largely thiol specific, and conjugations to amines or other nucleophiles occur at a markedly low rate. Analysis of the mBBr conjugates by reversed-phase high-performance liquid chromatography (RP-HPLC) allows the separation and distinction of hydrolysis products and other contaminants from the fluorescent mBBr-glutathione conjugate (mB-SG). By treating pre-glutathionylated AtDHAR2 with excess GSH and then blocking free thiols with an N-ethylmaleamide (NEM), the formation of GSSG was detected by reduction and subsequent mBBr derivatization (Figure. 3). From this, it could be concluded that GSH reacts with the mixed-disulfide of S-glutathionylated DHAR2, producing GSSG and a reduced thiol at Cys20.

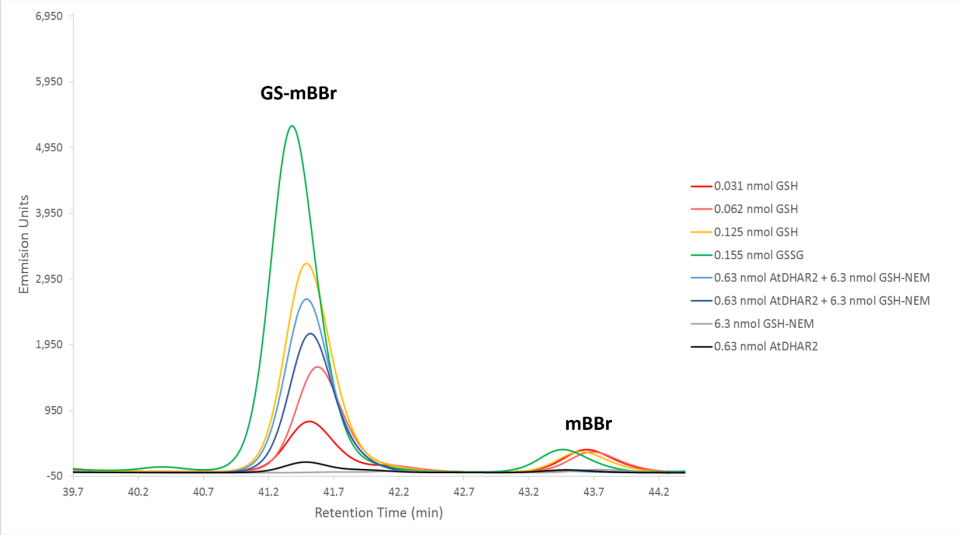

Figure 3. Reversed phase fluorescence elution profile of the glutathione monobromobimane (GS-MBBr) derivatives. Fluorescence peaks were assigned according to known standards. GSH was alkylated prior to reduction of GSSG, therefore, no mBBr derivatization of the GSH substrate was observed, as shown by the negative control of 6.3 nmol GSH-N-ethylmaleamide (NEM) (gray trace). AtDHAR2-SG without addition of free GSH was used as negative control (black trace). The fluorescence peak for two independent replicates with 0.63 nmol AtDHAR2 with 6.3 nmol GSH-N- ethylmaleamide (NEM) were observed (light and dark blue traces). Concentrations are given as final molar values for the total injected sample.

With the understanding that GSSG can be generated from S-glutathionylated AtDHAR2, we determined the catalytic rate of reaction step 2 by exploiting the intrinsic fluorescence of AtDHAR2 (which contains four tryptophan residues) in a stopped-flow analysis of the GSSG formation from a AtDHAR2-SG mixed-disulfide (Figure. 4A). A second-order rate constant of 1331±13 $M^{-1}s^{-1}$ was found and a rate of 5.6 (±0.02) s^{-1} at 4 mM GSH, which is an assumed average physiological concentration of GSH in the Arabidopsis cell cytoplasm (Meyer and Fricker 2000).

Characterization of the steady-state kinetics of AtDHAR2 under saturated DHA conditions (200 µM with $K_{0.5}$= 23± 1 µM for DHA) (Waszczak, Akter et al. 2014) with variable concentrations of GSH revealed a sigmoidal behavior of velocity dependence, indicative of cooperative interplay (Figure. 4B). Fitting data to equation 1 (see Materials and Methods) yielded a $K_{0.5}$= 3.9 ± 0.4 mM, V_{max}= 20 ± 1 µmol $min^{-1}mg^{-}$, k_{cat}= 7.8 ± 0.4 s^{-1}, and h = 1.6 ± 0.15. The Hill coefficient indicates either a positive heterotropic effect of GSH on DHA binding, or a positive homotropic effect of GSH on the affinity of the second molecule of GSH. Previous kinetic characterization of AtDHAR2 revealed a Hill coefficient of 2.6 when varying the concentration of DHA (Waszczak, Akter et al. 2014). Taken together, AtDHAR2 is the first DHAR to display allosteric behavior. The V_{max} of AtDHAR2 is markedly lower than that reported for OsDHAR1 (350 µmol $min^{-1}mg^{-1}$), although the kinetic parameters of OsDHAR1 were measured at pH 8 (the catalytic optimum) (Amako, Ushimaru et al. 2006), whereas the steady-state kinetics of AtDHAR2 were measured at pH 7 (Table 2).

Table 2. Summarized kinetic parameters of plant DHARs and GSTL

Enzyme	K_m^{GSH} **(mM)**	K_m^{DHA} **(mM)**	k_{cat} **(s^{-1})**	**Specific activity (µmol min^{-1} mg^{-1})**
DHAR1[a] **(*Oryza sativa*)**	1	0.35	----	350
DHAR1[b] **(*Spinacea oleracea*)**	2.5	0.07	----	370
DHAR2[c, d] **(*Arabidopsis thaliana*)**	3.9 ± 0.4	0.023 ± 0.01	7.8 ± 0.4	20 ± 1
DHAR3A[e] **(*Populus trichocarpa*)**	----	0.18 ± 0.02	315 ± 5	----
GSTL1[f] **(*Populus trichocarpa*)**	----	0.09 ± 0.01	1.5 ± 0.027	----

[a] Amako (2006), [b] Hossain (1984), [c] Present work, [d] Waszczak (2014), [e] Lallement (2016), [f] Lallement, (2014)

The catalytic activity of OsDHAR1 was almost 50% lower than the full activity at pH 7 and, therefore, caution should be taken when directly cross-comparing catalytic parameters of DHARs (Kato, Urano et al. 1997). The k_{cat}/K_M of OsDHAR1 for DHA is within the same range as the k_{cat}/K_M for GSH, 3.91×10^5 $M^{-1}s^{-1}$ and 1.37×10^5 $M^{-1}s^{-1}$, respectively, showing a comparable substrate specificity (Amako, Ushimaru et al. 2006). In contrast, the $k_{cat}/K_{0.5}$ of AtDHAR2 for DHA was significantly higher than for GSH, 3.39×10^5 $M^{-1}s^{-1}$ and 2×10^3 $M^{-1}s^{-1}$, respectively, hinting at a considerably higher substrate specificity for DHA in the case of AtDHAR2.

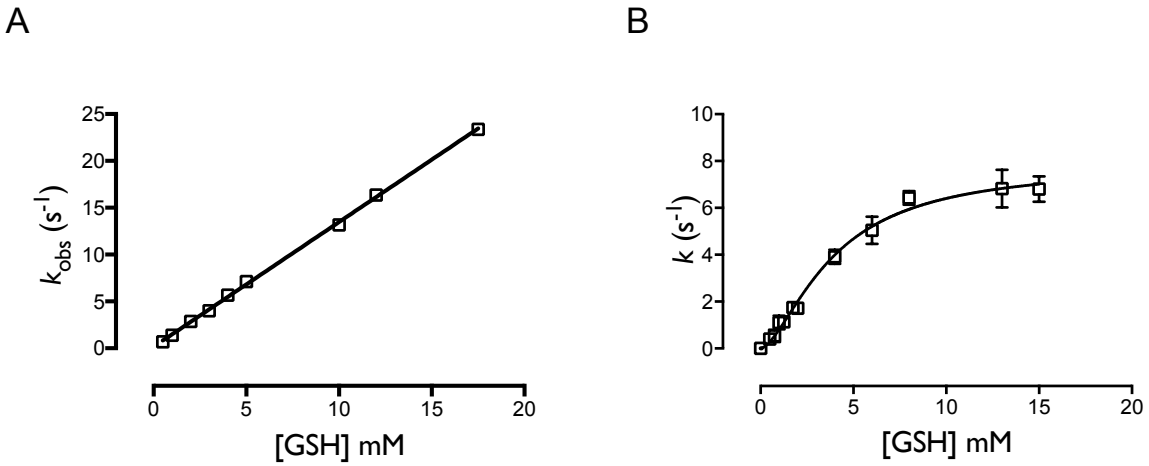

Figure 4. Pre-steady state kinetics of AtDHAR2. (A) Stopped flow analysis of the reaction of GSH with AtDHAR2: GSH. A linear dependence of the observable rate constants allowed the calculation of second-order rate constant of 1331 ± 13 $M^{-1}s^{-1}$ for the conversion of S-glutathionylated DHAR2 to its reduced form. (B) A sigmoidal rate variance with respect to GSH concentration with a fixed saturated concentration of DHA (200 μM), represented as a rate constant k (s^{-1}) versus the GSH concentration in mM.

The k of reaction step 2, i.e., AtDHAR2 reduction and GSSG formation at 4 mM GSH (as derived from the stopped-flow analysis), is relatively close to the steady-state k value at an equivalent GSH concentration (5.6 ± 0.02 s^{-1} and 3.8 ± 0.2 s^{-1}, respectively), and at GSH concentrations below 4 mM, k values from stopped-flow and steady-state converge even further. This indicates that at sub-physiological GSH concentrations (below 4 mM), reaction step 2 is probably the rate-limiting step in the catalytic cycle of AtDHAR2. Allosteric enzymes in a ping-pong mechanism are characterized by stable interconvertible macro-states throughout the reaction sequence, usually related to chemical modifications of the original enzyme, such as enzyme reduction (Sumi and Ui 1972). As stopped-flow analysis measures the overall

change in protein fluorescence, and considering the kinetic allostery implied in the steady-state kinetics, it is possible to conclude that the rate limitation is related to structural changes.

Overall structure of AtDHAR2

The crystal structure of AtDHAR2 in complex with GSH was solved by molecular replacement to a resolution of 2.3 Å in space group P21221. Due to the inherent flexibility of the terminal regions of the polypeptide chain, residues 1–4 and 212–213 of the 213-residue protein were undefined by electron density. AtDHAR2 crystallized as a monomer and exhibited the classic structural architecture common to the GST super-family, with an all-helical C-terminal domain, and a thioredoxin-like N-terminal domain consisting of a mixture of β-sheets and α-helices (Figure. 5). The overall structural fold of AtDHAR2 is almost identical to that of the structures of OsDHAR1 and PgDHAR1, albeit with the inclusion of an additional short-chain helical turn preceding the α1-helix (Figure. 5).

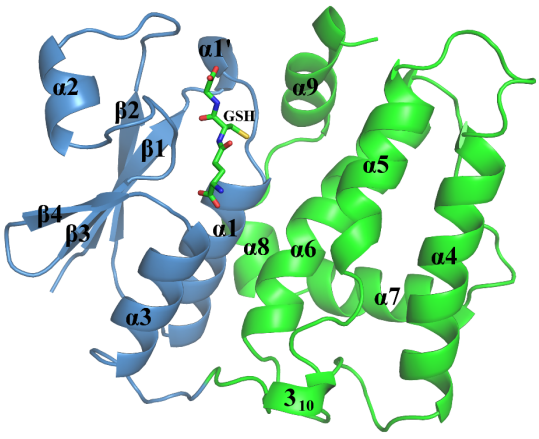

Figure 5. Crystal structure of the GSH-bound AtDHAR2. The N-terminal thioredoxin like domain (blue) and the C-terminal helical domain (green) are shown.

The AtDHAR2 structure superposes well with those of OsDHAR1 and PgDHAR1, aligning with a root-mean-square deviation of 0.85 Å over 193 Cα and 0.8 Å over 191 Cα, respectively, with structural differences arising primarily across the α2-helix-containing region. Structural overlay plant DHARs, plant GSTL1, human GSTO2, and human CLIC1 revealed a localized conformational variability in the α2-helical region (Figure 6). Comparative analysis of the structures of AtDHAR2 and OsDHAR1 by the DynDom server

(http://fizz.cmp.uea.ac.uk/dyndom/) (Hayward, Kitao et al. 1997) identified the α2-helix to be a hinged subdomain, spanning residues 32–63.

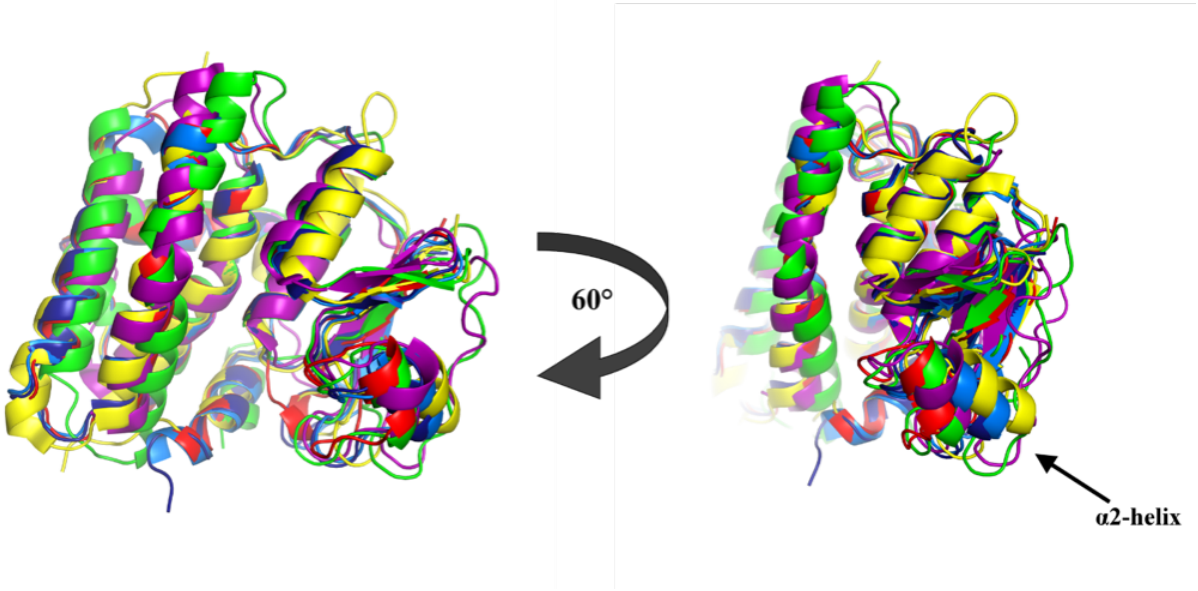

Figure 6. The superimposed structures of AtDHAR2 (red), GSTO-2 (green), PtGSTL1 (purple), AtDHAR1 (dark blue), OsDHAR1 (light blue), and CLIC1 (yellow) show a marked conformational variability in the α2-helix region.

Interactions of a putative hinged subdomain with G-site GSH

Glutaredoxins (Grx) and the GST enzyme family bind GSH in the solvent-exposed active site cleft at a region designated the G-site. Residues involved in the binding of GSH at the G-site are all located within the N-terminal thioredoxin-like domain, and a core interaction invariably occurs between the thiol of GSH and the catalytic motif consists of cysteine, serine and tyrosine residue of the α1-helix.

GSH was placed into the available electron density of the mF_O-DF_C difference map at the G-site of AtDHAR2 at full occupancy in a non-covalently bound state. The cysteinyl sulfur of GSH was in close proximity (2.8 Å) to the sulfur atom of Cys20, thereby indicating that the GSH was likely engaged in a mixed disulfide (for which a maximum bond length of 2.3Å is commonly applied) with Cys20 before disulfide cleavage by X-ray irradiation, a well-characterized phenomenon (Weik, Berges et al. 2002, Roberts, Wood et al. 2005, Sutton, Black et al. 2013). As an indication of the relative stability of GSH binding, the average B-factor for the G-site GSH (34.9 $Å^2$) is comparable to that determined for the polypeptide main-chain

atoms (34.8Å^2). The GSH γ-glutamyl is particularly well stabilized, as evidenced by low B-factor values of 24–29 Å^2, accepts H-bonds to its carboxylate from a water molecule and from the backbone amide and side-chain hydroxyl of Ser73, and forms a salt bridge interaction with Asp72 via its amine group (Figure. 7). The γ-glutamyl group is also engaged in van der Waals interactions with Phe22, and hydrogen-bonds the side-chain amine of Lys59 by its γ-glutamyl peptide carbonyl. The central cysteinyl region of the GSH molecule is stabilized by hydrogen bonding of the carbonyl and amide of the cysteine with the backbone amide and carbonyl groups of Val60. The glycinyl group of GSH is less tightly bound, as reflected by elevated B-factors of 39–48 Å^2, forming a single salt bridge with the side-chain amine of Lys47 through its carboxylate. Among the GST enzyme family, Asp72 and Ser73 are well conserved and are also present in the GSH-bound structures of PtGSTL and HsGSTO2, whereas Lys47 and Lys59 are less well conserved, although they are often substituted by equivalently charged residues. In the case of HsGSTO2, Lys47 is conserved (Lys59 in HsGSTO2) and forms a salt bridge interaction with GSH, and a histidine residue occupies the Lys59 position, but without forming an interaction with G-site GSH (Zhou, Brock et al. 2012). Similarly, in the PtGSTL structure, an arginine substitutes the salt bridge by Lys47, and although Lys59 is conserved (Lys78 in PtGSTL1), it does not form a hydrogen bond with GSH (Lallement, Meux et al. 2014). In the S-glutathionylated structure of HsCLIC1 (PDB, 1K0N), there are surprisingly few interactions with GSH. H-bonds are formed only through Thr77 (CLIC1 numbering) and the peptide backbone carbonyl of Leu54 (CLIC1 numbering), with Lys49 (Lys47 in AtDHAR2) too distant for salt bridge formation and Lys59 is not conserved (Glu63 in CLIC1) (Harrop, DeMaere et al. 2001).

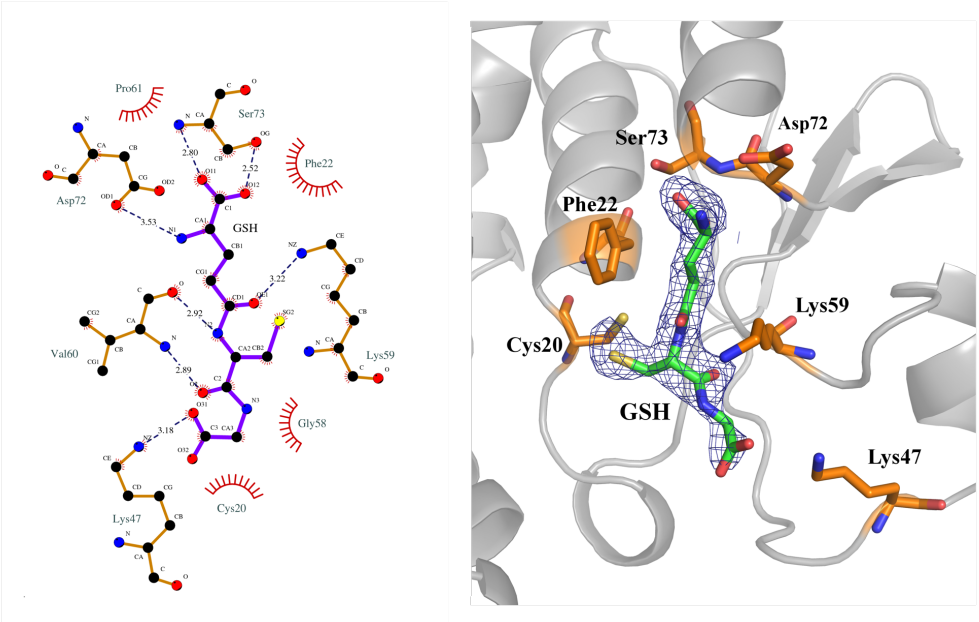

Figure 7. Schematic representation of the G-site GSH environment in AtDHAR2. The bonding environment of GSH at the G-site of AtDHAR2 is displayed in LIGPLOT (left panel) and PyMOL (right panel) (Sumi and Ui 1972). H-bonding and salt bridge interactions are illustrated in LIGPLOT by blue dashed lines. The mF_o-DF_c omit map for GSH is defined by a blue mesh contoured at 3σ. Waters interacting with GSH are omitted.

The H-site and the nature of DHA binding

In addition to the G-site, the GST enzyme family also possesses a second substrate binding site, designated the H-site, which mostly consists of residues from the C-terminal domain. In contrast to the conserved nature of the G-site, the H-site typically exhibits more structural plasticity among GSTs, relating to a substrate specificity variation. Based on the crystal structure of OsDHAR1, both DHA and a secondary GSH molecule are able to bind at the H-site of DHAR, albeit not simultaneously. From the structure of the AsA-bound OsDHAR1, Lys8, Asp19, and Lys210 are identified as forming H-bonds with AsA (Zhang, Wang et al. 2015). The structure of PgDHAR1 also supports the role of Lys8 and Asp19 in DHA binding, with glycerol as a mimic of the 1,2-dihydroxyethyl arm of AsA (Krishna Das, Kumar et al. 2016). In addition to the charged residues mentioned above, hydrophobic van der Waals interactions from Pro21, Phe104, and Trp207 contribute to the binding of AsA in the crystal structure of the AsA-bound OsDHAR1 (Do, Kim et al. 2016). All the residues observed to interact with AsA in the OsDHAR1 structure are conserved among DHARs (Figure 8).

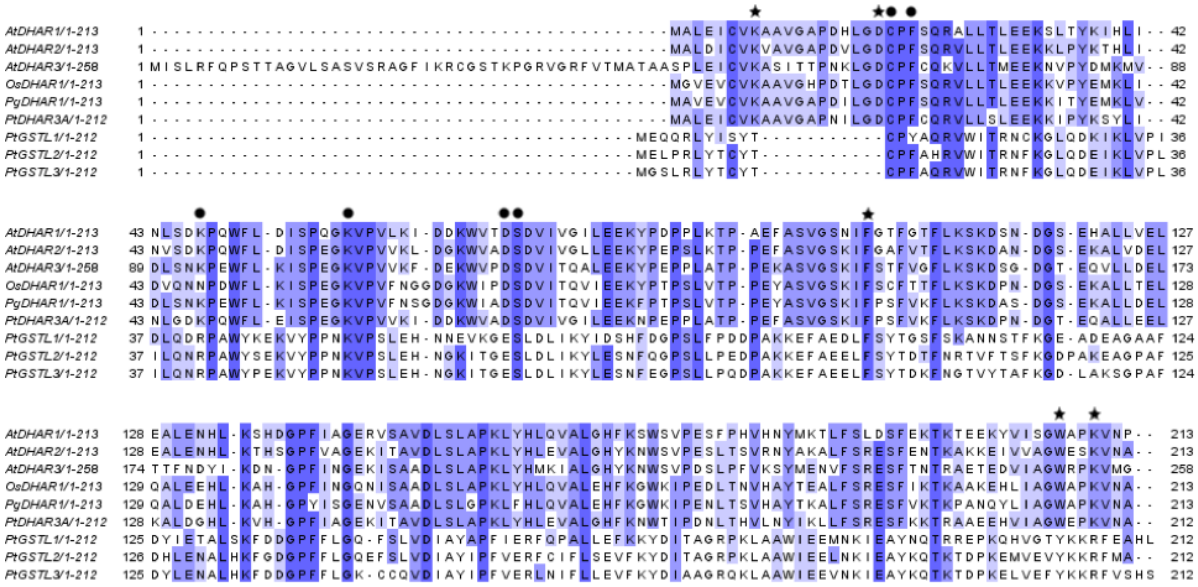

Figure 8. Sequence alignment of DHARs from *Arabidopsis* (AtDHAR1-3), *Oryza sativa* (OsDHAR1), *Pennisetum glaucum* (PgDHAR1), and *Populus trichocarpa* GSTL1-3. Residues that engage in side-chain

interactions with AsA in the structure of OsDHAR1 (PDB, 5D9W) are indicated by a star. Residues shown in the structure of AtDHAR2 to bind the G-site GSH through side-chain interactions are indicated by a circle. The additional N-terminal residue of AtDHAR3 represents the chloroplastic signal peptide.

Comparison of the H-site region of AtDHAR2 to that of PgDHAR1, OsDHAR1, and PtDHAR3A reveals a distinctive difference in the conformation of Asp19. The introduction of the α1'-helix in AtDHAR2 alters the peptide torsion of Asp19 in such a way as to redirect its side-chain carboxylate toward the protein interior, forming a hydrogen bond with His160. In the case of OsDHAR1, PgDHAR1, and PtDHAR3A, the side-chain of Asp19 is orientated outward into the H-site pocket and a polar interaction between His160 and Asp19 is instead formed via the backbone carbonyl of Asp19 (Lallement, Roret et al. 2016) (Figure 9). As Asp19 is proposed to be a significant residue in the binding and stabilization of DHA for catalytic reduction (Do, Kim et al. 2016, Krishna Das, Kumar et al. 2016), preclusion of its carboxylate side-chain from the H-site-binding region in AtDHAR2 complicates understanding of its role in DHA reduction.

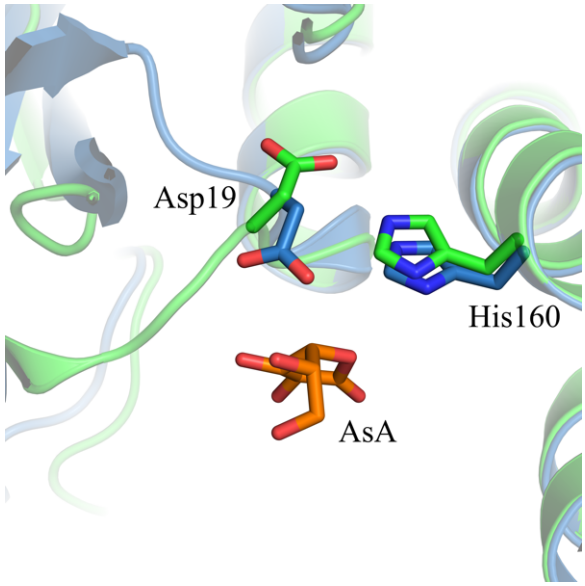

Figure 9. Differing conformations of Asp19 in the superimposed structures of AtDHAR2 (green) and AsA-bound OsDHAR1 (blue).

In the proposed molecular mechanism of enzymatic DHA reduction (Do, Kim et al. 2016), Lys8 has a central function in both binding and protonation of DHA and its site-directed mutagenesis in both OsDHAR1 and *Populus tomentosa* DHAR2 has been shown to significantly reduce the catalytic efficiency (Tang and Yang 2013, Do, Kim et al. 2016). However, although Lys8 is conserved in AtDHAR2, it is instead positioned at the beginning

of the β1-strand, distal from the active site cleft and 19 Å Cα-Cα from the positioning of Lys8 of OsDHAR1, and the equivalent position occupied by a glycine.

It is notable that in PtGSTL1, which also displays DHAR activity, Asp19 or Lys8 are not conserved, and are instead substituted by a threonine and serine, respectively. With the assumed functional significance of Lys8 and Asp19, the preclusion of such residues from the active site environment of AtDHAR2 would be expected to reduce its catalytic efficiency with respect to DHA. However, the kinetic parameters defined for AtDHAR2 reveal a markedly enhanced substrate specificity toward DHA relative to GSH, whereas such a difference in substrate specificity is not evident for OsDHAR1.

Normal mode analysis to assess structural flexibility

The allosteric behavior of DHAR2 activity could be ascribed to a structural rearrangement during GSH binding and/or GSSG release. The most likely place for such a structural rearrangement to occur would be the α2-helix and its connecting loops, in which many of the residues involved in G-site GSH-binding are located. The inherent flexibility of the α2-helix in *Homo sapiens* GST Pi (HsGSTP1–1) has been previously highlighted on the basis of high crystallographic temperature factors (Oakley, Lo Bello et al. 1998). For PgDHAR1, OsDHAR1, and AtDHAR2, crystallographic temperature factors for the α2-helix are within the range of the structural average, however, this is because intermolecular crystal contacts formed at the α2-helix interface provide stabilizing interactions and decrease the domain flexibility, thereby reducing the respective temperature factors. Computational simulation of macromolecular flexibility can provide valuable insight into the range and direction of potential motions, and one such computational approach is normal mode analysis (NMA). NMA uses a coarse-grained structural model, in which residues are considered as nodes of equal mass and a single-parameter potential energy function describes interactions between nodes within a defined interaction distance. Collective molecular motions are defined through eigenvectors across the potential energy matrix, corresponding to the vibrational normal modes, and through eigenvalues, which are the associated frequencies. Despite the significant simplification of energetic parameters and lack of explicit solvent, the lowest frequency modes calculated by NMA have been found to be particularly effective in predicting large-scale macromolecular motions (Delarue and Sanejouand 2002). Two separate NMA web servers were used to assess

the structural dynamics of AtDHAR2; elNémo (http:// igs-server.cnrs-mrs.fr/elnemo/index.html) (Suhre and Sanejouand 2004) and ANM 2.0 (http://anm.csb.pitt.edu) (Eyal, Lum et al. 2015). The two lowest-frequency normal modes calculated described either a twisting motion or breathing motion around an axis along the groove between the N-terminal thioredoxin-like domain and the all-helical C-terminal domain, relating to a partial opening and closing of the active site cleft. The largest amplitude of atomic displacement was observed in the α2-helix region and in a solvent-exposed loop connecting the α4- and α5-helices (Figure 10).

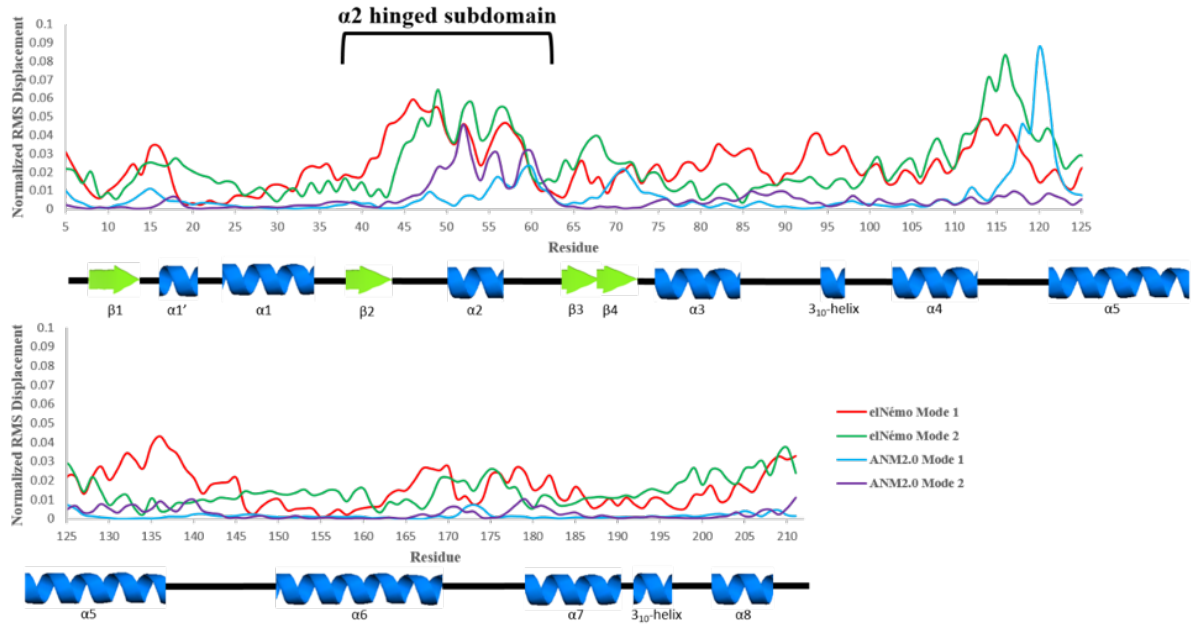

Figure 10. Normalized root mean square (RMS) C^{α} displacement across the polypeptide chain of AtDHAR2 in the direction of the two lowest frequency (non-trivial) normal modes calculated by elNémo (red and green) and ANM 2.0 (blue and purple). This provides a measure of structural change at the associated frequency of vibration for the simulation. For clarity, the associated secondary structure elements of AtDHAR2 are presented below the graph.

As this loop, does not contain residues involved in substrate binding, it was not considered to be a functionally significant region. These findings correlate well with the more in-depth molecular dynamics simulations used previously in the study of CLIC1, in which the same two types of concerted motions were identified and significant structural change of the α2-helix were observed as well (Jones, Curmi et al. 2013). Molecular dynamics simulations performed on HsGSTP1-1 have also found the largest structural change in the α2-helix (Stella, Di Iorio et al. 1999).

Motion of the α2-helix during the catalytic mechanism

Allosteric behavior in monomeric enzymes is relatively rare, and, in the context of ping-pong kinetics, interpretation of such allosteric behavior is largely a speculative task. One possible explanation for the allosteric behavior of AtDHAR2 takes GSH as a positive regulator, in which the G-site S-glutathionylation increases the GSH affinity for the H-site. Alternatively, the allosteric mechanism of AtDHAR2 may be purely related to structural changes, in which the α2-helix region dynamics regulate the affinity for GSH/GSSG. The tendency of the α2-helical region to switch conformations could be linked to the presence or absence of the G-site GSH, where H-bonding and salt bridge interactions between GSH and the α2-helical region would cause one conformation to be favored over the other. In the GSH-bound AtDHAR2, significant steric overlap (>0.5 Å) occurs between Val44 and Asp46 located within the α2 hinge region, indicative of a strained conformation. This observation could imply an induced-fit conformation in the S-glutathionylated state of the enzyme with a G-site-apo form representing an energetically favored resting conformation. Potential conformational flexibility of the α2-helix of GSTs has been studied in depth for HsGSTP1-1, with conclusions supporting an induced-fit model for GSH binding (Ricci, Caccuri et al. 1996, Stella, Caccuri et al. 1998, Stella, Di Iorio et al. 1999, Stella, Nicotra et al. 1999).

Interestingly, positive cooperativity in the catalytic activity of GSTP1-1 was shown to be induced upon site-directed mutation within the α2-helix, increasing both the $K_{0.5}$ GSH and the Hill coefficient (Lo Bello, Nuccetelli et al. 1998). For the *Phanerochaete chrysosporium* GST-class enzyme, Ure2p, which exhibits DHAR activity, GSSG-bound and apo crystal structures show that the α2-helix becomes disordered in the absence of bound GSSG, indicating a more extreme flexibility in this region which depends on the binding of GSSG (Roret, Thuillier et al. 2015). GSSG has been shown to be a competitive inhibitor of the DHAR activity with respect to DHA, with a reported 73% activity reduction at 2.5 mM GSSG (Shimaoka, Miyake et al. 2003, Tang and Yang 2013); therefore, rapid diffusion of GSSG from the active site could be an important factor and the α2-helix dynamics may release GSSG from the active site-binding cleft to allow DHA binding. Another possible functional implication of structural dynamics could be a cooperative relationship between the α2-helix and the α1′-helix. The α1′-helix is an unusual structural feature among the GST enzyme family. The formation of this coil precludes the side-chain Asp19 from interaction with H-site-bound DHA and also forces a

repositioning of the conserved Lys8 to a location distal from the active site. With the inward conformation of the α2-helix in AtDHAR2, uncoiling of the α1′-helix is not possible, which would reorient the Asp19 side-chain into the active site due to inevitable steric interference of the N-terminal loop of the α2 hinge region. If the α2-helix were to shift outward to a conformation more closely resembling that of OsDHAR1 or PgDHAR1, the steric hindrance would be relieved, allowing uncoiling of α1′.

Examples within the GST family of structural flexibility in the α2-helix provide a precedent for conformational change in the case of AtDHAR2, and prior evidence of an induced-fit mechanism and induced positive cooperativity in GSTP1-1 supports the possible influence of this helix on the allosteric behavior of AtDHAR2 (Lo Bello, Nuccetelli et al. 1998, Stella, Nicotra et al. 1999). However, as GSTP1-1 functions as a homodimer, direct comparison to the monomeric DHAR should be viewed with caution. AtDHAR2 is the first monomeric GST-family enzyme shown to display an allosteric enzymatic behavior, though whether this allostery is common to other isoforms of DHAR or specific to AtDHAR2 alone remains an open question.

Acknowledgements

We thank Didier Vertommen for generously providing mass spectrometry services, Nicolas Foloppe, Guido Verniest, and Brandán Pérez for discussion, Remy Loris and Inge Van Molle for collecting crystal diffraction data, Martine De Cock for help in preparing the manuscript, and the Proxima1 beamline scientists at SOLEIL for their technical support. This work was supported by the Research Foundation-Flanders (projects G.0305.12 and G0D7914N), Flanders Hercules Foundation (grants HERC16 and UABR/09/005, for the purification and in house X-ray crystallography platform, respectively), and the Vrije Universiteit Brussel Strategic Research Program (SRP34). N.B. is indebted to the Indian Council of Agricultural Research for a PhD fellowship

References

Al Khamici, H., L. J. Brown, K. R. Hossain, A. L. Hudson, A. A. Sinclair-Burton, J. P. M. Ng, E. L. Daniel, J. E. Hare, B. A. Cornell, P. M. G. Curmi, M. W. Davey and S. M. Valenzuela (2015). "Members of the chloride intracellular ion channel protein family demonstrate glutaredoxin-like enzymatic activity." Plos One **10**(1).

Amako, K., T. Ushimaru, A. Ishikawa, Y. Ogishi, R. Kishmoto and K. Goda (2006). "Heterologous expression of dehydroascorbate reductase from rice and its application to determination of dehydroascorbate concentrations." J Nutr Sci Vitaminol **52**(2): 89-95.

Bak, D. W. and E. Weerapana (2015). "Cysteine-mediated redox signalling in the mitochondria." Mol Biosyst **11**(3): 678-697.

Breen, A. P. and J. A. Murphy (1995). "Reactions of oxyl radicals with DNA." Free Radic Biol Med **18**(6): 1033-1077.

Bryan, P. N. and J. Orban (2010). "Proteins that switch folds." Curr Opin Struct Biol **20**(4): 482-488.

Chen, V. B., W. B. Arendall, 3rd, J. J. Headd, D. A. Keedy, R. M. Immormino, G. J. Kapral, L. W. Murray, J. S. Richardson and D. C. Richardson (2010). "MolProbity: all-atom structure validation for macromolecular crystallography." Acta Crystallogr D Biol Crystallogr **66**(Pt 1): 12-21.

Collaborative Computational Project, N. (1994). "The CCP4 suite: programs for protein crystallography." Acta Crystallogr D Biol Crystallogr **50**(Pt 5): 760-763.

Cotgreave, I. A. and P. Moldeus (1986). "Methodologies for the application of monobromobimane to the simultaneous analysis of soluble and protein thiol components of biological systems." J Biochem Biophys Methods **13**(4-5): 231-249.

Delarue, M. and Y. H. Sanejouand (2002). "Simplified normal mode analysis of conformational transitions in DNA-dependent polymerases: the elastic network model." J Mol Biol **320**(5): 1011-1024.

Do, H., I.-S. Kim, B. W. Jeon, C. W. Lee, A. K. Park, A. R. Wi, S. C. Shin, H. Park, Y.-S. Kim, H.-S. Yoon, H.-W. Kim and J. H. Lee (2016). "Structural understanding of the recycling of oxidized ascorbate by dehydroascorbate reductase (OsDHAR) from *Oryza sativa* L. japonica." Sci. Rep. **6**: 19498.

Elter, A., A. Hartel, C. Sieben, B. Hertel, E. Fischer-Schliebs, U. Luttge, A. Moroni and G. Thiel (2007). "A plant homolog of animal chloride intracellular channels (CLICs) generates an ion conductance in heterologous systems." J Biol Chem **282**(12): 8786-8792.

Emsley, P. and K. Cowtan (2004). "Coot: model-building tools for molecular graphics." Acta Crystallogr D Biol Crystallogr **60**(Pt 12 Pt 1): 2126-2132.

Evans, P. (2006). "Scaling and assessment of data quality." Acta Crystallogr D Biol Crystallogr **62**(Pt 1): 72-82.

Evans, P. R. and G. N. Murshudov (2013). "How good are my data and what is the resolution?" Acta Crystallogr D Biol Crystallogr **69**(Pt 7): 1204-1214.

Eyal, E., G. Lum and I. Bahar (2015). "The anisotropic network model web server at 2015 (ANM 2.0)." Bioinformatics **31**(9): 1487-1489.

Fahey, R. C. and G. L. Newton (1987). "Determination of low-molecular-weight thiols using monobromobimane fluorescent labeling and high-performance liquid chromatography." Methods Enzymol **143**: 85-96.

Foyer, C. H. and B. Halliwell (1977). "Purification and properties of dehydroascorbate reductase from spinach leaves." Phytochemistry **16**(9): 1347-1350.

Gill, S. S. and N. Tuteja (2010). "Reactive oxygen species and antioxidant machinery in abiotic stress tolerance in crop plants." Plant Physiol Biochem **48**(12): 909-930.

Gupta, V. and K. S. Carroll (2014). "Sulfenic acid chemistry, detection and cellular lifetime." Biochim Biophys Acta **1840**(2): 847-875.

Harrop, S. J., M. Z. DeMaere, W. D. Fairlie, T. Reztsova, S. M. Valenzuela, M. Mazzanti, R. Tonini, M. R. Qiu, L. Jankova, K. Warton, A. R. Bauskin, W. M. Wu, S. Pankhurst, T. J. Campbell, S. N. Breit and P. M. G. Curmi (2001). "Crystal structure of a soluble form of the intracellular chloride ion channel CLIC1 (NCC27) at 1.4-angstrom resolution." J Biol Chem **276**(48): 44993-45000.

Hayward, S., A. Kitao and H. J. Berendsen (1997). "Model-free methods of analyzing domain motions in proteins from simulation: a comparison of normal mode analysis and molecular dynamics simulation of lysozyme." Proteins **27**(3): 425-437.

Heinig, M. and D. Frishman (2004). "STRIDE: a web server for secondary structure assignment from known atomic coordinates of proteins." Nucleic Acids Res **32**(Web Server issue): W500-502.

Hernandez, J. A., A. Jimenez, P. Mullineaux and F. Sevilla (2000). "Tolerance of pea (*Pisum sativum* L.) to long-term salt stress is associated with induction of antioxidant defences." Plant Cell Environ **23**(8): 853-862.

Jones, P. M., P. M. G. Curmi, S. M. Valenzuela and A. M. George (2013). "Computational analysis of the foluble form of the intracellular chloride ion channel protein CLIC1." Biomed Research International.

Kabsch, W. (2010). "Integration, scaling, space-group assignment and post-refinement." Acta Crystallogr D Biol Crystallogr **66**(Pt 2): 133-144.

Kato, Y., J. Urano, Y. Maki and T. Ushimaru (1997). "Purification and characterization of dehydroascorbate reductase from rice." Plant Cell Physiol **38**(2): 173-178.

Kiddle, G., G. M. Pastori, S. Bernard, C. Pignocchi, J. Antoniw, P. J. Verrier and C. H. Foyer (2003). "Effects of leaf ascorbate content on defense and photosynthesis gene expression in *Arabidopsis thaliana*." Antioxid Redox Signal **5**(1): 23-32.

Koussevitzky, S., N. Suzuki, S. Huntington, L. Armijo, W. Sha, D. Cortes, V. Shulaev and R. Mittler (2008). "Ascorbate peroxidase 1 plays a key role in the response of *Arabidopsis thaliana* to stress combination." J Biol Chem **283**(49): 34197-34203.

Krieger-Liszkay, A., C. Fufezan and A. Trebst (2008). "Singlet oxygen production in photosystem II and related protection mechanism." Photosynth Res **98**(1-3): 551-564.

Krishna Das, B., A. Kumar, P. Maindola, S. Mahanty, S. K. Jain, M. K. Reddy and A. Arockiasamy (2016). "Non-native ligands define the active site of Pennisetum glaucum (L.) R. Br dehydroascorbate reductase." Biochem Biophys Res Commun.

Lallement, P. A., E. Meux, J. M. Gualberto, P. Prosper, C. Didierjean, F. Saul, A. Haouz, N. Rouhier and A. Hecker (2014). "Structural and enzymatic insights into Lambda glutathione transferases from *Populus trichocarpa*, monomeric enzymes constituting an early divergent class specific to terrestrial plants." Biochem J **462**(1): 39-52.

Lallement, P. A., T. Roret, P. Tsan, J. M. Gualberto, J. M. Girardet, C. Didierjean, N. Rouhier and A. Hecker (2016). "Insights into ascorbate regeneration in plants: investigating the redox and structural properties of dehydroascorbate reductases from *Populus trichocarpa*." Biochem J **473**(6): 717-731.

Littler, D. R., S. J. Harrop, W. D. Fairlie, L. J. Brown, G. J. Pankhurst, S. Pankhurst, M. Z. DeMaere, T. J. Campbell, A. R. Bauskin, R. Tonini, M. Mazzanti, S. N. Breit and P. M. G. Curmi (2004). "The intracellular chloride ion channel protein CLIC1 undergoes a redox-controlled structural transition." J Biol Chem **279**(10): 9298-9305.

Lo Bello, M., M. Nuccetelli, E. Chiessi, A. Lahm, A. P. Mazzetti, A. Battistoni, A. M. Caccuri, A. J. Oakley, M. W. Parker, A. Tramontano, G. Federici and G. Ricci (1998). "Mutations of Gly to Ala in human glutathione transferase P1-1 affect helix 2 (G-site) and induce positive cooperativity in the binding of glutathione." J Mol Biol **284**(5): 1717-1725.

McCoy, A. J., R. W. Grosse-Kunstleve, P. D. Adams, M. D. Winn, L. C. Storoni and R. J. Read (2007). "Phaser crystallographic software." J Appl Crystallogr **40**(Pt 4): 658-674.

Meyer, A. J. and M. D. Fricker (2000). "Direct measurement of glutathione in epidermal cells of intact Arabidopsis roots by two-photon laser scanning microscopy." J Microsc **198**(Pt 3): 174-181.

Murshudov, G. N., P. Skubak, A. A. Lebedev, N. S. Pannu, R. A. Steiner, R. A. Nicholls, M. D. Winn, F. Long and A. A. Vagin (2011). "REFMAC5 for the refinement of macromolecular crystal structures." Acta Crystallogr D Biol Crystallogr **67**(Pt 4): 355-367.

Oakley, A. J., M. Lo Bello, G. Ricci, G. Federici and M. W. Parker (1998). "Evidence for an induced-fit mechanism operating in pi class glutathione transferases." Biochemistry **37**(28): 9912-9917.

Price, A. H., N. M. Atherton and G. A. Hendry (1989). "Plants under drought-stress generate activated oxygen." Free Radic Res Commun **8**(1): 61-66.

Ricci, G., A. M. Caccuri, M. Lo Bello, N. Rosato, G. Mei, M. Nicotra, E. Chiessi, A. P. Mazzetti and G. Federici (1996). "Structural flexibility modulates the activity of human glutathione transferase P1-1. Role of helix 2 flexibility in the catalytic mechanism." J Biol Chem **271**(27): 16187-16192.

Roberts, B. R., Z. A. Wood, T. J. Jonsson, L. B. Poole and P. A. Karplus (2005). "Oxidized and synchrotron cleaved structures of the disulfide redox center in the N-terminal domain of *Salmonella typhimurium* AhpF." Protein Sci **14**(9): 2414-2420.

Roos, G. and J. Messens (2011). "Protein sulfenic acid formation: from cellular damage to redox regulation." Free Radic Biol Med **51**(2): 314-326.

Roret, T., A. Thuillier, F. Favier, E. Gelhaye, C. Didierjean and M. Morel-Rouhier (2015). "Evolutionary divergence of Ure2pA glutathione transferases in wood degrading fungi." Fungal Genet Biol **83**: 103-112.
Schrodinger, LLC (2015). The PyMOL Molecular Graphics System, Version 1.8.

Sharma, P. and R. S. Dubey (2005). "Drought induces oxidative stress and enhances the activities of antioxidant enzymes in growing rice seedlings." Plant Growth Regul **46**(3): 209-221.

Shigeoka, S., R. Yasumoto, T. Onishi, Y. Nakano and S. Kitaoka (1987). "Properties of monodehydroascorbate reductase and dehydroascorbate reductase and their participation in the regeneration of ascorbate in *Euglena-Gracilis*." J Gen Microbiol **133**: 227-232.

Shimaoka, T., C. Miyake and A. Yokota (2003). "Mechanism of the reaction catalyzed by dehydroascorbate reductase from spinach chloroplasts." Eur J Biochem **270**(5): 921-928.

Stella, L., A. M. Caccuri, N. Rosato, M. Nicotra, M. Lo Bello, F. De Matteis, A. P. Mazzetti, G. Federici and G. Ricci (1998). "Flexibility of helix 2 in the human glutathione transferase P1-1. time-resolved fluorescence spectroscopy." J Biol Chem **273**(36): 23267-23273.

Stella, L., E. E. Di Iorio, M. Nicotra and G. Ricci (1999). "Molecular dynamics simulations of human glutathione transferase P1-1: conformational fluctuations of the apo-structure." Proteins **37**(1): 10-19.

Stella, L., M. Nicotra, G. Ricci, N. Rosato and E. E. Di Iorio (1999). "Molecular dynamics simulations of human glutathione transferase P1-1: analysis of the induced-fit mechanism by GSH binding." Proteins **37**(1): 1-9.

Suhre, K. and Y. H. Sanejouand (2004). "ElNemo: a normal mode web server for protein movement analysis and the generation of templates for molecular replacement." Nucleic Acids Res **32**(Web Server issue): W610-614.

Sumi, T. and M. Ui (1972). "Allosteric properties of enzymes with "ping-pong" mechanism." Biochim Biophys Acta **276**(1): 12-18.

Sutton, K. A., P. J. Black, K. R. Mercer, E. F. Garman, R. L. Owen, E. H. Snell and W. A. Bernhard (2013). "Insights into the mechanism of X-ray-induced disulfide-bond cleavage in lysozyme crystals based on EPR, optical absorption and X-ray diffraction studies." Acta Crystallogr D Struct Biol **69**: 2381-2394.

Tang, Z. X. and H. L. Yang (2013). "Functional divergence and catalytic properties of dehydroascorbate reductase family proteins from Populus tomentosa." Mol Biol Rep **40**(8): 5105-5114.

Turell, L., H. Botti, S. Carballal, G. Ferrer-Sueta, J. M. Souza, R. Duran, B. A. Freeman, R. Radi and B. Alvarez (2008). "Reactivity of sulfenic acid in human serum albumin." Biochem. **47**(1): 358-367.

Vass, I. and K. Cser (2009). "Janus-faced charge recombinations in photosystem II photoinhibition." Trends Plant Sci **14**(4): 200-205.

Washko, P. W., R. W. Welch, K. R. Dhariwal, Y. Wang and M. Levine (1992). "Ascorbic acid and dehydroascorbic acid analyses in biological samples." Anal Biochem **204**(1): 1-14.

Waszczak, C., S. Akter, D. Eeckhout, G. Persiau, K. Wahni, N. Bodra, I. Van Molle, B. De Smet, D. Vertommen, K. Gevaert, G. De Jaeger, M. Van Montagu, J. Messens and F. Van Breusegem (2014). "Sulfenome mining in *Arabidopsis thaliana*." Proc Natl Acad Sci U S A **111**(31): 11545-11550.

Weik, M., J. Berges, M. L. Raves, P. Gros, S. McSweeney, I. Silman, J. L. Sussman, C. Houee-Levin and R. B. G. Ravelli (2002). "Evidence for the formation of disulfide radicals in protein crystals upon X-ray irradiation." J. Synchrotron Radiat **9**: 342-346.

Winkler, B. S., S. M. Orselli and T. S. Rex (1994). "The redox couple between glutathione and ascorbic acid: a chemical and physiological perspective." Free Radic Biol Med **17**(4): 333-349.

Winters, R. A., J. Zukowski, N. Ercal, R. H. Matthews and D. R. Spitz (1995). "Analysis of glutathione, glutathione disulfide, cysteine, homocysteine, and other biological thiols by high-performance liquid chromatography following derivatization by n-(1-pyrenyl)maleimide." Anal Biochem **227**(1): 14-21.

Wu, M. J., P. J. O'Doherty, P. A. Murphy, V. Lyons, M. Christophersen, P. J. Rogers, T. D. Bailey and V. J. Higgins (2011). "Different reactive oxygen species lead to distinct changes of cellular metal ions in the eukaryotic model organism *Saccharomyces cerevisiae*." Int J Mol Sci **12**(11): 8119-8132.

Zhang, Y. J., W. Wang, H. L. Yang, Y. Li, X. Y. Kang, X. R. Wang and Z. L. Yang (2015). "Molecular properties and functional divergence of the dehydroascorbate reductase gene family in lower and higher plants." PLoS One **10**(12): e0145038.

Zhou, H. N., J. Brock, D. Liu, P. G. Board and A. J. Oakley (2012). "Structural insights into the dehydroascorbate reductase activity of human omega-class glutathione transferases." J Mol Biol **420**(3): 190-203.

Chapter 3

Arabidopsis thaliana mitogen activated kinase 4 cysteine mutant affects the phosphorylation activity

A modified version of this chapter will be submitted as a research article in future.

Author contributions: Nandita Bodra, Jingjing Huang, Leonardo Rosado, David Young Frank Van Breusegem and Joris Messens designed the experiments. Nandita Bodra performed all the experiments. Nandita Bodra wrote the paper with help of with the help of Frank Van Breusegem and Joris Messens.

Chapter 3

Arabidopsis thaliana mitogen activated kinase 4 cysteine mutant affects the phosphorylation activity

Abstract

Plants regularly encounter various biotic and abiotic stresses that adversely affect their growth and development. Such stresses can lead to generation of reactive oxygen species (ROS), which at low levels are involved in cellular signalling pathways, but at elevated levels can cause cellular damage. The amino acid cysteine has the highest reactivity towards ROS, with oxidation occurring on its sulfur atom. Oxidation of a cysteinyl sulfur first results in the formation of sulfenic acid, a post-translational modification associated with signal transduction pathways. However, how ROS-induced signals are translated into stress defence response is not yet clearly defined. ROS were known to activate mitogen activated kinases (MAPKs or MPKs), which are involved highly conserved signalling pathways. In Arabidopsis, three MPKs have been identified as sulfenylated proteins: MPK4, MPK2 and MPK7. However, the role of cysteine residues in the kinase activities of MPKs are not known. Here, we demonstrate that *Arabidopsis thaliana* MPK4 (AtMPK4) is sulfenylated on cysteine 181. We show that the site directed mutagenesis of cysteine 181 to serine lowers the AtMPK4 phosphorylation activity in the *in vitro* test substrate myelin basic protein (MBP). Further, mass spectrometry confirms that the AtMPK4 auto-phosphorylates on tyrosine 203. These biochemical characterization of AtMPK4 might uncover new mechanisms of oxidative stress response in plants and this knowledge will guide in manipulating genes to generate stress tolerant plant.

3.1 Introduction

Reactive oxygen species (ROS), such as hydrogen peroxide (H_2O_2), hydroxyl radical ($HO^{\bullet-}$), singlet oxygen ($^1O_2$) and superoxide anion ($O_2^{\bullet-}$), are formed upon partial reduction of oxygen (O_2). ROS are produced as the by-products of cellular respiration, photosynthesis, protein folding and several metabolic reactions in plants (Foyer and Noctor 2009). Additionally, in an aerobic environment, plants are constantly exposed to a variety of biotic and abiotic stresses (Xiong and Yang 2003, Chinnusamy, Schumaker et al. 2004) that generate ROS. ROS formation occurs under normal growth conditions that accelerates upon biotic or abiotic

stresses, such as plant-pathogen interactions, high light, salinity and drought (Torres and Dangl 2005, Suzuki, Koussevitzky et al. 2012). ROS generation in various subcellular compartments may lead to ROS accumulation in other compartments (Noctor and Foyer 2016). High levels of ROS lead to harmful effects such as direct or indirect ROS-mediated damage of a variety of molecules including lipid peroxidation in cellular membranes, protein denaturation, pigment breakdown and carbohydrate oxidation which eventually lead to cellular damage (Moller, Jensen et al. 2007). The ROS-scavenging systems such as enzymatic and non-enzymatic mechanisms keep the balance of ROS inside the cell (Foyer and Noctor 2009). However, the rapid and transient increase of ROS in plant cells act as signal that facilitate the regulation of various cellular activities and the adaptation of plants to abiotic and biotic stresses (Xing, Jia et al. 2007, Wan and Liu 2008). H_2O_2 is a key signalling molecule in plants and controls stomatal closure, root growth and programmed cell death, including hypersensitive responses and the regulation of gene expression (Foreman, Demidchik et al. 2003, Laloi, Mestres-Ortega et al. 2004, Pitzschke and Hirt 2006). In plants, mitogen-activated protein kinase cascade induction is an important signalling event that ensues in response to H_2O_2 (Wang, Du et al. 2010, Liu and He 2017).

The mitogen-activated protein kinase (MAPK or MPK) cascade is an intracellular pathway conserved among eukaryotes. It comprises three kinases, MPK, MPK kinase (MKK) and MPKK kinases (MPKKK or MEKK) (Group 2002). These three kinases form the basic module of MPK cascade, MEKK-MKK-MPK, in which MEKK phosphorylates and activates MKK, and the activated MKK phosphorylates and activates MPK. MPK cascades are involved in many aspects of plant physiology, such as cell division (Komis, Illes et al. 2011), plant growth and development, plant resistance to pathogens and plant response to abiotic stresses (Liu 2012, Smekalova, Doskocilova et al. 2014, Bigeard, Colcombet et al. 2015, Hettenhausen, Schuman et al. 2015, Xu and Zhang 2015). The *Arabidopsis thaliana* genome encodes 60 MEKKs, 10 MKKs and 20 MPKs (Group 2002). Evidence suggests that ROS signalling and MAP kinase activation are strongly intertwined in plants (Meng and Zhang 2013). The exogenous application of H_2O_2 or O_3 activates components of MPK cascades that initiate signalling and further lead to changes in MPK cascade, while the manipulation of MPK cascades results in the initiation of ROS responses (Pitzschke and Hirt 2006, Pitzschke and Hirt 2009). In higher plants, four subgroups of MPKs—subgroups A, B, C and D—have been identified based on the phosphorylation motifs within their kinase domains (Miles, Samuel et al. 2005, Hamel, Nicole et al. 2006). The ROS act upstream of the stress-activated MPK cascades. Here, we

study Arabidopsis MPK4 (AtMPK4), which is a terminal kinase in the MPK cascade and functions as a negative regulator in plant immune responses (Li, Jiang et al. 2015). It is involved in cytokinesis during mitosis and meiosis and the root hair development process (Kosetsu, Matsunaga et al. 2010). It modulates the expression of genes responding to biotic and abiotic stress (Petersen, Brodersen et al. 2000, Teige, Scheikl et al. 2004). Waszczak *et al.* have identified the AtMPK4 as one of the sulfenylated proteins of *Arabidopsis thaliana* upon H_2O_2 treatment (Waszczak, Akter et al. 2014). Till today it is not clear how the cysteine sulfenylation is involved in the regulation of the AtMPK4 activity. To unscramble the link between cysteine oxidation and the AtMPK4 function, we determined the biochemical properties of the AtMPK4. We demonstrated that Cys 181 is involved in the substrate phosphorylation activity of AtMPK4.

3.2 Materials and methods

Expression and purification of the AtMPK4

The *Arabidopsis thaliana* MPK4 (AT4G01370) gene sequence was codon-optimized for protein expression in *Escherichia coli* (*E.coli*). Further the att L sites were introduced to the N-terminal and C-terminal of the sequence to perform the LR reaction with pDEST17 plasmid and the gene was cloned in *E.coli* DH5α and transformed into *E.coli* C41 (DE3) cells by heat shock for protein expression. The bacterial cell culture was grown in Luria Bertani (LB) media to an optical density of 0.6 at 37°C and subsequently transferred to 20°C. The protein expression was induced with a 0.5 mM Isopropyl β-D-1-thiogalactopyranoside (IPTG) and left for overnight growth. The cells were harvested by centrifugation and the pellets were stored at -20°C prior to purification. For purification, cell pellets were thawed and resuspended in lysis buffer with 50 mM Tris-HCl, pH 7.8, 200 mM NaCl, 2 mM dithiothreitol (DTT), 5 mM imidazole, 20 mM $MgCl_2$, 50 µg/mL Dnase I, 1 µg/mL leupeptine, 0.1 mg/mL 4-(2-Aminoethyl) benzenesulfonyl fluoride hydrochloride (AEBSF), and cells were lysed by cell cracker at 20 KPsi. The cell lysate containing His-tagged protein was loaded on a Ni^{2+} Sepharose column (GE Healthcare) equilibrated with 50 mM Tris-HCl pH 7.8, 500 mM NaCl, 2 mM DTT. The flow-through and wash samples were collected using an AKTA pure (GE Healthcare) purification system. With the gradient increase in the concentration of imidazole, recombinant AtMPK4 was eluted from the column and the purity of the protein sample was analysed on Coomassie–stained sodium dodecyl sulfate polyacrylamide electrophoresis (SDS-

PAGE) gels. Further, the protein concentration was calculated by measuring the sample absorbance at 280 nm with a Bio-photometer (Eppendorf).

Dimedone labelling and sulfenylation detection

To assess the *in vitro* sulfenylation of recombinant AtMPK4 upon H_2O_2 treatment, dimedone labelling was performed. Briefly, purified AtMPK4 was reduced using 20 mM DTT and the excess of DTT was removed using Bio-Spin size exclusion columns (Bio-Rad). Next, 20 µM of reduced AtMPK4 protein was incubated with 2 mM dimedone, and 1:50 molar ratio of protein versus H_2O_2 was added. Further, this mixture was incubated at room temperature for 1 h in the dark. Then, the excess H_2O_2 and dimedone were removed using Bio-Spin size exclusion columns (Bio-Rad). Further, 4 mM N-ethylmaleimide (NEM) was added to the reaction mixture and incubated in the dark at room temperature for 10 min to block the free thiols of AtMPK4. Later, samples were separated by SDS-PAGE gel, and sulfenylation was visualized by Western blot using an anti-cysteine sulfenic acid antibody (Merck Millipore, Darmstadt, Germany). The protein band on the gel corresponding to the signal detected by the antibody was cut for mass spectrometric analysis. The protein gel band was washed and digested using trypsin or chymotrypsin. The obtained peptide mixture was analysed by liquid chromatography tandem mass spectrometry (LC-MS/MS), and the obtained data was searched using the SEQUEST bioinformatics search tool against *Escherichia coli* and *Arabidopsis thaliana* protein databases.

Site directed mutagenesis

The QuikChange® site-directed mutagenesis kit was used to make point mutations. This was performed using Pfu DNA polymerase and thermal cycler. Two synthetic oligonucleotide primers containing serine as a mutated amino acid were designed as shown in Table 1. For the polymerase chain reaction (PCR) a total of 50 µl reaction mixture containing 4 µl dNTPs, 5 µl Pfu buffer with $MgSO_4$, 1 µl DNA Pfu polymerase, 0.9 µl forward and reverse primers and 1 µl DNA template (AtMPK4 plasmid) was prepared.

Table 1. Primers used for site directed mutagenesis

Mutation	**Primers**
MPK4 C181S	Forward Primer: CTG TTG AAT GCT AAT **AGC** GAC CTT AAG CTG GGG G
	Reverse Primer: C CCC CAG CTT AAG GTC **GCT** ATT AGC ATT CAA CAG

Codon highlighted in bold represents the serine mutation

For the polymerase chain reaction (PCR), the temperature cycling was set as follows: 1 cycle at 95ºC for 30 s followed by 16 cycles at 95ºC for 30 s, 55 ºC for 1 min, and 68 ºC for 7.5 min. After PCR, the product was treated with DpnI endonuclease for 1 h at 37°C, and the resultant product was transformed into DH5α competent cells. Then, plasmid was isolated from DH5α cells using Pure Yield™; the Plasmid Miniprep System kit and mutations were validated by sequencing. Further, correct plasmid was transformed into *E.coli* C41 (DE3) cells.

Expression and Purification of MPK4 C181S mutant

Recombinant MPK4 C181S was expressed in *E.coli* C41 (DE3) cells using 6 L Luria Bertani media supplemented with 100 µg/µl ampicilline to an OD_{600} of 0.6 at 37°C and subsequently transferred to 25°C. Next, protein expression was induced by 0.5 mM isopropyl-β-D-thiogalactopyranoside (IPTG) and culture was further grown for 4 h in a shaking incubator. The cells were harvested by centrifugation and the pellets were stored at -20°C. The pellets were thawed at 4°C and cells were resuspended in a lysis buffer containing 50 mM Tris/HCl, pH 7.8, 200 mM NaCl, 2 mM DTT, 5 mM imidazole, 20 mM $MgCl_2$, 50 µg/ml DNaseI, 1 µg/ml leupeptine, 0.1 mg/ml AEBSF and lysed by sonication. The cell lysate was loaded onto a Ni^{2+}Sepharose column pre-equilibrated in buffer with 50 mM Tris-HCl, pH 7.8, 500 mM NaCl and 2 mM DTT. The flow through and wash samples were collected using an AKTA Pure (GE Healthcare) purification system. By increasing the concentration of imidazole, MPK4 C181S was eluted. The purity of the MPK4 C181S fractions were analyzed on a Coomassie-stained SDS-polyacrylamide gel electrophoresis (SDS-PAGE) gels. After collecting the elution fractions from the Ni^{2+}Sepharose column, samples were applied on a Source 30Q anion exchange column pre-equilibrated with 50 mM Tris-HCl, pH 7.8 and 2 mM DTT. Further, MPK4 C181S was eluted with increasing concentration of salt with buffer containing 1 M NaCl, 50 mM Tris-HCl, pH 7.8 and 2 mM DTT. The protein concentration was calculated by measuring the sample absorbance at 280 nm with a Bio-photometer (Eppendorf).

Kinase assay

To measure the activity of the AtMPK4 and MPK4 C181S mutant, a radioactive kinase assay was performed. Reduced AtMPK4 and MPK4 C181S mutant were prepared by incubating AtMPK4 and MPK4 C181S mutant protein with 20 mM DTT for 30 min at room temperature,

and the excess of DTT was removed using Bio Spin Columns. For the kinase assay, 10 µM Myelin Basic Protein, MBP (Sigma Aldrich), 50 µM ATP, 1 mM DTT and 0.5 mM P^{32}-ATP (Perkin Elmer) were pre-incubated at 30°C for 30 min, and subsequently, 10 µM AtMPK4 protein was added to the mixture to start the reaction. Similarly, 10 µM MPK4 C181S mutant protein was added to the reaction mixture in separate tube. All the components were prepared in the kinase buffer with 250 mM Tris-HCl, pH 7.5 and 10 mM $MgCl_2$. The reaction was stopped by the addition of SDS sample loading buffer after 0, 1, 10, 20, 30, and 60 min followed by heating the samples at 95°C for 5 min. Each sample was analysed on SDS PAGE gels followed by coomassie brilliant blue staining and destaining. The destained gels were dried on a gel drier and the gels were exposed to the phosphor screen overnight. The phosphorylation signal was detected using phosphorimager (Bio Rad) (Figure 4A). The obtained signal was quantified using Image Lab™ 6.0 software, and the data were processed using the Graphpad Prism 7 software (Figure 4B.).

ATP/NADH coupled assay

To measure the auto-phosphorylation activity of wild type (WT) AtMPK4, ATP/NADH coupled enzyme assay was performed. Briefly, before starting the assay, WT AtMPK4 was treated with 4 U/mg alkaline phosphatase (Roche) overnight to remove the endogenously bound ATP from AtMPK4. Next, the alkaline phosphatase and AtMPK4 were separated on a Superdex200 10/30 column. Next, the WT AtMPK4 was reduced using 20 mM DTT for 30 min at room temperature and the excess of DTT was removed using Bio Spin Columns. Next, the ATP in a concentration range of 0.1–3 mM was mixed using 1.5 mM phospho (enol) pyruvic acid, PEP (Sigma Aldrich), 0.2 mM nicotinamide adenine dinucleotide reduced, NADH (Sigma), 6 U/mL pyruvate kinase (Sigma Aldrich) and 9 U/mL of lactate dehydrogenase (Sigma Aldrich), in 1 cm path length quartz cuvette with a final volume of 0.5 mL, and the consumption of NADH (with a molar extinction coefficient of 6220 $M^{-1}cm^{-1}$) was followed in the function of time at 340 nm. The reduced WT AtMPK4 (5 µM) was added last into the reaction mixture, and the reactions were carried out for 15 min at 30°C. Each of the samples was prepared in 250 mM Tris-HCl, pH 7.5 and 10 mM $MgCl_2$ for the kinase assay. The experimental data fitted Michaelis-menten curve with V_{max} of 0.001830 µmol. min^{-1}, K_m of 1.12 mM and k_{cat} of 3.5 *10^{-7} min^{-1}. All the experiments were done in duplicate and the data were analysed with the GraphPad Prism 7.0 software (Figure 2B).

Oligomeric state determination of WT MPK4

The oligomeric state of WT MPK4 was determined by analytical gel filtration on a Superdex 200 HR column. The column was equilibrated with 20 mM Tris, pH 7.8, 50 mM NaCl and 2 mM DTT for a reduced sample and 20 mM Tris, pH 7.8, 50 mM NaCl for an oxidized sample. Firstly, the reduced samples were prepared by incubating 1 mg/ml of WT AtMPK4 with 20 mM DTT for 30 min at room temperature. For the oxidized sample, 1 mg/ml of AtMPK4 was incubated with 1mM H_2O_2 for 1 h at room temperature. Afterwards, excess of DTT and H_2O_2 were removed by micro Bio-spin chromatography columns, and the samples were injected onto the column. Next, 0.2 ml of Bio-Rad standard sample was injected onto the column. The elution volumes of reduced and oxidized, standard samples were obtained by peak integration, and partition coefficient (K_{av}) were calculated using Eq. 1, where V_o and V_t represented void volume and total volume of the column respectively. The V_e indicated the elution volume of each protein sample.

$$K_{av} = (V_e - V_o) / (V_t - V_o) \qquad \text{Eq. 1}$$

Circular dichroism measurements

Circular dichroism (CD) spectra were measured on Jasco J-715 spectropolarimeter. The reduced WT AtMPK4 and oxidized WT AtMPK4 were prepared in 50 mM ammonium bicarbonate buffer with pH 7.4. In short, to prepare reduced sample, the WT AtMPK4 was incubated using 20 mM DTT for 30 min at room temperature, and the excess of DTT was removed using micro Bio-spin chromatography columns. Additionally, 1 mM of H_2O_2 was used to oxidize the WT AtMPK4 for 1 h at room temperature, and subsequently, the excess of H_2O_2 was removed with micro Bio-spin chromatography columns. Samples were put in quartz cuvettes with optical path length of 0.1 cm up to a final volume of 0.5 mL. The spectra were measured from 260 to 190 nm. Five scans were measured for each sample. The temperature was kept constant at 30ºC. The CD spectra data were obtained as ellipticity (θ) with millidegrees (mdeg) units. Furthermore, molar ellipticity [θ] were calculated using eq. 2, where θ represents ellipticity, MW-molecular weight, c-concentration of protein sample, l-path length of the cuvette and n-number of amino acid. To analyse the CD data, the GraphPad prism 7.0 software was used.

$$[\theta] = \frac{\theta \times 100 \times \mathrm{MW}}{c \times l \times n} \qquad \text{Eq. 2}$$

Intrinsic tryptophan fluorescence measurements

The AtMPK4 contains two tryptophan residues: Trp 208 and Trp 228. The change in fluorescence of the reduced WT AtMPK4 sample (prepared as described above) with adenylyl-imidodiphosphate AMP-PNP which is an ATP analogue was determined using a SX-20 stopped-flow spectrometer equipped with a fluorescence detector. The final concentration of 1 μM WT AtMPK4 was mixed with the AMP-PNP concentrations ranging from 0.5 to 5 mM in 250 mM Tris-HCl, pH 7.5 and 10 mM $MgCl_2$. Samples were excited at 290 nm with an emission cut-off of 320 nm. All measurements were done at 30°C. The preliminary experimental data showed the binding of AMP-PNP to reduced WT AtMPK4.

Determination of the number of free thiols

The free thiol content was determined by the 5,5'-dithio-bis- [2-nitrobenzoic acid] (DTNB) spectrophotometric assay in 1.0-cm path-length quartz cuvettes with 100 Bio UV-visible spectrophotometer (Cary 100 Bio). The reduced and oxidized AtMPK4 samples were prepared as described above in 100 mM sodium phosphate buffer, with pH 8.0. Diamide treated samples were prepared using 1 mM diamide incubated with reduced WT AtMPK4 for 30 min at room temperature, and the excess of diamide was removed using Hitrap desalting column (GE Healthcare). For each reaction, 0.5 μM sample and 5 μM DTNB were incubated for 5 min at room temperature in a 0.5-mL final volume. Further, 2-nitro-5-thiobenzoate (TNB), DTNB reduction product was followed at 412 nm. An absorption coefficient of 14,150 $M^{-1}cm^{-1}$ (Tossounian, Pedre et al. 2015) was used to quantify the formation of 2-nitro-5-thiobenzoate. All the experiments were performed in duplicate.

Homology modelling of AtMPK4

To visualize the three-dimensional structure of AtMPK4 homology modelling was performed. Homology modelling is a comparative modelling technique which predict the protein 3D structure using a known experimental structure of a homologous protein called template. For AtMPK4 structure prediction, AtMPK6 (pdb:5ci6) was used as a template.

3.3 Results and discussion

AtMPK4 sulfenylates on Cys 181

We studied AtMPK4 that has been identified previously as a sulfenylated protein in *Arabidopsis thaliana* cell suspensions (Waszczak, Akter et al. 2014). We recombinantly produced and purified N- terminal His-tagged AtMPK4. Recombinant AtMPK4 eluted from Ni^{2+} metal affinity column and migrated as a 46-kDa band on a SDS-PAGE gel (Figure 1A). Previous studies have shown that map kinase pathways can be induced by hydrogen peroxide treatments (Liu and He 2017). We confirmed that AtMPK4 is sulfenylated *in vitro* upon H_2O_2 treatment with dimedone (5,5-Dimethyl-1,3-cyclohexadione) based sulfenic acid labelling (Figure 1A). Dimedone specifically binds to sulfenic acid residues (Klomsiri, Nelson et al. 2010). Mass spectrometry analysis identified Cys181 (AtMPK4 C181) sulfenylated upon 1 mM H_2O_2 treatment (Figure. 1B). The AtMPK4 contains eight cysteine residues among which we found that only Cys 181 showed sulfenylation, which implied that sulfenylation occurred on specific cysteine residues in this protein. To the best of our knowledge, this is the first report that shows AtMPK4 sulfenylation on Cys 181.

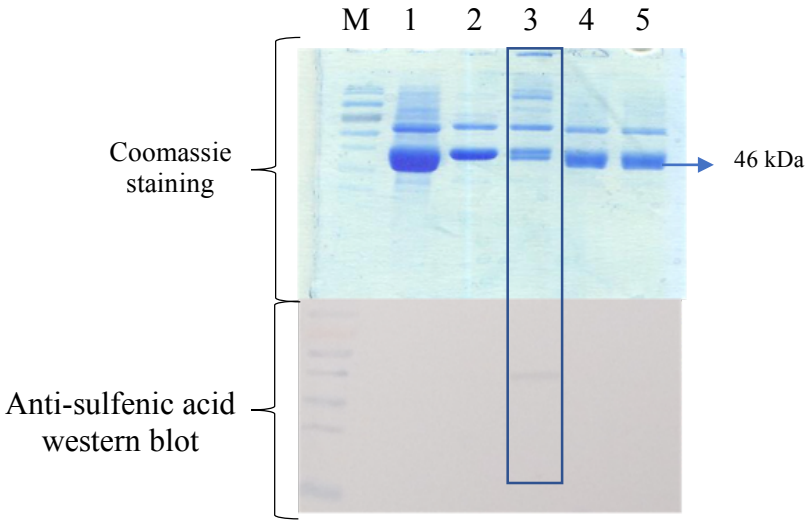

Figure: 1A

Figure 1A: Visualization of protein samples on SDS PAGE gel and sulfenylation signal detection on western blot: Sample 3 shows sulfenylation signal on western blot with anti sulfenic acid antibody and sample 3 band was cut for mass spectrometric analysis.
M: Marker; sample 1: Reduced MPK4; sample 2: Reduced MPK4 treated with 1:8 molar ratio H_2O_2 and 2 mM dimedone and 4 mM NEM; sample 3: Reduced MPK4 treated with 1:50 molar ratio H_2O_2 and 2 mM dimedone and 4 mM NEM; sample 4: Reduced MPK4 treated with 1:8 molar ratio H_2O_2 and 2 mM dimedone; sample 5: Reduced MPK4 with 2 mM Dimedone

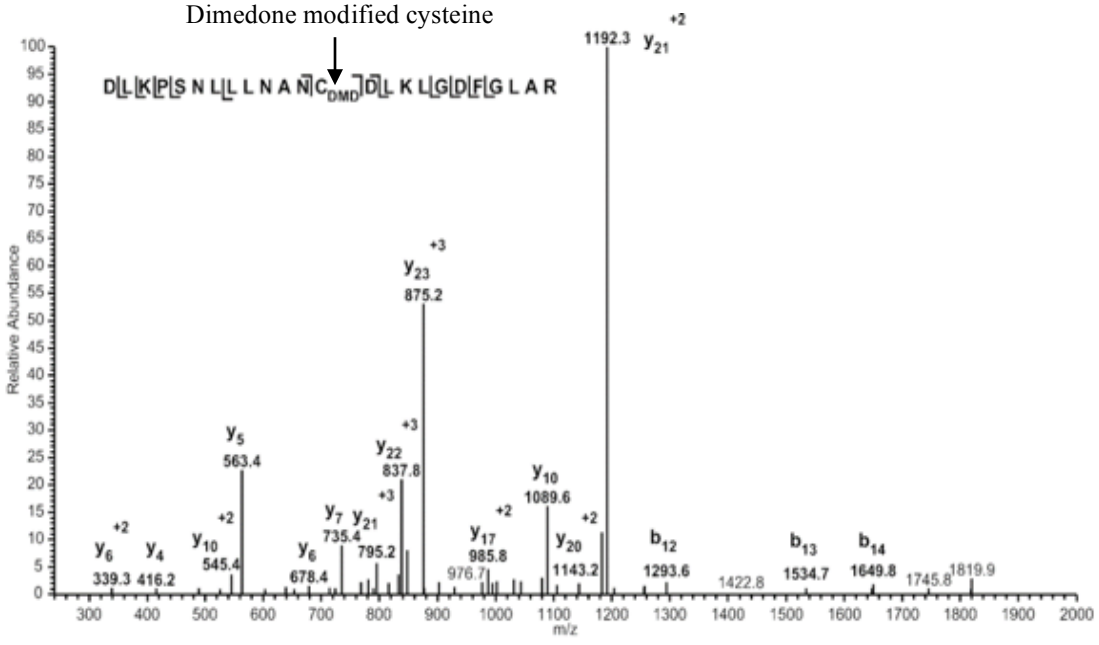

Figure: 1B

Figure 1B: Identification of sulfenylation site on AtMPK4: MS/MS spectrum of DLKPSNLLLNANC$_{DMD}$DLKLGDFGLAR from AtMPK4 showing sulfenylation on Cys181.

AtMPK4 is a monomer and oxidation causes oligomerization

We determined the oligomeric state of reduced and oxidised AtMPK4 by analytical gel filtration column. The purified recombinant AtMPK4 reduced with DTT eluted as a monomer from analytical gel filtration column. Furthermore, our result showed that H_2O_2 treated AtMPK4 oligomerised and formed aggregates. Zhang et al. have reported that *Brassica napus* MPK4 (BnMPK4), which shares 94.95 % amino acid identity with AtMPK4 forms aggregates in the presence of H_2O_2 (Zhang, Zhu et al. 2015). This result indicate that AtMPK4 is sensitive to oxidation. With the DTNB-based assay, we estimated the apparent number of free thiols present in AtMPK4. We found that reduced AtMPK4 had 7.1 free thiols, which is close to the expected value of 8 (Table 2). Whereas the H_2O_2 -treated and diamide-treated AtMPK4 samples have free thiols value of 0.2 and 1.7, respectively.

All together, these results indicate that reduced AtMPK4 contain eight cysteine residues, one of which cannot be reached by DTNB, suggesting that it is buried inside the protein core. The number of free thiols obtained using H_2O_2 -and diamide -treated AtMPK4 samples indicate that cysteine residues might over-oxidise to form a sulfinic or sulfonic acid, or might be involved

in disulfide bond formation. Although this is yet to be confirmed. Furthermore, this result invites a question if AtMPK4 could be a thioredoxin target.

Table 2. DTNB assay

Sample	Obtained value	Expected value
1. Reduced WT MPK4	7.1	8
2. H_2O_2 treated WT MPK4	0.2	0
3. Diamide treated WT MPK4	1.7	0
4. No treatment	1.3	-

Auto-phosphorylation of AtMPK4 and reaction rates

AtMPK4 has been reported to get auto-phosphorylated (Huang, Li et al. 2000). In order to detect the auto-phosphorylation site of AtMPK4, we removed endogenously bound ATP from AtMPK4 by treating AtMPK4 with alkaline phosphatase and further analysed the sample with mass spectrometry. We showed that the AtMPK4 auto-phosphorylates tyrosine 203 without the involvement of upstream kinases (Figure 2A). The MAP kinases have been reported to get auto-phosphorylated (Wu, Rossomando et al. 1991), and highly active MAP kinase required phosphorylation of tyrosine and threonine residues on its TEY motif (Payne, Rossomando et al. 1991). Huang et al. reported that Arabidopsis MEK1 (AtMEK1), which is a map kinase, acts upstream to map kinases, phosphorylates AtMPK4 *in vitro* and primarily phosphorylates its threonine 201 in its TEY motif (Huang, Li et al. 2000). Additionally, they reported that AtMPK4 auto-phosphorylated tyrosine, however they have not described which tyrosine auto-phosphorylates. Our result showed for the first time that AtMPK4 auto-phosphorylates tyrosine 203 on its TEY motif. Moreover, it has been suggested that auto-phosphorylation of map kinase on a Tyr residue increased the affinity for MEK (Haystead, Dent et al. 1992). It will be intriguing to check the reaction rates of auto-phosphorylation of AtMPK4 in the presence of upstream kinase, such as AtMEK1.

Recently, it has been shown that the map kinase 4 of *Brassica napus* auto-phosphorylates threonine and tyrosine at its TEY motif in the presence of its substrate map kinase substrate 1 (MKS1) (Zhang, Zhu et al. 2015). These results indicated that to become phosphorylated at both threonine and tyrosine at the same time on the TEY motif, AtMPK4 most probably required upstream kinases or presence of its substrate while performing the phosphorylation

activity.

Further, to estimate the reaction rate of auto-phosphorylation (Figure 2B), we used an ATP/NADH coupled enzyme assay as described (Truong, Ung et al. 2016). Briefly, in the presence of adenosine triphosphate (ATP) MPK4 auto-phosphorylates and releases adenosine diphosphate (ADP). This ADP reacts with phosphoenol pyruvate (PEP) and forms pyruvate catalysed by pyruvate kinase (PK). In the next step, the resultant pyruvate reacts with nicotinamide adenine dinucleotide reduced (NADH) and produces lactate and NAD+. During the reaction, the consumption of NADH can be monitored spectrophotometrically at a wavelength of 340 nm We obtained V_{max} of 0.001830 µmol. min^{-1}, K_m of 1.12 mM and k_{cat} of $1.23*10^{-6}$ s^{-1}.

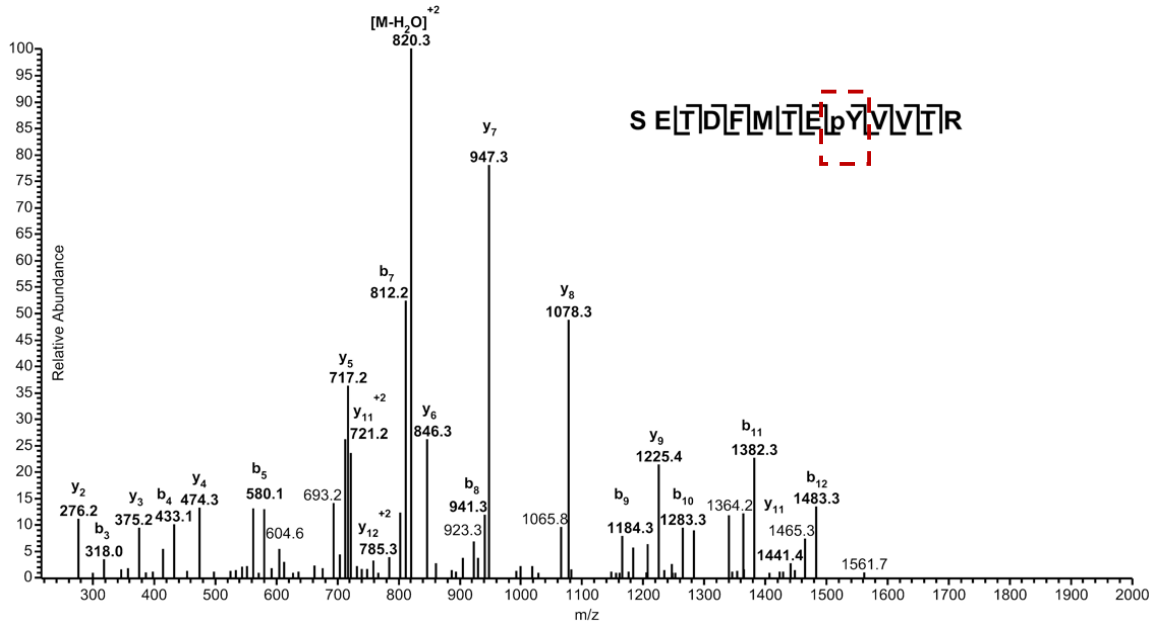

Figure 2A

Figure 2A. Identification of AtMPK4 auto-phosphorylation site: The MS/MS spectrum of SETDFMTEpYVVTR from AtMPK4 showing phosphorylation site on Tyr 203 in the TEY motif.

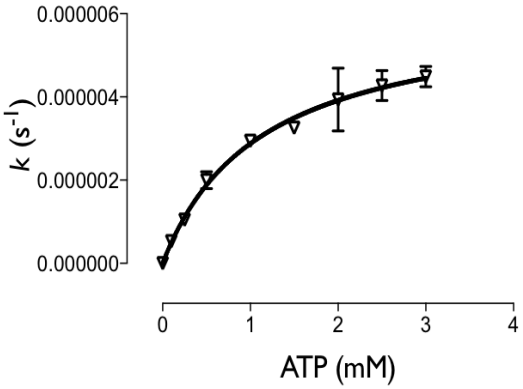

Figure 2B

Figure 2B: Auto-phosphorylation activity of reduced AtMPK4. The experimental data fitted Michaelis-menten curve with V_{max} of 0.001830 µmol. min^{-1}, K_m of 1.12 mM and k_{cat} of 1.23 * 10^{-6} s^{-1}.

Circular dichroism study of AtMPK4

To evaluate the possible structural modifications resulting from the oxidation of AtMPK4, we performed a circular dichroism spectropolarimetry experiment. AtMPK4 does not show any difference between reduced and oxidized AtMPK4 at secondary structure level (Figure. 3).

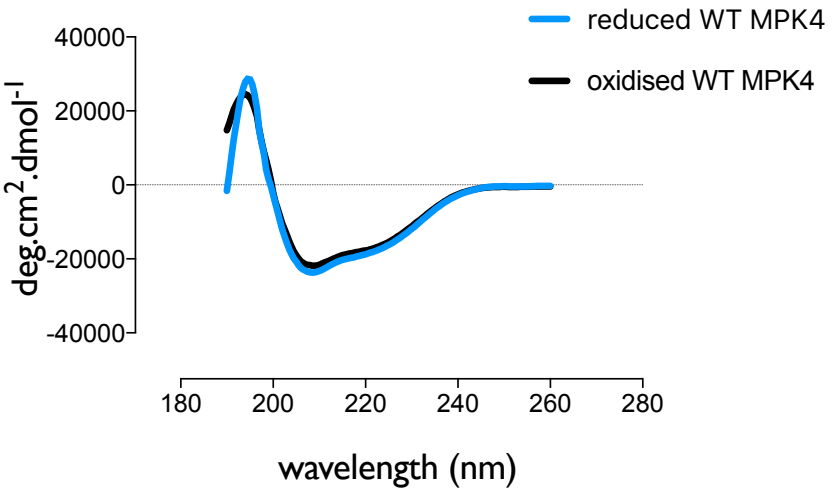

Figure 3: The circular dichroism spectra of the wild-type reduced and oxidized AtMPK4: The comparison of the spectra obtained for wild-type reduced (blue) and oxidized AtMPK4 (black). In the experiment, the spectra were recorded from 190 to 260 nm; five successive spectra were accumulated for each sample. The proteins were used at a final concentration of 2 µM in 50 mM ammonium bicarbonate buffer, pH 7.4 at 30ºC.

Cysteine 181 mutation to serine decreases the phosphorylation activity of AtMPK4

There are eight cysteine residues present in AtMPK4, among which we show that AtMPK4 is sulfenylated on cysteine 181 upon 1 mM H_2O_2 treatment. Therefore, we mutated Cys 181 to serine by site-directed mutagenesis and examined the MBP phosphorylation activity of the AtMPK4 C181S mutant (MPK4 C181S) using a radioactive kinase assay. MBP is a kinase substrate and it has been reported to get phosphorylated by map kinases (Adam, Pike et al. 1997). While comparing the MBP phosphorylation activity of wild type MPK4 (WT MPK4) with MPK4 C181S mutant, we observed significant decrease in the MBP phosphorylation activity of MPK4 C181S mutant (Figure. 4). This result suggested that the Cys181 might play a role in the catalysis of MBP phosphorylation. Nevertheless, it is not yet clear how Cys181 is involved in MBP phosphorylation at molecular level. Nakagami et al. have shown that MEKK1 activates AtMPK4 in protoplasts (Nakagami, Soukupova et al. 2006). MEKK1 is a mitogen activated protein kinase kinase that acts upstream to AtMPK4 and activates AtMPK4 (Kong, Qu et al. 2012). Our result indicated that AtMPK4 can exhibit phosphorylation activity in absence of upstream kinase. The DFG motif present in kinase subdomain VII is utterly conserved in all protein kinases responsible for the catalysis of phosphate transfer (Huang, Li et al. 2000). In the homology model of AtMPK4 structure, we see that Cys181 is not in proximity with the DFG motif (Figure. 5).

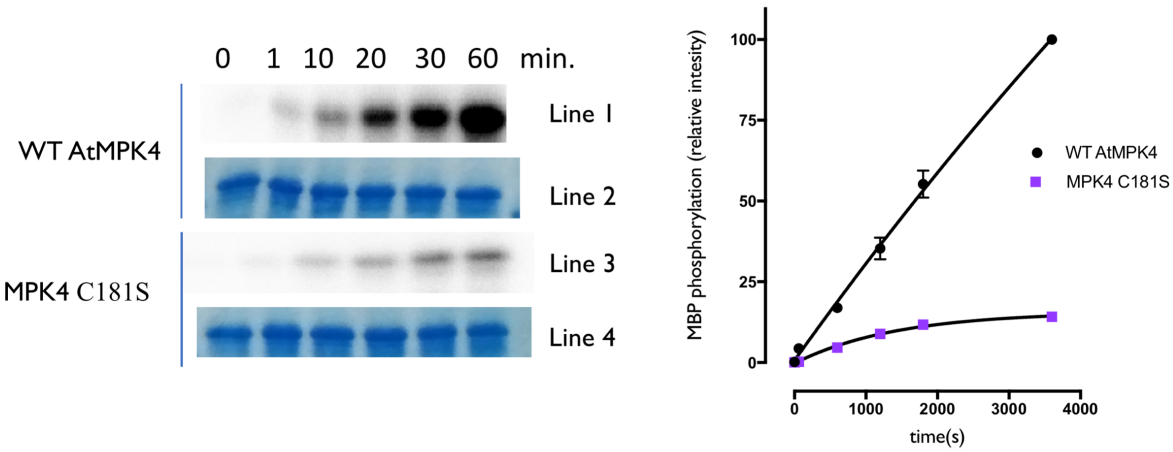

Figure. 4. Phosphorylation of myelin basic protein (MBP) by WT AtMPK4 and MPK4 C181S mutant. A comparison of the MBP phosphorylation of WT AtMPK4 and MPK4 C181S with radioactive kinase assay. A. Line 1 and 3 represent phosphorylation signal from MBP detected on phosphor screen by phosphoimager at different time points. Line 2 and 4 represent coomassie brilliant blue (CBB) stained MBP bands on SDS PAGE gel. B. The phosphorylated MBP signal was quantified with Image Lab™ 6.0 software, and the graph was plotted using GraphPad Prism 7.0 software. All the experiments were done in duplicate.

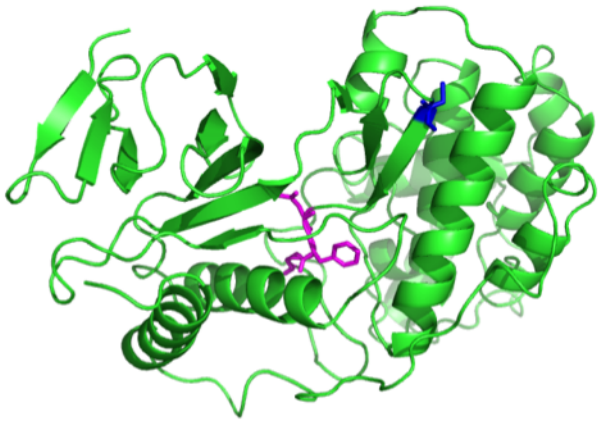

Figure 5. The homology model of AtMPK4 based on the structure of AtMPK6. The location of Cys181 (blue) and the amino acid ATP-binding motif DFG (pink) are shown in stick representation.

AtMPK4 does not bind glutathione

Next, we investigated whether the AtMPK4 binds to glutathione. For this, we used the tryptophan fluorescence spectroscopy to follow the sensitivity of tryptophan as a fluorescence probe toward the changes in its environment upon glutathione binding. Therefore, we used 1 µM reduced WT AtMPK4 and 1 µM oxidized WT AtMPK4, and mixed each sample with glutathione in concentrations of 2 mM and 5 mM in 250 mM Tris-HCl, pH 7.5 and 10 mM $MgCl_2$. Samples were excited at 290 nm with an emission cut-off of 320 nm in stop flow analysis. Our result does not show glutathione binding of AtMPK4 in fluorescence emission spectra (Figure 6.). Xie *et al.* suggested that the glutathione directly inhibited the *in vitro* and *in vivo* kinase activities of *Oryza sativa* MPK3 (OsMPK3) and *Oryza sativa* MPK6 (OsMPK6) through interaction with the fourth Cys in the ATP-binding sites of kinase subdomain VII in OsMPK3 and OsMPK6 (Xie, Sasaki et al. 2014) . They propose that the fourth cysteine, i.e., Cys 179 in OsMPK3 and Cys 210 in case of OsMPK6 can be glutathionylated.

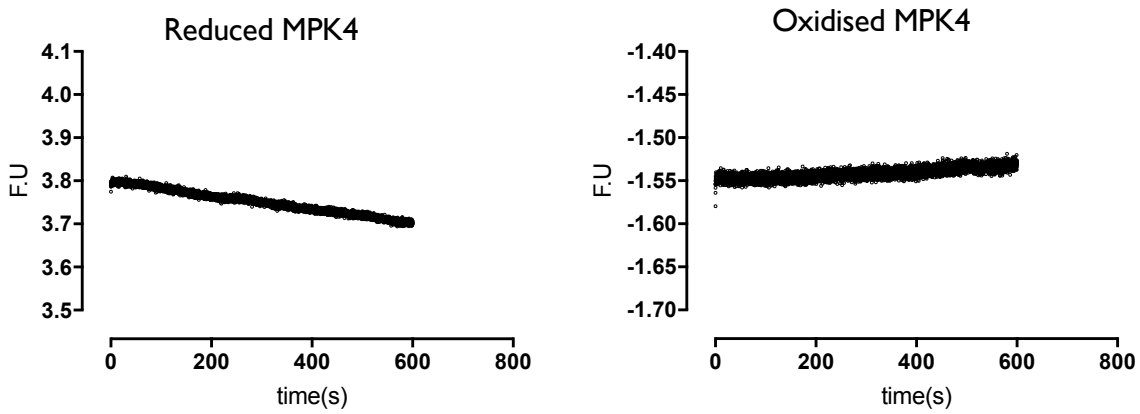

Figure. 6. The stop flow analysis of glutathione binding to AtMPK4. Both reduced and oxidized AtMPK4 do not show GSH binding. The left panel represents reduced AtMPK4 and the right panel represents oxidized AtMPK4.

The sequence alignment of OsMPK3, OsMPK6 and AtMPK4 revealed that AtMPK4 has a Gly residue at the fourth cysteine position, which could be the reason why AtMPK4 does not show binding with GSH (Figure 7.).

```
BnMPK4/1-373     1 MSAEN----------------------------CFGGGGGDQSTKGL 19
AtMPK4/1-376     1 MSAES----------------------------CFGSSGDQSSSKGV 19
OsMPK6/1-398     1 MDAGAQPPDTEMAEAGGGQQPPAAAAAAAGAGAGAGMMENIQAT 43
OsMPK3/1-369     1 MDGAP----------------------------VAEFRPT 12

BnMPK4/1-373    20 ATHGGQYVQYNVYGNIFEVTRKYVPPLRPIGRGAYGIVCAATN 62
AtMPK4/1-376    20 ATHGGSYVQYNVYGNLFEVSRKYVPPLRPIGRGAYGIVCAATN 62
OsMPK6/1-398    44 LSHGGRFIQYNIFGNVFEVTAKYKPPILPIGKGAYGIVCSALN 86
OsMPK3/1-369    13 MTHGGRYLLYDIFGNKFEVTNKYQPPIMPIGRGAYGIVCSVMN 55

BnMPK4/1-373    63 SETGEEVAIKKIGNAFDNIIDAKRTLREIKLLKHMDHENVIAV 105
AtMPK4/1-376    63 SETGEEVAIKKIGNAFDNIIDAKRTLREIKLLKHMDHENVIAV 105
OsMPK6/1-398    87 SETGEQVAIKKIANAFDNKIDAKRTLREIKLLRHMDHENIVAI 129
OsMPK3/1-369    56 FETREMVAIKKIANAFNNDMDAKRTLREIKLLRHLDHENIIGI 98

BnMPK4/1-373   106 KDIIRPPLRENFNDVYIVYELMDTDLHQIIRSNQPLTDDHCRF 148
AtMPK4/1-376   106 KDIIKPPQRENFNDVYIVYELMDTDLHQIIRSNQPLTDDHCRF 148
OsMPK6/1-398   130 RDIIPPPQRNSFNDVYIAYELMDTDLHQIIRSNQALSEEHCQY 172
OsMPK3/1-369    99 RDVIPPPIPQAFNDVYIATELMDTDLHHIIRSNQELSEEHCQY 141

BnMPK4/1-373   149 FLYQLLRGLKYVHSANVLHRDLKPSNLLLNANCDLKLGDFGLA 191
AtMPK4/1-376   149 FLYQLLRGLKYVHSANVLHRDLKPSNLLLNANCDLKLGDFGLA 191
OsMPK6/1-398   173 FLYQILRGLKYIHSANVLHRDLKPSNLLLNANCDLKICDFGLA 215
OsMPK3/1-369   142 FLYQILRGLKYIHSANVIHRDLKPSNLLLNANCDLKICDFGLA 184

BnMPK4/1-373   192 RTKSETDFMTEYVVTRWYRAPELLLNCSEYTAAIDIWSVGCIL 234
AtMPK4/1-376   192 RTKSETDFMTEYVVTRWYRAPELLLNCSEYTAAIDIWSVGCIL 234
OsMPK6/1-398   216 RTTSETDFMTEYVVTRWYRAPELLLNSSEYTAAIDVWSVGCIF 258
OsMPK3/1-369   185 RPSSESDMMTEYVVTRWYRAPELLLNSTDYSAAIDVWSVGCIF 227

BnMPK4/1-373   235 GETMTREPLFPGKDYVHQLRLITELIGSPDDSSLGFLRSDNAR 277
AtMPK4/1-376   235 GETMTREPLFPGKDYVHQLRLITELIGSPDDSSLGFLRSDNAR 277
OsMPK6/1-398   259 MELMDRKPLFPGRDHVHQLRLLMELIGTPNEADLDFV-NENAR 300
OsMPK3/1-369   228 MELINRQPLFPGRDHMHQMRLITEVIGTPTDDELGFIRNEDAR 270

BnMPK4/1-373   278 RYVKQLPQYPRQNFAARFPNMSAGAADLLEKMLVFDPSRRITV 320
AtMPK4/1-376   278 RYVRQLPQYPRQNFAARFPNMSAGAVDLLEKMLVFDPSRRITV 320
OsMPK6/1-398   301 RYIRQLPRHARQSFPEKFPHVHPLAIDLVEKMLTFDPRQRITV 343
OsMPK3/1-369   271 KYMRHLPQYPRRTFASMFPRVQPAALDLIERMLTFNPLQRITV 313

BnMPK4/1-373   321 DEALCHPYLAPLHDINEEPVCVRPFNFDFEQPSLTEENIKELI 363
AtMPK4/1-376   321 DEALCHPYLAPLHDINEEPVCVRPFNFDFEQPTLTEENIKELI 363
OsMPK6/1-398   344 EGALAHPYLASLHDISDEPVCSSPFSFDFEQHALSEEQMKDLI 386
OsMPK3/1-369   314 EEALDHPYLERLHDIADEPICLEPFSFDFEQKALNEDQMKQLI 356

BnMPK4/1-373   364 YRETVKFNPQ---                              373
AtMPK4/1-376   364 YRETVKFNPQDSV                            376
OsMPK6/1-398   387 YQEGLAFNPDYQ-                            398
OsMPK3/1-369   357 FNEAIEMNPNIRY                            369
```

Figure 7: The sequence alignment of AtMPK4, OsMPK6, OsMPK3 and BnMPK4. The multiple sequence alignment was performed using Clustal omega. The graphical representation of sequence alignment was shown by Jalview. The blue arrow shows the presence of glycine residue in AtMPK4 and BnMPK4.

The kinases catalyse the transfer of the phosphoryl group from ATP to itself in the auto-phosphorylaltion reaction. Therefore, we prompted to see the binding of ATP and adenylyl-imidodiphosphate (AMP-PNP), which is a non-hydrolysable ATP to AtMPK4. Our results do not show the binding of ATP to AtMPK4, but our preliminary data shows that AMP-PNP binds to AtMPK4 (Figure 8) in stop flow analysis.

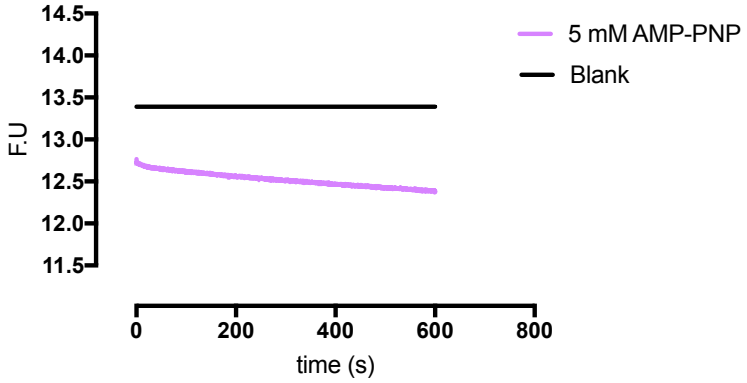

Figure 8: The binding of adenylyl-imidodiphosphate (AMP-PNP) to AtMPK4: The final concentration of 1 µM WT AtMPK4 was mixed with the 5 mM AMP-PNP in 250 mM Tris-HCl, pH 7.5 and 10 mM $MgCl_2$ at 30ºC and fluorescence emission spectra was obtained.

3.4 Conclusion and perspectives

Mitogen Activated Protein kinase pathways are known to be activated by biotic and abiotic stresses. *Arabidopsis* MPK4 has been reported to be activated by salt, drought, touch, cold and wound stress (Ichimura, Mizoguchi et al. 2000), which indicates that MPK4 plays a crucial role in transducing the stress signal response. It has also shown that AtMPK4 involved in various physiological function such as in the regulation of plant cytokinesis during mitosis and meiosis, microtubule organization as well as in root hair development(Beck, Komis et al. 2010). Our novel finding on AtMPK4 indicates that it is one of the sulfenylated protein kinase and the involvement of cysteine 181 may play a role in substrate phosphorylation activity. Also, we observe that oxidation causes oligomerization and reduces the number of free thiols

of the AtMPK4 indicating conformational change in the AtMPK4. Although it remains unclear if oxidation affects the activity of AtMPK4.

To assess the oxidation effects and role of cysteine 181 on AtMPK4 more efforts are required both in vitro and in planta. To investigate the role of sulfenylation in biological function, it is very crucial to know the involvement of Cys181 under non-stressed and stressed conditions in the plants. It has been reported that an AtMPK4 knockout mutant plant has a dwarf phenotype (Kosetsu, Matsunaga et al. 2010). It will be fascinating to complement the AtMPK4 knockout plant with MPK4 C181S mutant gene to know if complementation has any affect in the phenotype.

Recently, Truong et al. have shown that the activity of epidermal growth factor receptor kinase is regulated by sulfenylation of its Cys 797 (Truong, Ung et al. 2016). It might be interesting to evaluate the impact of a MPK4 C181D mutant activity in vitro and in plants, as aspartic acid mimics a sulfinic acid. Additionally, the structural aspects describing the active site of AtMPK4 need to be investigated. The structure of AtMPK4 and its mutants along with the structural complex of AtMPK4 with its substrate could unravel the molecular mechanism behind the role of sulfenylation on its activity. Furthermore, fishing out the interactors of AtMPK4 and its mutant upon oxidative stress condition will be interesting as it has been reported that AtMPK4 interacts with transcription factors, such as ASR3 and MYB75 (Li, Jiang et al. 2015, Li, Wang et al. 2016).

Acknowledgements

We thank Didier Vertommen for generously providing mass spectrometry service. We also thank Leonardo Rosado, David Young and Brandán Pérez for their fruitful discussions. Nandita Bodra is indebted to the Indian Council of Agricultural Research for a PhD fellowship.

References

Adam, A. L., S. Pike, M. E. Hoyos, J. M. Stone, J. C. Walker and A. Novacky (1997). "Rapid and transient activation of a myelin basic protein kinase in tobacco leaves treated with harpin from *Erwinia amylovora*." Plant Physiol **115**(2): 853-861.

Beck, M., G. Komis, J. Muller, D. Menzel and J. Samaj (2010). "*Arabidopsis* homologs of nucleus- and phragmoplast-localized kinase 2 and 3 and mitogen-activated protein kinase 4 are essential for microtubule organization." Plant Cell **22**(3): 755-771.

Bigeard, J., J. Colcombet and H. Hirt (2015). "Signaling mechanisms in pattern-triggered immunity (PTI)." Mol Plant **8**(4): 521-539.

Chinnusamy, V., K. Schumaker and J. K. Zhu (2004). "Molecular genetic perspectives on cross-talk and specificity in abiotic stress signalling in plants." J Exp Bot **55**(395): 225-236.

Foreman, J., V. Demidchik, J. H. Bothwell, P. Mylona, H. Miedema, M. A. Torres, P. Linstead, S. Costa, C. Brownlee, J. D. Jones, J. M. Davies and L. Dolan (2003). "Reactive oxygen species produced by NADPH oxidase regulate plant cell growth." Nature **422**(6930): 442-446.

Foyer, C. H. and G. Noctor (2009). "Redox regulation in photosynthetic organisms: signaling, acclimation, and practical implications." Antioxid Redox Signal **11**(4): 861-905.

Group, M. (2002). "Mitogen-activated protein kinase cascades in plants: a new nomenclature." Trends Plant Sci **7**(7): 301-308.

Hamel, L. P., M. C. Nicole, S. Sritubtim, M. J. Morency, M. Ellis, J. Ehlting, N. Beaudoin, B. Barbazuk, D. Klessig, J. Lee, G. Martin, J. Mundy, Y. Ohashi, D. Scheel, J. Sheen, T. Xing, S. Zhang, A. Seguin and B. E. Ellis (2006). "Ancient signals: comparative genomics of plant MAPK and MAPKK gene families." Trends Plant Sci **11**(4): 192-198.

Haystead, T. A., P. Dent, J. Wu, C. M. Haystead and T. W. Sturgill (1992). "Ordered phosphorylation of p42mapk by MAP kinase kinase." FEBS Lett **306**(1): 17-22.

Hettenhausen, C., M. C. Schuman and J. Wu (2015). "MAPK signaling: a key element in plant defense response to insects." Insect Sci **22**(2): 157-164.

Huang, Y., H. Li, R. Gupta, P. C. Morris, S. Luan and J. J. Kieber (2000). "ATMPK4, an Arabidopsis homolog of mitogen-activated protein kinase, is activated in vitro by AtMEK1 through threonine phosphorylation." Plant Physiol **122**(4): 1301-1310.

Ichimura, K., T. Mizoguchi, R. Yoshida, T. Yuasa and K. Shinozaki (2000). "Various abiotic stresses rapidly activate *Arabidopsis* MAP kinases ATMPK4 and ATMPK6." Plant J **24**(5): 655-665.

Klomsiri, C., K. J. Nelson, E. Bechtold, L. Soito, L. C. Johnson, W. T. Lowther, S. E. Ryu, S. B. King, C. M. Furdui and L. B. Poole (2010). "Use of dimedone-based chemical probes for sulfenic acid detection evaluation of conditions affecting probe incorporation into redox-sensitive proteins." Methods Enzymol **473**: 77-94.

Komis, G., P. Illes, M. Beck and J. Samaj (2011). "Microtubules and mitogen-activated protein kinase signalling." Curr Opin Plant Biol **14**(6): 650-657.

Kong, Q., N. Qu, M. Gao, Z. Zhang, X. Ding, F. Yang, Y. Li, O. X. Dong, S. Chen, X. Li and Y. Zhang (2012). "The MEKK1-MKK1/MKK2-MPK4 kinase cascade negatively regulates immunity mediated by a mitogen-activated protein kinase kinase kinase in Arabidopsis." Plant Cell **24**(5): 2225-2236.

Kosetsu, K., S. Matsunaga, H. Nakagami, J. Colcombet, M. Sasabe, T. Soyano, Y. Takahashi, H. Hirt and Y. Machida (2010). "The MAP kinase MPK4 is required for cytokinesis in *Arabidopsis thaliana*." Plant Cell **22**(11): 3778-3790.

Laloi, C., D. Mestres-Ortega, Y. Marco, Y. Meyer and J. P. Reichheld (2004). "The Arabidopsis cytosolic thioredoxin h5 gene induction by oxidative stress and its W-box-mediated response to pathogen elicitor." Plant Physiol **134**(3): 1006-1016.

Li, B., S. Jiang, X. Yu, C. Cheng, S. Chen, Y. Cheng, J. S. Yuan, D. Jiang, P. He and L. Shan (2015). "Phosphorylation of trihelix transcriptional repressor ASR3 by MAP KINASE4 negatively regulates *Arabidopsis* immunity." Plant Cell **27**(3): 839-856.

Li, S., W. Wang, J. Gao, K. Yin, R. Wang, C. Wang, M. Petersen, J. Mundy and J. L. Qiu (2016). "MYB75 phosphorylation by MPK4 Is required for light-induced anthocyanin accumulation in *Arabidopsis*." Plant Cell **28**(11): 2866-2883.

Liu, Y. (2012). "Roles of mitogen-activated protein kinase cascades in ABA signaling." Plant Cell Rep **31**(1): 1-12.

Liu, Y. and C. He (2017). "A review of redox signaling and the control of MAP kinase pathway in plants." Redox Biol **11**: 192-204.

Meng, X. and S. Zhang (2013). "MAPK cascades in plant disease resistance signaling." Annu Rev Phytopathol **51**: 245-266.

Miles, G. P., M. A. Samuel, Y. Zhang and B. E. Ellis (2005). "RNA interference-based (RNAi) suppression of AtMPK6, an Arabidopsis mitogen-activated protein kinase, results in hypersensitivity to ozone and misregulation of AtMPK3." Environ Pollut **138**(2): 230-237.

Moller, I. M., P. E. Jensen and A. Hansson (2007). "Oxidative modifications to cellular components in plants." Annu Rev Plant Biol **58**: 459-481.

Nakagami, H., H. Soukupova, A. Schikora, V. Zarsky and H. Hirt (2006). "A Mitogen-activated protein kinase kinase kinase mediates reactive oxygen species homeostasis in *Arabidopsis*." J Biol Chem **281**(50): 38697-38704.

Noctor, G. and C. H. Foyer (2016). "Intracellular Redox Compartmentation and ROS-Related Communication in regulation and signaling." Plant Physiol **171**(3): 1581-1592.

Payne, D. M., A. J. Rossomando, P. Martino, A. K. Erickson, J. H. Her, J. Shabanowitz, D. F. Hunt, M. J. Weber and T. W. Sturgill (1991). "Identification of the regulatory phosphorylation sites in pp42/mitogen-activated protein kinase (MAP kinase)." EMBO J **10**(4): 885-892.

Petersen, M., P. Brodersen, H. Naested, E. Andreasson, U. Lindhart, B. Johansen, H. B. Nielsen, M. Lacy, M. J. Austin, J. E. Parker, S. B. Sharma, D. F. Klessig, R. Martienssen, O. Mattsson, A. B. Jensen and J. Mundy (2000). "Arabidopsis map kinase 4 negatively regulates systemic acquired resistance." Cell **103**(7): 1111-1120.

Pitzschke, A. and H. Hirt (2006). "Mitogen-activated protein kinases and reactive oxygen species signaling in plants." Plant Physiol **141**(2): 351-356.

Pitzschke, A. and H. Hirt (2009). "Disentangling the complexity of mitogen-activated protein kinases and reactive oxygen species signaling." Plant Physiol **149**(2): 606-615.

Smekalova, V., A. Doskocilova, G. Komis and J. Samaj (2014). "Crosstalk between secondary messengers, hormones and MAPK modules during abiotic stress signalling in plants." Biotechnol Adv **32**(1): 2-11.

Suzuki, N., S. Koussevitzky, R. Mittler and G. Miller (2012). "ROS and redox signalling in the response of plants to abiotic stress." Plant Cell Environ **35**(2): 259-270.

Teige, M., E. Scheikl, T. Eulgem, R. Doczi, K. Ichimura, K. Shinozaki, J. L. Dangl and H. Hirt (2004). "The MKK2 pathway mediates cold and salt stress signaling in *Arabidopsis*." Mol Cell **15**(1): 141-152.

Torres, M. A. and J. L. Dangl (2005). "Functions of the respiratory burst oxidase in biotic interactions, abiotic stress and development." Curr Opin Plant Biol **8**(4): 397-403.

Tossounian, M. A., B. Pedre, K. Wahni, H. Erdogan, D. Vertommen, I. Van Molle and J. Messens (2015). "*Corynebacterium diphtheriae* methionine sulfoxide reductase a exploits a unique mycothiol redox relay mechanism." J Biol Chem **290**(18): 11365-11375.

Truong, T. H., P. M. Ung, P. B. Palde, C. E. Paulsen, A. Schlessinger and K. S. Carroll (2016). "Molecular basis for redox activation of epidermal growth factor receptor kinase." Cell Chem Biol **23**(7): 837-848.

Wan, X. Y. and J. Y. Liu (2008). "Comparative proteomics analysis reveals an intimate protein network provoked by hydrogen peroxide stress in rice seedling leaves." Mol Cell Proteomics **7**(8): 1469-1488.

Wang, P., Y. Du, Y. Li, D. Ren and C. P. Song (2010). "Hydrogen peroxide-mediated activation of MAP kinase 6 modulates nitric oxide biosynthesis and signal transduction in *Arabidopsis*." Plant Cell **22**(9): 2981-2998.

Waszczak, C., S. Akter, D. Eeckhout, G. Persiau, K. Wahni, N. Bodra, I. Van Molle, B. De Smet, D. Vertommen, K. Gevaert, G. De Jaeger, M. Van Montagu, J. Messens and F. Van Breusegem (2014). "Sulfenome mining in *Arabidopsis thaliana*." Proc Natl Acad Sci U S A **111**(31): 11545-11550.

Wu, J., A. J. Rossomando, J. H. Her, R. Del Vecchio, M. J. Weber and T. W. Sturgill (1991). "Autophosphorylation in vitro of recombinant 42-kilodalton mitogen-activated protein kinase on tyrosine." Proc Natl Acad Sci U S A **88**(21): 9508-9512.

Xie, G., K. Sasaki, R. Imai and D. Xie (2014). "A redox-sensitive cysteine residue regulates the kinase activities of OsMPK3 and OsMPK6 in vitro." Plant Sci **227**: 69-75.

Xing, Y., W. Jia and J. Zhang (2007). "AtMEK1 mediates stress-induced gene expression of CAT1 catalase by triggering H_2O_2 production in *Arabidopsis*." J Exp Bot **58**(11): 2969-2981.

Xiong, L. and Y. Yang (2003). "Disease resistance and abiotic stress tolerance in rice are inversely modulated by an abscisic acid-inducible mitogen-activated protein kinase." Plant Cell **15**(3): 745-759.

Xu, J. and S. Zhang (2015). "Mitogen-activated protein kinase cascades in signaling plant growth and development." Trends Plant Sci **20**(1): 56-64.

Zhang, T., M. Zhu, W. Y. Song, A. C. Harmon and S. Chen (2015). "Oxidation and phosphorylation of MAP kinase 4 cause protein aggregation." Biochim Biophys Acta **1854**(2): 156-165.

General conclusion

Plants require diverse responses and adjustment of multiple adaptation mechanisms to cope with the multiple stresses that occur in nature including biotic and abiotic stresses. As a consequence of stress exposure, reactive oxygen species (ROS) production occur that could either be beneficial or detrimental to the plant cells. Various types of ROS such as hydrogen peroxide (H_2O_2), hydroxyl radical ($HO^{\bullet}$), singlet oxygen ($^1O_2$) or superoxide anion ($O_2^{\bullet-}$) and their production in subcellular sites decides the biochemical, physiological and molecular responses. It has been anticipated that ROS signals or signatures by the cell occur through different redox reactions in which ROS such as H_2O_2 oxidizes sulfur-containing residues of proteins that is the SH group of cysteine and alter protein structure and function via the formation of disulfide bonds. Such protein modification can further lead to regulate the binding of transcription factors (TFs) to DNA and affect transcription (Dietz, Turkan et al. 2016). Therefore, the study of ROS-induced protein modifications is fundamental to our understanding of how ROS can modify gene expression and metabolism during various stress conditions. Among the most important ROS-induced post-translational modifications are sulfenic acid, sulfinic/ sulfonic acid and glutathionylation which have been reviewed in the chapter 1. One of the mechanisms that regulates the activity of several enzymes and TFs in plants is the oxidation of sulfhydryl groups. H_2O_2 mainly induces the oxidation and generate sulfenic acid (R-SOH) that can lead to the formation of disulfide (S–S) bonds between cysteine residues which in turn result in conformational changes that alter protein/enzyme activity. Further, the protein can recover from the oxidation and attain its reduced form by reacting with thioredoxin, peroxiredoxin or glutathione and in this way protein respond to oxidative stress and regulate redox homeostasis.

In my PhD research, I studied two proteins, dehydroascorbate reductase 2 and mitogen activated kinase 4 which we found to be sulfenylated in *Arabidopsis thaliana* cells under hydrogen peroxide stress. The genome of *Arabidopsis thaliana* encodes three isoforms of dehydroascorbate reductases (DHARs) namely the mitochondrial DHAR1, the cytosolic DHAR2 and a chloroplastic DHAR3. In planta studies on perturbation of DHARs have shown to affect the rate of plant growth and leaf aging due to ROS mediated damage (Chen and Gallie 2006).The overexpression of DHAR in plants have shown to increase the level of ascorbic acid

through improved ascorbate recycling (Chen, Young et al. 2003). DHAR2 catalyzes the reduction of oxidized ascorbate with a concomitant oxidation of glutathione (GSH) to oxidized glutathione (GSSG) and therefore it is one of the core enzymes of the GSH/ascorbate cycle that maintains reduced ascorbate pools in the cell (Shimaoka, Yokota et al. 2000). DHAR2 contains two cysteine residues and to understand the possible function of cysteine residue of DHAR2, Waszczak et al. modified the free thiols with iodoacetamide and oxidized DHAR2 with increasing concentration of H_2O_2 and showed that the activity of DHAR2 is affected which indicate the importance of cysteine residue (Dixon, Davis et al. 2002, Waszczak, Akter et al. 2014).

The chapter 2 of my thesis elaborates the findings of DHAR2. Our steady state kinetics study revealed that DHAR2 exhibit an allosteric behavior which is a rare phenomenon for a monomeric enzyme. Also, we showed that DHAR2 is glutathionylated on cysteine 20 and determined the crystal structure of glutathione bound DHAR2 which showed glutathione interacting environment. We compared the glutathione binding site of DHAR2 with its structural homologs such as glutathione transferases and chloride ion channel proteins. Furthermore, we proposed the possible mechanism of DHAR2 catalysis and confirmed the release of oxidized glutathione (GSSG) upon reaction of glutathionylated DHAR2 with reduced glutathione. Our in depth structural analysis of DHAR2 exposed the local conformational variability in alpha 2 helical region which demonstrated the structural flexibility of DHAR2 (Bodra, Young et al. 2017)..

Next, we chose mitogen activated kinase 4 (MPK4) from the YAP1C and DYn-2 sulfenome list. The mitogen activated kinase signaling cascades are integral part of plant biotic and abiotic stress signaling pathways (Kovtun, Chiu et al. 2000, Zhou, Xia et al. 2014). Human and yeast model systems showed that MPKs are redox regulated through upstream regulators and through direct cysteine oxidation events (Truong and Carroll 2013). In the human p38 MPK a cysteine oxidation had been shown to act as a functional regulatory switch (Templeton, Aye et al. 2010). Although, till date in plant mitogen activated cascade no such thiol modification has been reported. Therefore, to understand the possible role of cysteine residues in plant MPKs we characterized *Arabidopsis* MPK4. Mitogen activated kinase cascades are conserved signaling modules found in all eukaryotes, which transduce environmental and developmental cues into intracellular responses (Tena, Asai et al. 2001, Jonak, Okresz et al. 2002). In *Arabidopsis thaliana* mitogen activated kinase cascades have been shown to be involved in signaling

pathways activated by abiotic stresses such as cold, salt, touch, wounding and osmotic shock (Ichimura, Mizoguchi et al. 2000, Droillard, Boudsocq et al. 2002, Ahlfors, Macioszek et al. 2004, Teige, Scheikl et al. 2004). It has been reported that H_2O_2 is a potent activator of mitogen activated protein kinases in Arabidopsis leaf cells (Kovtun, Chiu et al. 2000). The complex role of mitogen activated protein kinase cascades in ROS signaling and responses has been revealed in regulation of ROS-related genes, executing plant cell death, and modulating stomatal function but how ROS activates this cascade is still not understood. In chapter 3 we investigated Arabidopsis MPK4 which is a terminal kinase located in cytosol and nucleus and part of a typical MAP kinase cascade module involved in signal perception and transduction induced by oxidative stress. It plays an important role in defense responses and *mpk4* knockout (KO) plants display constitutive stress responses and enhanced resistance to biotrophic pathogens (Petersen, Brodersen et al. 2000). The function of MPK4 has been extensively studied in plants. It has been reported to be involved in cortical microtubule organization, cell plate formation in cytokinesis, pollen development and systemic acquired resistance (Petersen, Brodersen et al. 2000, Beck, Komis et al. 2010, Zeng, Chen et al. 2011, Suzuki, Matsushima et al. 2016). Recently, it has been reported that MPK4 is essential for light induced anthocyanin accumulation in Arabidopsis (Li, Wang et al. 2016). Anthocyanins are non-photosynthetic pigments likely to scavenge reactive oxygen species produced under light stress (Gould 2004, Maier, Schrader et al. 2013). *Nicotiana benthiana* MPK4 which is homolog of Arabidopsis MPK4 is engaged in ozone tolerance via stomatal movement in tobacco (Gomi, Ogawa et al. 2005). Silencing *Nicotiana attenuata* MPK4 (NaMPK4) delayed senescence and increased photosynthetic rates (Hettenhausen, Baldwin et al. 2012).The overexpression of *Brassica napus* MPK4 (BnMPK4) significantly enhances the resistance to *Sclerotinia sclerotiorum* and *Botrytis cinerea* in transgenic oilseed rape (Wang, Mao et al. 2009).

In our study, we presented the biochemical aspects of *Arabidopsis* MPK4. We validated that H_2O_2 treatment on recombinant MPK4 lead to sulfenylation and identified that cysteine 181 forms sulfenic acid. We also showed that cysteine 181 mutation to serine residue resulted in lower substrate phosphorylation activity compared to wild type MPK4. Furthermore, we showed that reduced and oxidized MPK4 have no secondary structural differences. Also, we confirmed that both reduced and oxidized MPK4 do not interact with glutathione. Additionally, we showed that MPK4 exhibit auto-phosphorylation activity and phosphorylates on tyrosine 203. Next, we speculated that H_2O_2 induced oxidation of MPK4 might lead to form either disulfide bond or over-oxidation to form sulfinic and sulfonic acid.

Future perspectives

The study on post-translational modifications of cysteine residues has gained interest in recent years because of the demonstrated involvement of cysteine residues in the regulation of both protein stability, confirmation and activity. With the use of the YAP1C and DYn-2 probes, we explored the *Arabidopsis thaliana* sulfenome during hydrogen peroxide exposure (Waszczak, Akter et al. 2014, Akter, Huang et al. 2015). These efforts have provided us a first inventory plant proteins which undergo cysteine oxidation to form cysteine sulfenic acid. These proteins were before reported to be involved in signal perception and transduction, redox regulation, protein degradation, RNA binding-translation, primary metabolism, amino acid metabolism, hormone homeostasis and several unknown functions. Until now, only for a fraction of these proteins, the relevance of cysteine oxidation has been investigated. Therefore, in order to understand better the function effect of sulfenic acid formation on these proteins, it is necessary to characterize these sulfenylated proteins individually. Because the amount of sulfenylated proteins to be investigated outnumbers the available hands and brains in one lab, a prioritization effort is needed. The major criteria to prioritise the sulfenylated proteins that are detected through the various direct proteomics approaches could be their involvement in a biological process or mechanism of interest; more pragmatic characteristics like the availability of loss and gain of function mutants, and prior art information about the critical cysteine that undergoes the post-translational modification of interest. Once prioritized, again pragmatic issues like feasibility of recombinant protein production in standard hosts like *E.coli*, available enzymatic assays and potentially available structural information of the protein can be taken into account.

Although we are making progress with DEHYDROASCORBATE REDUCTASE 2 and MITOGEN ACTIVATED KINASE 4 in understanding the role of cysteine oxidation, there still remain several open questions. The most important, but also the most difficult one, is to nail down the physiological relevance of these sulfenylation events in planta. To obtain a first-line answer, a phenotypic complementation effort of a loss-of-function line with a mutated version of DHAR2 and MPK4 (in which the critical Cys residue is altered into serine) mutant line will be done. Once available, these transgenic events will be phenotypically evaluated under normal growth conditions, as well as under under stress conditions, such as high light and salt stress.

The effect of oxidation on *Arabidopsis* MPK4 auto-phosphorylation and substrate phosphorylation activity remains to be determined. Intriguingly, (artificial) substrate phosphorylation activity of the (in vitro) MPK4 C181S mutant is lower as compared to wild type MPK4.

A plausible hypothesis to explain this observation is that the C181S mutation trigger a conformational change in MPK4 mutant due to which activity goes down. Therefore, a structural analysis of MPK4 C181S mutant could be the further step to visualize the difference between wild type MPK4 and MPK4 C181S mutant which could also unravel the possible reaction mechanism behind the substrate phosphorylation of *Arabidopsis* MPK4. So far only the structural information of *Arabidopsis* MPK6 from plant has been deposited in the protein data bank (Wang, Qin et al. 2016). In contrast with our in vitro data, Wang et al. showed that Arabidopsis MPK6 (F364L) and MPK6 (F368L) mutants, in which Phe364 and Phe368 were mutated to Leu respectively had higher intrinsic kinase activity. Moreover, to further examine the role of sulfenylation in plants, the cysteine 181 of MPK4 could be mutated to aspartate. Aspartate will mimic the structure of a sulfenic acid. Upon oxidation, we showed that the number of free thiols present in the MPK4 reduces which raise the question if MPK4 could be the target of thioredoxin system. Also, it is interesting to know if MPK4 C181S mutant could still localizes to the nucleus upon stress. Several studies have been done to find the substrate and interactors of Arabidopsis MPK4 (Petersen, Qiu et al. 2010, Li, Jiang et al. 2015, Li, Wang et al. 2016, Suzuki, Matsushima et al. 2016, Rayapuram, Bigeard et al. 2018). In future MPK4 C181S mutant interactors could be identified and compared with wild type MPK4.

In summary, the characterization of the sulfenylated proteins demand a keen effort to overcome the difficulty to express recombinant plant proteins, to design appropriate activity assays, to get the mutant phenotypes, to have information about the role and function of the identified proteins and to get the structural view of each protein. However, we hope that such type of efforts will contribute to evaluate the potential for biotechnological applications by modifying sulfenylated proteins. E.g. to improve stress tolerance in plants.

References

Ahlfors, R., V. Macioszek, J. Rudd, M. Brosche, R. Schlichting, D. Scheel and J. Kangasjarvi (2004). "Stress hormone-independent activation and nuclear translocation of mitogen-activated protein kinases in *Arabidopsis thaliana* during ozone exposure." Plant J **40**(4): 512-522.

Akter, S., J. Huang, N. Bodra, B. De Smet, K. Wahni, D. Rombaut, J. Pauwels, K. Gevaert, K. Carroll, F. Van Breusegem and J. Messens (2015). "DYn-2 based identification of *Arabidopsis* sulfenomes." Mol Cell Proteomics **14**(5): 1183-1200.

Beck, M., G. Komis, J. Muller, D. Menzel and J. Samaj (2010). "Arabidopsis homologs of nucleus- and phragmoplast-localized kinase 2 and 3 and mitogen-activated protein kinase 4 are essential for microtubule organization." Plant Cell **22**(3): 755-771.

Bodra, N., D. Young, L. Astolfi Rosado, A. Pallo, K. Wahni, F. De Proft, J. Huang, F. Van Breusegem and J. Messens (2017). "*Arabidopsis thaliana* dehydroascorbate reductase 2: Conformational flexibility during catalysis." Sci Rep **7**: 42494.

Chen, Z. and D. R. Gallie (2006). "Dehydroascorbate reductase affects leaf growth, development, and function." Plant Physiol **142**(2): 775-787.

Chen, Z., T. E. Young, J. Ling, S. C. Chang and D. R. Gallie (2003). "Increasing vitamin C content of plants through enhanced ascorbate recycling." Proc Natl Acad Sci U S A **100**(6): 3525-3530.

Dietz, K. J., I. Turkan and A. Krieger-Liszkay (2016). "Redox- and Reactive Oxygen Species-Dependent signaling into and out of the photosynthesizing chloroplast." Plant Physiol **171**(3): 1541-1550.

Dixon, D. P., B. G. Davis and R. Edwards (2002). "Functional divergence in the glutathione transferase superfamily in plants. Identification of two classes with putative functions in redox homeostasis in Arabidopsis thaliana." J Biol Chem **277**(34): 30859-30869.

Droillard, M., M. Boudsocq, H. Barbier-Brygoo and C. Lauriere (2002). "Different protein kinase families are activated by osmotic stresses in *Arabidopsis thaliana* cell suspensions. Involvement of the MAP kinases AtMPK3 and AtMPK6." FEBS Lett **527**(1-3): 43-50.

Gomi, K., D. Ogawa, S. Katou, H. Kamada, N. Nakajima, H. Saji, T. Soyano, M. Sasabe, Y. Machida, I. Mitsuhara, Y. Ohashi and S. Seo (2005). "A mitogen-activated protein kinase NtMPK4 activated by SIPKK is required for jasmonic acid signaling and involved in ozone tolerance via stomatal movement in tobacco." Plant Cell Physiol **46**(12): 1902-1914.

Gould, K. S. (2004). "Nature's Swiss Army Knife: The Diverse Protective Roles of Anthocyanins in Leaves." J Biomed Biotechnol **2004**(5): 314-320.

Hettenhausen, C., I. T. Baldwin and J. Wu (2012). "Silencing MPK4 in Nicotiana attenuata enhances photosynthesis and seed production but compromises abscisic acid-induced stomatal closure and guard cell-mediated resistance to Pseudomonas syringae pv tomato DC3000." Plant Physiol **158**(2): 759-776.

Ichimura, K., T. Mizoguchi, R. Yoshida, T. Yuasa and K. Shinozaki (2000). "Various abiotic stresses rapidly activate Arabidopsis MAP kinases ATMPK4 and ATMPK6." Plant J **24**(5): 655-665.

Jonak, C., L. Okresz, L. Bogre and H. Hirt (2002). "Complexity, cross talk and integration of plant MAP kinase signalling." Curr Opin Plant Biol **5**(5): 415-424.

Kovtun, Y., W. L. Chiu, G. Tena and J. Sheen (2000). "Functional analysis of oxidative stress-activated mitogen-activated protein kinase cascade in plants." Proc Natl Acad Sci U S A **97**(6): 2940-2945.

Li, B., S. Jiang, X. Yu, C. Cheng, S. Chen, Y. Cheng, J. S. Yuan, D. Jiang, P. He and L. Shan (2015). "Phosphorylation of trihelix transcriptional repressor ASR3 by MAP KINASE4 negatively regulates Arabidopsis immunity." Plant Cell **27**(3): 839-856.

Li, S., W. Wang, J. Gao, K. Yin, R. Wang, C. Wang, M. Petersen, J. Mundy and J. L. Qiu (2016). "MYB75 phosphorylation by MPK4 is required for light-induced anthocyanin accumulation in *Arabidopsis*." Plant Cell **28**(11): 2866-2883.

Maier, A., A. Schrader, L. Kokkelink, C. Falke, B. Welter, E. Iniesto, V. Rubio, J. F. Uhrig, M. Hulskamp and U. Hoecker (2013). "Light and the E3 ubiquitin ligase COP1/SPA control the protein stability of the MYB transcription factors PAP1 and PAP2 involved in anthocyanin accumulation in *Arabidopsis*." Plant J **74**(4): 638-651.

Petersen, K., J. L. Qiu, J. Lutje, B. K. Fiil, S. Hansen, J. Mundy and M. Petersen (2010). "Arabidopsis MKS1 is involved in basal immunity and requires an intact N-terminal domain for proper function." PLoS One **5**(12): e14364.

Petersen, M., P. Brodersen, H. Naested, E. Andreasson, U. Lindhart, B. Johansen, H. B. Nielsen, M. Lacy, M. J. Austin, J. E. Parker, S. B. Sharma, D. F. Klessig, R. Martienssen, O. Mattsson, A. B. Jensen and J. Mundy (2000). "*Arabidopsis* map kinase 4 negatively regulates systemic acquired resistance." Cell **103**(7): 1111-1120.

Rayapuram, N., J. Bigeard, H. Alhoraibi, L. Bonhomme, A. M. Hesse, J. Vinh, H. Hirt and D. Pflieger (2018). "Quantitative phosphoproteomic analysis reveals shared and specific targets of *Arabidopsis* Mitogen-Activated Protein Kinases (MAPKs) MPK3, MPK4, and MPK6." Mol Cell Proteomics **17**(1): 61-80.

Shimaoka, T., A. Yokota and C. Miyake (2000). "Purification and characterization of chloroplast dehydroascorbate reductase from spinach leaves." Plant Cell Physiol **41**(10): 1110-1118.

Suzuki, T., C. Matsushima, S. Nishimura, T. Higashiyama, M. Sasabe and Y. Machida (2016). "Identification of Phosphoinositide-Binding Protein PATELLIN2 as a Substrate of Arabidopsis MPK4 MAP Kinase during Septum Formation in Cytokinesis." Plant Cell Physiol **57**(8): 1744-1755.

Teige, M., E. Scheikl, T. Eulgem, R. Doczi, K. Ichimura, K. Shinozaki, J. L. Dangl and H. Hirt (2004). "The MKK2 pathway mediates cold and salt stress signaling in Arabidopsis." Mol Cell **15**(1): 141-152.

Templeton, D. J., M. S. Aye, J. Rady, F. Xu and J. V. Cross (2010). "Purification of reversibly oxidized proteins (PROP) reveals a redox switch controlling p38 MAP kinase activity." PLoS One **5**(11): e15012.
Tena, G., T. Asai, W. L. Chiu and J. Sheen (2001). "Plant mitogen-activated protein kinase signaling cascades." Curr Opin Plant Biol **4**(5): 392-400.

Truong, T. H. and K. S. Carroll (2013). "Redox regulation of protein kinases." Crit Rev Biochem Mol Biol **48**(4): 332-356.

Wang, B., X. Qin, J. Wu, H. Deng, Y. Li, H. Yang, Z. Chen, G. Liu and D. Ren (2016). "Analysis of crystal structure of Arabidopsis MPK6 and generation of its mutants with higher activity." Sci Rep **6**: 25646.

Wang, Z., H. Mao, C. Dong, R. Ji, L. Cai, H. Fu and S. Liu (2009). "Overexpression of *Brassica napus* MPK4 enhances resistance to *Sclerotinia sclerotiorum* in oilseed rape." Mol Plant Microbe Interact **22**(3): 235-244.

Waszczak, C., S. Akter, D. Eeckhout, G. Persiau, K. Wahni, N. Bodra, I. Van Molle, B. De Smet, D. Vertommen, K. Gevaert, G. De Jaeger, M. Van Montagu, J. Messens and F. Van Breusegem (2014). "Sulfenome mining in *Arabidopsis thaliana*." Proc Natl Acad Sci U S A **111**(31): 11545-11550.

Zeng, Q., J. G. Chen and B. E. Ellis (2011). "AtMPK4 is required for male-specific meiotic cytokinesis in *Arabidopsis*." Plant J **67**(5): 895-906.

Zhou, J., X. J. Xia, Y. H. Zhou, K. Shi, Z. Chen and J. Q. Yu (2014). "RBOH1-dependent H_2O_2 production and subsequent activation of MPK1/2 play an important role in acclimation-induced cross-tolerance in tomato." J Exp Bot **65**(2): 595-607.

Words of thanks

I would like to express my sincere gratitude to my supervisors Professor Joris Messens and Professor Frank Van Breusegem for the continuous support of my Ph.D. study and related research, for their patience, motivation, and immense knowledge. Their guidance helped me in all the time of research and writing of this thesis. For their unwavering support, I am truly grateful.

I would like to thank all the lab members of VIB Center for Structural Biology, Brussels and VIB Center for Plant System Biology, Ghent. I am very thankful to Brandan and Maria for giving me the advice in performing experiments. I am also very thankful to Jingjing, Leonardo, David and Inge for their continuous support and advice. I would like to thank Barbara and Amna for helping me with the experiments in Ghent. I am also grateful to other members of my lab Aleksandra, Ting, Jasmine, Tom, Bo, Simon, Alvaro, Huaming, Valerie, Pavel, Inge, Xi, Katrien, Patrick, Sam- thank you all for your help throughout my stay at VUB and PSB.

My very special thanks to Khadija for providing me enormous support in the lab. Whenever I faced any problem in administrative and technical perspective; I always have been to you for your help and suggestions.

I would like to acknowledge the Indian Council of Agricultural Research Organization for providing me the funding and opportunity to start Ph.D. research in excellent labs at VIB Center for Structural Biology, Brussels and VIB Center for Plant System Biology.

Further, I would like to thank almighty GOD, my family, and all my friends.

Thank you all

Nandita Bodra

Joint PhD Fellow
Center for Structural Biology, Brussels Center for Redox Biology, VIB-VUB
Department of Plant Systems Biology, VIB-UGent

ACADEMIC RECORDS

PhD in Bio-engineering Sciences, VUB (on going)

PhD in Sciences: Biochemistry and Biotechnology, UGent (on going)
Research Topic: The plant sulfenome: Mining for new targets for crop improvement
Institutes:
1) Faculty of Sciences and Bioengineering Sciences, Department of Bioengineering Sciences, Structural Biology Brussels, Vrije Universiteit Brussel, Belgium
2) Faculty of Sciences, Department of Plant Biotechnology and Genetics, Universiteit Gent, Belgium

Master of Science in Biotechnology
Institute: Indian Institute of Technology Roorkee, India
Year: 2013
Result: 1st division

Bachelor of Science in Biotechnology
Institute: Ranchi Women's College, Ranchi University
Year: 2011
Result: 1st division

Intermediate of Science
Mahilla College Chaibasa, Jharkhand
Year: 2008
Result: 1st division

Senior Secondary (Matriculation)
ST. Xavier's Girls High School Chaibasa, Jharkhand
Year: 2006
Result: 1st division

PUBLICATIONS

1. *Arabidopsis thaliana* dehydroascorbate reductase 2: Conformational flexiblity during catalysis; **Bodra N**, Young D, Astolfi Rosado, Pallo A, Wahni K, D Proft F, Huang

J, Van Breusegem F, Messens J; Scientific Reports, 2017 Feb 14;7:42494. doi: 10.1038/srep42494.

2. DYn-2 based identification of Arabidopsis sulfenomes; Akter S,Huang J, **Bodra N**, De Smet B, Wahni K Rombaut D, Pauwels J, Gevaert K, Carroll K, Van Breusegem F, Messens J; Molecular and Cellular Proteomics, 2015 May;14(5):1183-200. doi: 10.1074/mcp.M114 10.1074/mcp.M114.046896.

3. Sulfenome mining in *Arabidopsis thaliana*; Waszczak C, Akter S, Eeckhout D, Persiau G, Wahni K, **Bodra N**, Van Molle I, De Smet B, Vertommen D, Gevaert K, De Jaeger G, Van Montagu M, Messens J, Van Breusegem F; Proceedings of the National Academy of Sciences of United States of America, 2014. Aug 5;111(31):11545-50. doi: 10.1073/pnas.1411607111.

EDUCATIONAL TASKS

IPMB practical course
Teaching protein purification techniques specifically immobilized metal ion affinity chromatography and anion exchange chromatography, Site directed mutagenesis (2-19 May, 2016)

Bioengineer's practical course
Teaching protein purification techniques including affinity chromatography anion exchange chromatography and gel filtration, ATP/NADH coupled enzyme assay (Mar 20- Mar 30, 2017)

ORAL AND POSTER PRESENTATIONS

Oral presentations

1. VUB PhD Research Day (27 May, 2016)
2. International workshop on Biochemistry, Physiology and Pharmacology of oxidative stress, Rome (July 2-4, 2015)

Poster presentations

1. EMBO workshop 2017, Sant Feliu de Guixols, Spain (17-21 Sept, 2017)
2. GBM redox meeting 2016, Dusseldorf (4-5 July, 2016)
3. 9th Belgian crystallography symposium (26 Oct, 2016)
4. PhD-symposium on modulation of oxidative stress, Brussels (May 29, 2015)

EXPERIMENTAL SKILLS

Molecular biology techniques: Genomic and plasmid DNA isolation, Primer design, Restriction digestion and ligation, PCR, Gene cloning, SDS-PAGE, Western blot analysis

Biophysical techniques: Protein crystallization, UV-Visible Spectroscopy, Fluorescence Spectroscopy, Circular Dichroism Spectroscopy

Microbiological techniques: Bacterial culture maintenance, preparation of chemical competent cells and transformation
Biochemical methods: Protein purification (Affinity chromatography, Ion-exchange chromatography, Size Exclusion Chromatography), Dialysis

SCIENTIFIC AND SOFT SKILL COURSES

Lecture on *Creating Effective Research Posters* by Dr ir Jean- luc Dumont

9 Mar. 2017, Institute: ULB

Initiation Gimp and Inkscape
6 Dec. 2016**,** Institute: VIB

Essentials of Image Editing
13 Dec.2016**,** Institute: VIB

Seminar series on Protein folding and protein stability, Liege
29-30 Aug, 2016, Institute: University of Liege

Scientific writing and oral presentation
Nov 12- 13, 2015 and Dec 1- 2, 2015, Institute: VIB

PERSONAL DETAILS

Date of birth: 15th May, 1990

Father's Name: Krishna Bodra

Mother's Name: Anita Bodra

Nationality: Indian

Languages known: English, Hindi, Ho

I hereby declare that all the information given herewith is correct.